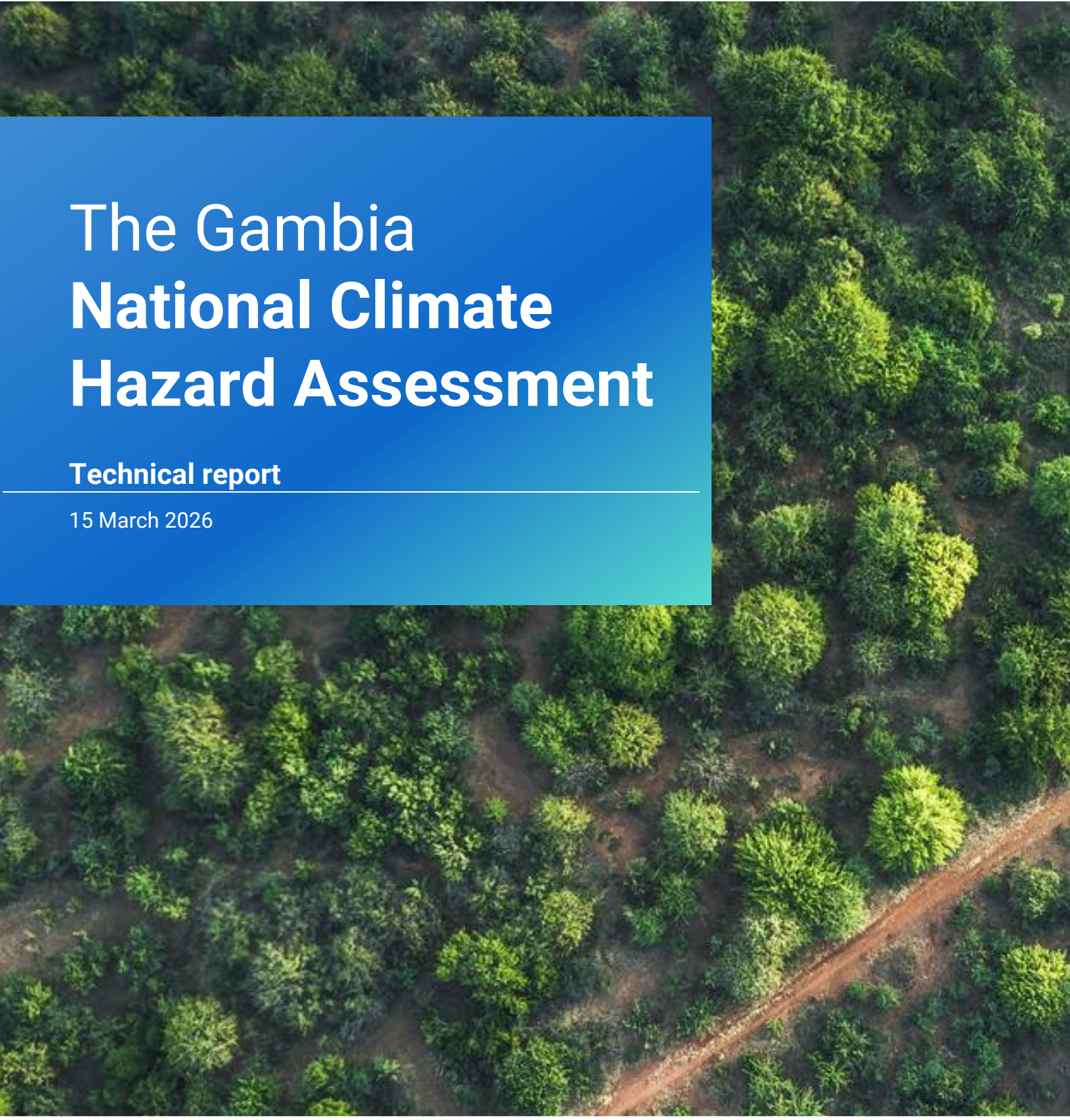

The Gambia
National Climate Hazard Assessment

Technical report

15 March 2026

GLOBAL
CENTER ON
ADAPTATION

AUTHORS & ACKNOWLEDGMENTS

This report was developed by:

Global Center on Adaptation: Martin Garcia Perez, Program Officer; Merita Salihu, Senior Program Officer; Edwina Mercer, Senior Program Office; Anne-Laure Solnon, Senior Specialist; Adele Cadario, Global Lead, Infrastructure and Nature-based Solutions.

Partnerships: The World Bank Group

Consultants: Haskoning, Lobelia Earth, City Scape Associates, and Rebel Group.

Acknowledgements :

This report builds on analyses conducted by GCA under the Africa Adaptation Acceleration Program (AAAP), an initiative launched by the GCA in collaboration with the African Development Bank, endorsed by the African Union. The work benefited from collaboration with the World Bank teams for The Gambia Infrastructure Project and CCDR, as well as insights shared by the Ministry of Transport Works & Infrastructure, the Ministry of Environment and Climate Change, the Department of Water Resources, and the National Roads Authority of The Gambia.

GLOBAL CENTER ON ADAPTATION

ABOUT THE GLOBAL CENTER ON ADAPTATION

The Global Center on Adaptation (GCA) is an international organization, hosted by the Netherlands, which works as a solutions broker to accelerate action and support for adaptation solutions from the international to the local, in partnership with the public and private sector, to ensure we learn from each other and work together for a climate resilient future.

AFRICA ADAPTATION ACCELERATION PROGRAM

GCA is providing technical assistance under the African Adaptation Acceleration Program (AAAP), a joint initiative launched by the GCA and the African Development Bank in 2021.

In Partnership with:

WORLD BANK GROUP

Consultants:

Royal HaskoningDHV
Enhancing Society Together

REBEL

CITYSCAPE ASSOCIATES

Lobelia.

CONTEXT

The Global Center on Adaptation (GCA) is an international organization working to accelerate action on adapting to climate change and building resilient economies.

Under the African Adaptation Acceleration Program (AAAP), GCA supports The Gambia in embedding climate resilience into national planning and infrastructure investment projects – including The World Bank Gambia Infrastructure Project, The African Development Bank Banjul Port 4th Expansion and Senegambia Bridge Asset Recycling projects. Since 2024, GCA has partnered with IFIs, the Ministry of Transport Works and Infrastructure, the Ministry of Environment and Climate Change, NAWEC, the Water Resources Department and the National Roads Authority of The Gambia to assess climate risks to the transport sector, water resources, identify adaptation solutions, and strengthen local capacity though training activities.

In this context, GCA is supporting the World Bank and governmental institutions on a $50 million investment to enhance climate resilience in The Gambia's transport and energy infrastructure. The project focuses on improving last-mile connectivity by expanding low-voltage electricity access in 225 rural communities, strengthening urban energy grid redundancy, and upgrading 150 kilometers of seasonal roads to ensure reliable year-round access. Additionally, the project focuses on strengthening The Gambia's transport and energy sectors through policy reforms, institutional capacity building, and improved planning for sustainability, resilience, and universal access. It includes support for road sector management, climate-resilient design standards, and enabling frameworks for renewable energy investment, energy efficiency, and private sector participation.

GCA's support focuses on prioritizing infrastructure investments from an adaptation perspective, with the aim of strengthening connectivity, identifying and assessing targeted adaptation measures, and developing implementation guidelines to improve existing design standards. In parallel, GCA is contributing to related initiatives. This work seeks to reinforce sectoral ambitions by integrating climate change considerations with development objectives, while promoting the incorporation of long-term strategies for climate resilience.

Table of contents

ABBREVIATIONS

Acronyms	Definitions
CMIP5	Coupled Model Intercomparison Project Phase 5
CMIP6	Coupled Model Intercomparison Project Phase 6
CORDEX	Coordinated Regional Downscaling Experiment
ENSO	El Niño-Southern Oscillation
FWI	Fire Weather Index
GCA	Global Center on Adaptation
GCM	Global Climate Models
IPCC	Intergovernmental Panel on Climate Change
ITCZ	Intertropical Convergence Zone
NOAA	National Oceanic and Atmospheric Administration
RCM	Regional Climate Models
RCPs	Representative Concentration Pathways
SPEI	Standardised Evapotranspiration Precipitation Index
SPI	Standardised Precipitation Index
SSPs	Shared Socioeconomic Pathways
WB	World Bank

EXECUTIVE SUMMARY

The Gambia, with its low-lying topography and extensive fluvial networks, faces significant climate challenges that threaten critical infrastructure across its transport, energy, and water resource sectors. These sectors are vital for the nation's socio-economic stability, yet they are increasingly vulnerable to climate-induced hazards such as flooding and extreme weather events. The impacts of these hazards disrupt mobility, trade, and access to essential services, posing risks to livelihoods and economic development.

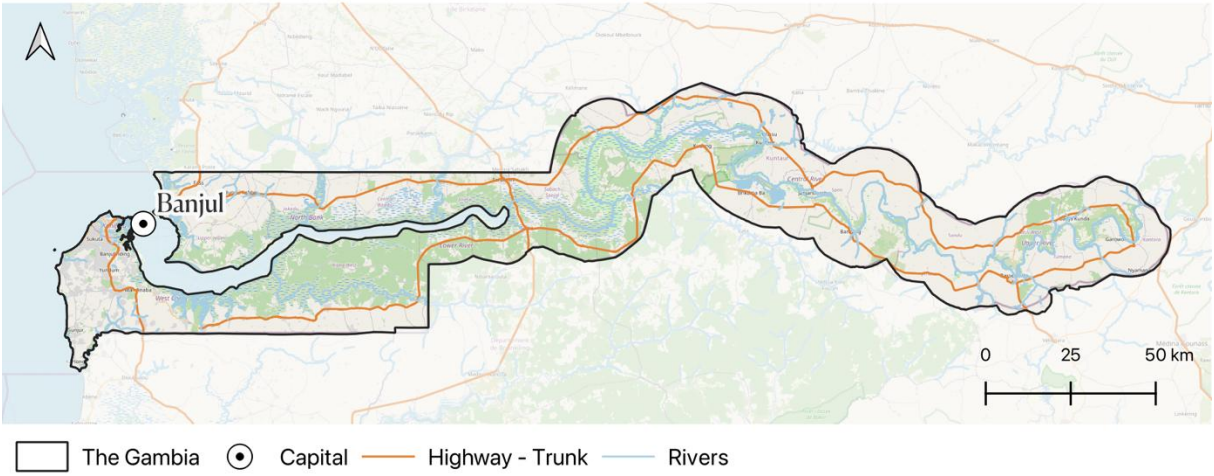

This assignment focuses specifically on assessing climate hazards affecting The Gambia currently, as well as how they will change in the next few decades. The analysis covered key hazards identified to be relevant in the country: extreme temperatures, extreme precipitation, extreme winds, drought and wildfires. Additionally, precipitation data for the river basin was examined and provided for a separate water balance analysis (separate from this report). Supplementary, a flood hazard assessment was conducted covering three flood types: coastal flooding, rainfall-driven flooding, and riverine flooding.

While the focus of this report lies on the climate hazards and their evolution over time, the overarching goal of the project has been kept in focus throughout the analysis. The hazards covered here closely relate to The Gambia's infrastructure, with an emphasis on the transport sector, including roads, bridges, and fluvial systems. The analysis is aimed at supporting the integration of resilience and adaptation measures into national-level planning, particularly in collaboration with ongoing efforts to develop a new Transport Masterplan and inform investment projects in transport and energy. By providing a detailed assessment of climate hazards, this work establishes a foundation for identifying priority interventions and nature-based solutions that will enhance the resilience of critical infrastructure while safeguarding the country's water resources and key socio-economic activities.

The Gambia climate lies at the border between tropical savanna climate and hot semi-arid climates, according to the Köppen climate classification. The seasons are shaped by the movement of the Intertropical Convergence Zone (ITCZ), the main rain-producing mechanism over Western Africa. The country experiences a long, dry season from November to May and a short, wet season from June to October. Temperatures vary little throughout the year, ranging from 25ºC to 30ºC year round. Year-to-year temperature variations have been linked to El Niño-Southern Oscillation (ENSO) patterns, and the Dakar Niño/Niña phenomenon on a more localised scale. Like its larger counterpart, Dakar El Niño years are characterised by higher temperatures, while Dakar La Niña years bring cooler conditions. Temperature and precipitation spatial patterns are influenced by the proximity to the ocean. Regions closer to the Atlantic Ocean experience lower temperatures. Precipitation varies from approximately 650 mm/year in the east to 1100 mm/year in the west, with a country-wide average of 800 mm/year.

This climate hazard assessment aims to provide a comprehensive analysis of the risks associated to drought, wildfire, extreme temperature, precipitation, wind, and the different flood types on The Gambia transportation and energy infrastructure and water resource availability. To assess the risks associated with these climate hazards, we used several independent sources of evidence depending on data

availability. Firstly, we examined long-term historical climate records from CHIRPS[1] and CHIRTS[2] climatologies, and from one reanalysis (ERA5[3]), to assess the already observed trends. These datasets have been validated and compared using in-situ data from meteorological stations in bordering regions (see Section 3.2.3). Secondly, we used climate projections from 16 state-of-the-art simulations from the international CORDEX program to estimate future hazards[4]. By using a large ensemble of models, we have quantified the corresponding model uncertainty and analyse the agreement between different models to provide reliable estimates of the future. The high spatial resolution (25 km) of the CORDEX simulations represents better small-scale processes that drive the occurrence of extreme events such as intense precipitation or heat waves compared to global climate projections from the Coupled Model Intercomparison Project[5] (CMIP5-CMIP6). We compared two different scenarios for the possible future, including the high greenhouse emissions RCP8.5 scenario and the RCP4.5 scenario characterised by a notable reduction in global emissions[6]. Future climate projections were given for 20-year periods centred in 2030, 2050, 2070 and 2090.

Results per hazard are summarised below:

Extreme temperature: Future projections indicate a consistent warming trend in maximum temperatures across the country, supported by strong model agreement. Extreme temperature events are expected to become more intense. Inland areas will see a significant shift, with extreme temperatures that occurred every 25 years during the reference period projected to occur every 2 years by 2050 under the moderate emissions scenario. The coastal areas are expected to see a greater increase in the average number of days exceeding 35ºC per year by 2050 (around two more weeks), whilst the northeastern region will experience the largest rise in the frequency of days exceeding 40ºC. There, typical conditions will experience over twice as many days over 40ºC compared to the reference period.

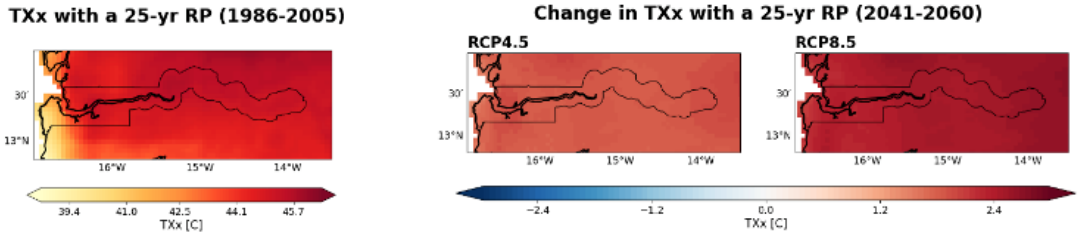

Extreme precipitation: Extreme precipitation events with a return period of 25 years are expected to increase significantly, with rises of 17% in the west and 34% in the east under RCP4.5, and 17% in the west and 45% in the east under RCP8.5. By mid-century, the highest daily precipitation levels are projected to reach 130 mm/day in the eastern tip of the country under both scenarios, while in Banjul, extreme one-day precipitation is forecasted to reach 110 mm/day for both emission scenarios. Future model projections indicate no significant changes in the frequency of days with extreme precipitation. Mean precipitation accumulated over the year is expected to decrease particularly on coastal areas, with little to no change inland.

---

[1] Climate Hazards Group InfraRed Precipitation with Station data (CHIRPS) https://doi.org/10.1038/sdata.2015.66

[2] Climate Hazards Group InfraRed Temperature with Station data (CHIRTS) https://doi.org/10.1038/s41597-020-00643-7

[3] ERA5 dataset. https://cds.climate.copernicus.eu/cdsapp#!/dataset/reanalysis-era5-single-levels

[4] CMIP6 was used for future projections for the flood hazard assessment.

[6] The flood hazard assessment uses the corresponding SSP scenarios : SSP2-4.5 and SSP5-8.5.

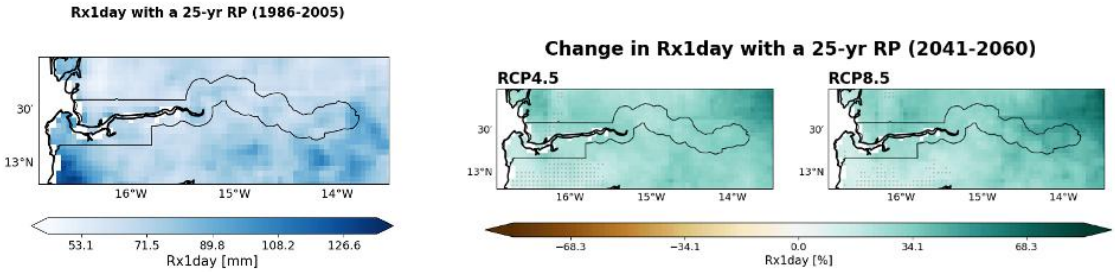

Extreme Wind: Future projections suggest that the average maximum wind gusts will remain largely unchanged across most of the country. For 25-year return period events, wind gusts are projected to peak mid-century, with increases of up to 10% under RCP4.5 by 2050 in the central regions, and returning to values similar to the reference period under both emissions scenarios. The frequency of days with wind gusts exceeding the 90th percentile is projected to rise in the future. Years with extreme wind gust events for a 25-year return period are expected to see up to 90 days and 95 days of such occurrences, under RCP4.5 and RCP8.5 respectively, from the 60 days in the historical period. Geographically, the centre of the country is the region expected to see the most noticeable increases in wind.

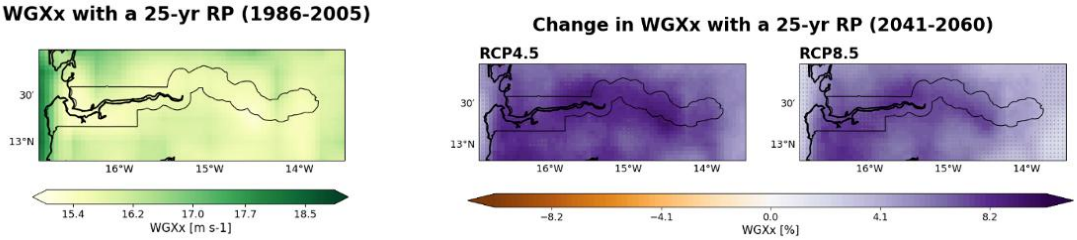

Drought: Drought risk is expected to increase consistently over time. Based on a widely used drought indicator, the Standardised Precipitation and Evapotranspiration Index (SPEI), by 2050, droughts that occur once every two years are projected to decrease by 0.4 to 0.8 on the SPEI scale, shifting the whole country from today's Normal conditions to Moderately dry conditions (SPEI < -1). By the end of the century the increase trend in drought conditions will lead to most of the country reaching to levels of Severely dry conditions (SPEI < -1.5) under RCP4.5 and reaching in some areas Extremely dry conditions (SPEI < -2).

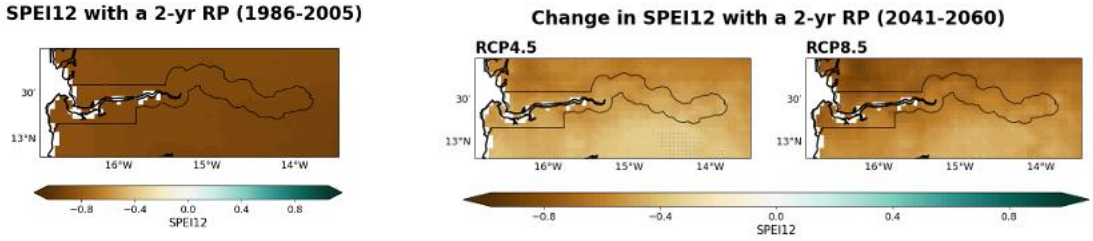

Wildfire: Future projections under mean conditions show a gradual westward expansion of very extreme wildfire risk zones under both RCP 4.5 and RCP 8.5 scenarios. By the mid-21st century, Fire Weather Index (FWI) is expected to increase uniformly by 2-3% across The Gambia, with a slightly greater increase under RCP 8.5. An increasing trend in the number of days per year when FWI surpasses the historical 90th percentile (dFWI90p) is projected across The Gambia, indicating a rise in the frequency of high-risk days. By the mid-21th century (2040–2060), dFWI90p is projected to increase by 30-39 days, resulting in 62-72 high-risk days annually.

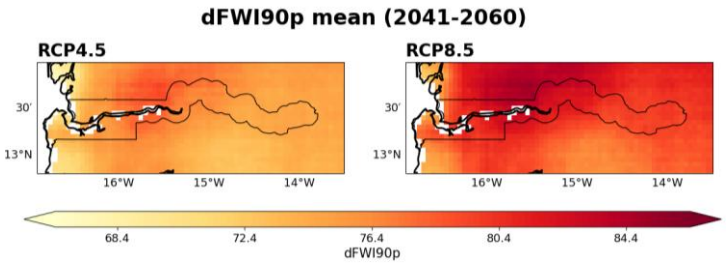

Coastal Flooding: The coastal flood assessment reveals particular hazard in the Greater Banjul Area and the Gambia River estuarine area. Current coastal floods are concentrated in low-lying areas around Banjul, with significant inundation during extreme water level events. Mangrove areas west of Banjul show high inundation levels, underlining their crucial role and potential in flood attenuation. Sea level rise will amplify coastal flood risks, with projected increases in flood depths under the SSP5-8.5 climate scenario of 0.25 meters by 2050 and 0.42m by 2070. The combination of sea level rise and storm surge creates compound effects that will increasingly challenge coastal infrastructure. Banjul and Brikama regions show the highest projected increases in flood depths for extreme events between the current and 2050 time horizons. These findings suggest an urgent need for coastal adaptation strategies, particularly for critical infrastructure in the Greater Banjul Area.

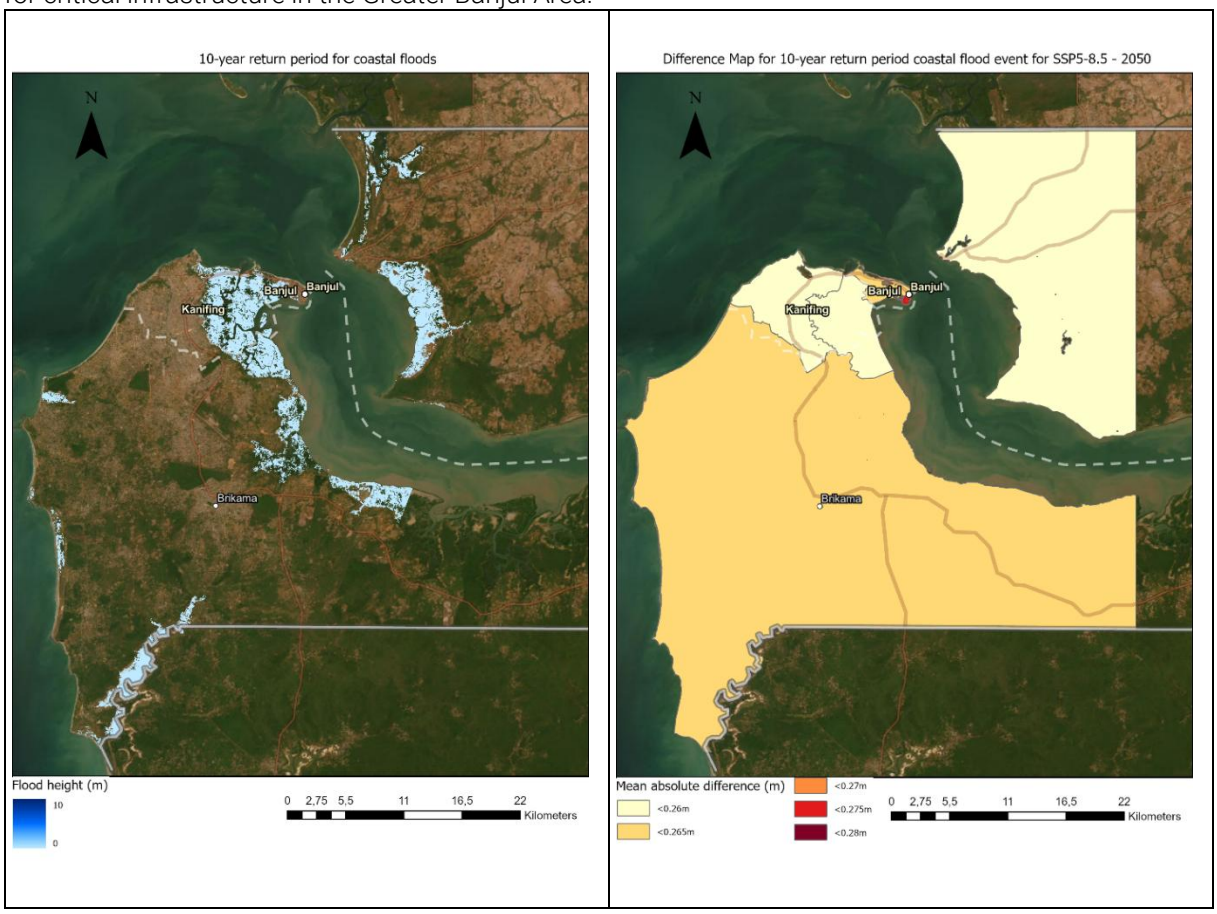

Pluvial Flooding: The analysis of rainfall-driven flooding reveals widespread pluvial flood hazard across The Gambia, with distinct spatial patterns. Eastern regions, particularly Basse, show the highest susceptibility to pluvial flooding and the largest projected increases in flood depth under future climate scenarios. Urban areas demonstrate particular vulnerability to local flash flooding, with Kanifing showing significant localized impacts around Kotu Stream. Short-duration, high-intensity rainfall events are projected to increase in frequency and severity under future climate scenarios, leading to increased flooding. The east-west gradient in increased flood exposure suggests the need for regionally differentiated adaptation strategies. These patterns highlight the importance of improving urban drainage systems and localized flood management strategies.

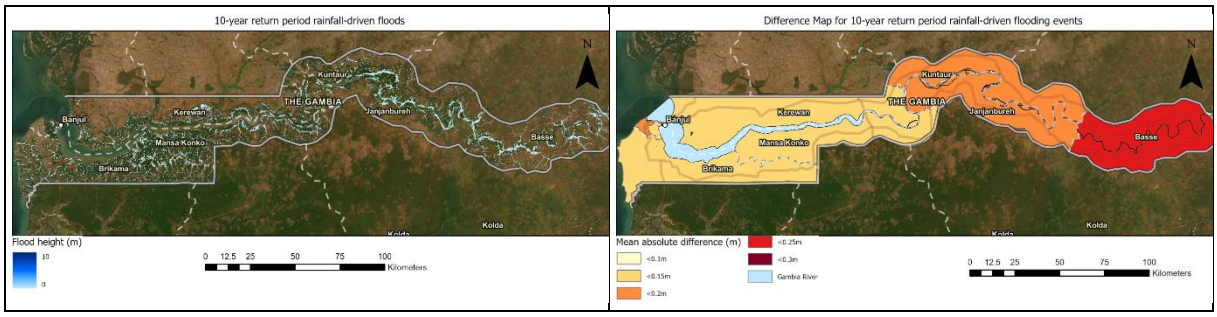

Fluvial Flooding: The assessment of riverine flooding reveals complex interactions between river dynamics and flood exposure. The Gambia River and its tributaries have extensive flood plains, particularly in middle river regions (Mansa Konko, Kuntaur, and Janjanbureh) which also show the most significant fluvial flood hazard. Under future climate scenarios, the effect of increased sea levels is transmitted up the Gambia River as far as the tidal effect, resulting in increased flooding in the lower river regions under these scenarios. Up to 2050, the 7-day precipitation change ratio for future climate scenarios is positive, reflecting increased long-duration rainfall; however after 2050 it then reflects a pronounced decline in total cumulative rainfall under the high-emission scenario SSP5-8.5. This shift points to a strong decrease in long-duration extreme precipitation, and thus in the magnitude of fluvial floods between 2050 and 2070. The spatial pattern of fluvial flood hazard contrasts with pluvial hazard patterns requiring integrated flood management. The validation against 2007 flood events demonstrates the model's capability to capture major flood patterns with sufficient accuracy for the purposes of this assessment.

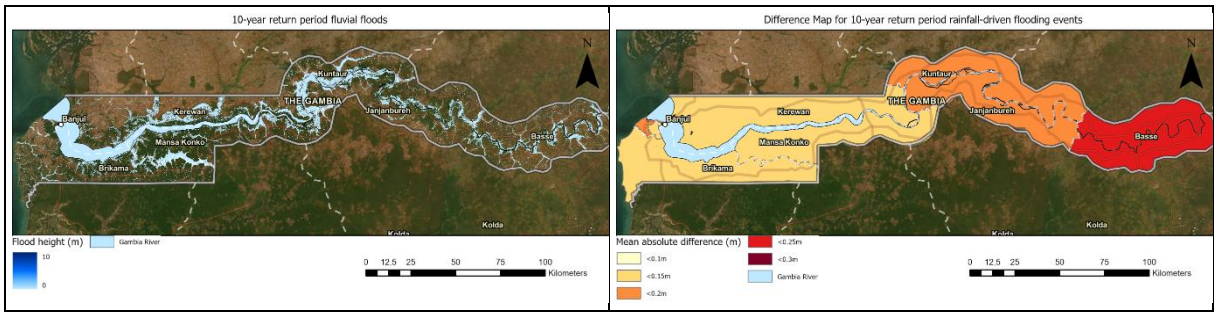

In general terms, The Gambia faces multiple climate hazards, but flooding, extreme temperatures, and drought stand out as the most significant due to their far-reaching impacts. The different types of flooding having an extensive range over the whole of The Gambia, threatening communities and infrastructure. Rising temperatures, particularly inland, contribute to severe heat stress and threaten vulnerable populations and transport infrastructure, while also amplifying water demand. Projections indicate an alarming increase in the frequency and intensity of extreme heat events, with inland areas experiencing temperatures above 40°C for up to 290 days annually under high-emissions scenarios by mid-century. Coupled with this, drought risks are expected to escalate as higher temperatures exacerbate water scarcity, pushing the country toward severely dry conditions, particularly in northern regions.

While extreme precipitation, wind, and wildfires are also noteworthy, their impacts are more localized or uncertain. Flooding from extreme rainfall events, though severe, lacks consistent future trends in annual precipitation. Wind hazards are projected to rise slightly in frequency, and wildfire risks, though driven by extreme dry conditions, remain secondary to the direct effects of heat and drought. Collectively, these hazards underscore the urgent need for climate resilience, but addressing floods, extreme temperatures and drought will be critical for safeguarding The Gambia's communities, ecosystems and transport infrastructure.

1. INTRODUCTION

The objective of the Climate Hazard Assessment Report is to analyse different climate-related hazards that might have an impact on the Transport, Energy and Water Sectors in The Gambia, considering the available observational records from the last decades and future projections provided by high-resolution climate models.

The first section of this report presents a general introduction to the climate in The Gambia and the observed trends in the last few decades. The following sections are an in-depth description of the most relevant hazards projected to affect the country. A description of the methodology is presented in the last section, outlining the data sources, the integration of data from local stakeholders, and the method for validation and calibration of climate data.

1.1 Climatology of the Gambia

Climate

The Gambia is the smallest country in Africa, characterised by a narrow horizontal shape that stretches along the Gambia River. It is surrounded entirely by Senegal except for an 80-kilometre coastline in the west, along the Atlantic Ocean. According to the Köppen climate classification, The Gambia lies at the border between tropical savanna climate and hot semi-arid climates. The country experiences a long, dry season from November to May and a short, wet season from June to October (Figure 1). Temperatures vary little throughout the year, ranging from 25ºC to 30ºC year round. The topography of the country is flat, with over 50% of the country below 20m altitude and with no point surpassing 60m altitude.

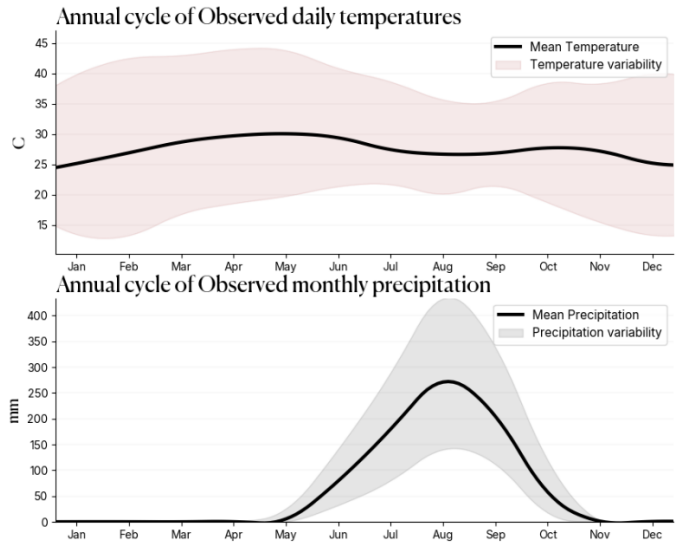

Figure 1-1. Annual cycle of mean temperature and precipitation with their variability. Data obtained from CHIRPS 0.25 and CHIRTS.

Drivers of climate variability

The seasons are shaped by the movement of the Intertropical Convergence Zone (ITCZ), the main rain-producing mechanism over Western Africa. Over The Gambia, it remains inactive until early or mid-May, reaching its peak in August and giving the Gambia its main rains before it propagates southwards. Year-to-year temperature variations have been linked to ENSO patterns, with La Niña years typically associated with cooler temperatures. Additionally, the Dakar Niño/Niña phenomenon mirrors the broader ENSO system but operates on a more localised scale. Like its larger counterpart, Dakar El Niño years are characterised by higher temperatures, while Dakar La Niña years bring cooler conditions.

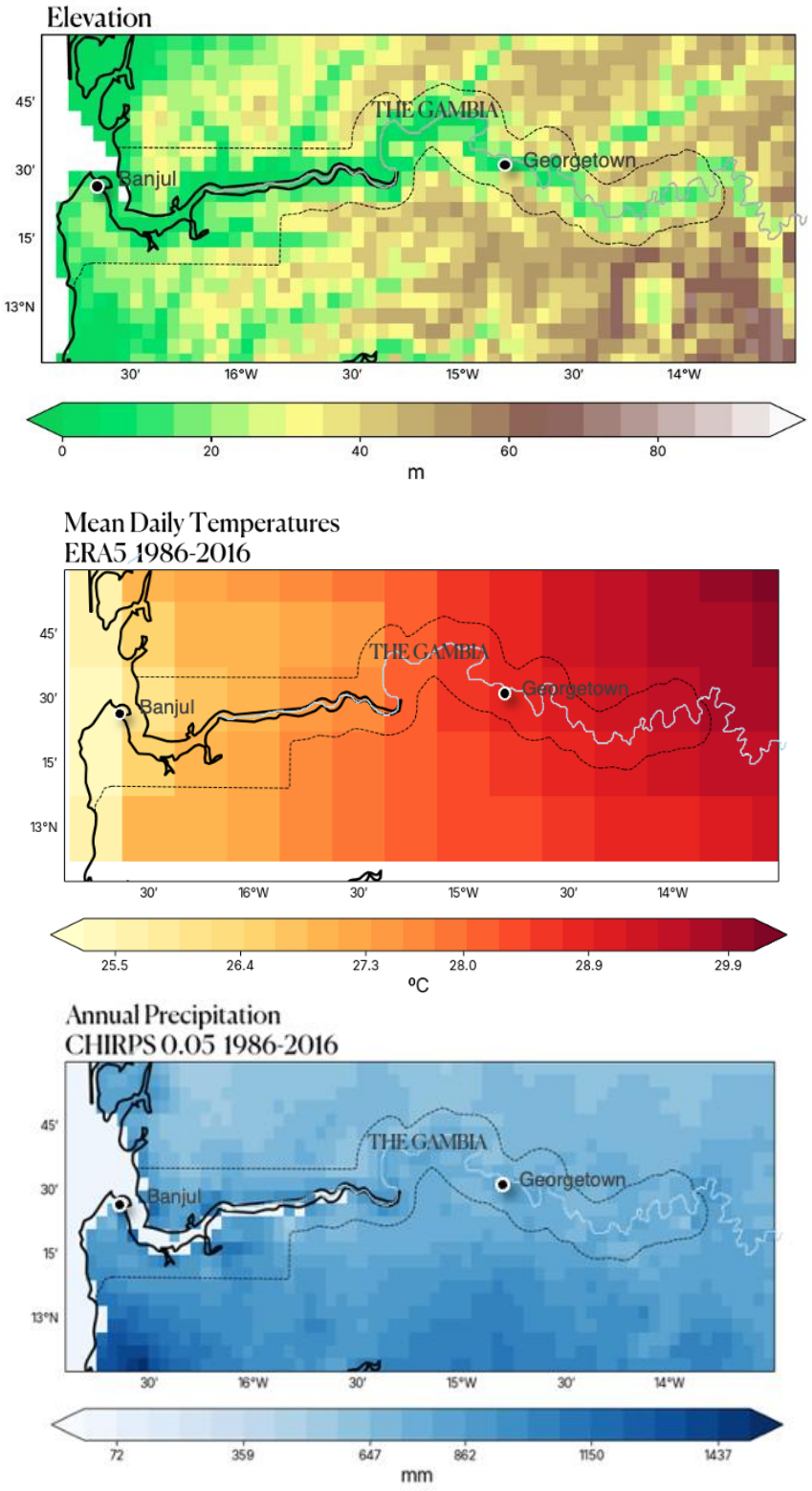

Figure 1-2. Land elevation and mean fields of mean daily temperature and mean annual precipitation. Data obtained from CHIRPS 0.25 and CHIRTSmax data.

Country-wide variations

Temperature and precipitation patterns are influenced by proximity to the ocean. Regions closer to Banjul and the Atlantic Ocean experience lower temperatures due to the ocean's regulatory effect and higher levels of precipitation. Between 1980 and 2023, average temperatures ranged from 25ºC along the western coast to 29ºC in the eastern region, with the national annual average settling at 28ºC. Extreme

temperatures reached up to 38ºC on the coast but climbed up to 44ºC in the east of Georgetown. Precipitation varies from approximately 650 mm/year in the east to 1100 mm/year in the west, with a country-wide average of 800 mm/year.

Recent trends

Annual temperature anomalies of the whole country indicate a continuous warming pattern during the last 40 years (Figure 3). Mean annual temperature has increased steadily, gaining nearly a whole degree on average since 1980. During the months of April and May 2024, the Sahel and West Africa suffered extreme heatwaves[7].

Precipitation patterns are variable, showing no significant change. The lowest national average was recorded in 1983, at just over 550 mm per year, while the highest occurred in 1999, reaching approximately 1100 mm per year. The country has a long record of droughts over the past years, being the 2011-2012, the 2014, 2018 and 2023 years under drought conditions in recent years.

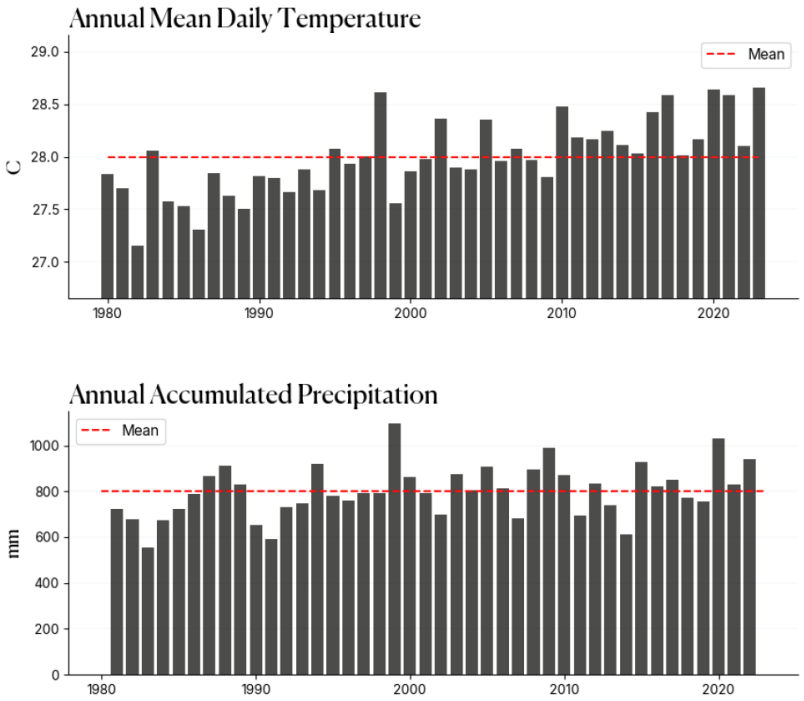

Figure 1-3. Temporal evolution of anomalies of annual mean annual precipitation and temperature in the period 1981-2022 (top and bottom respectively) around the asset. Data obtained from CHIRPS 0.25 and CHIRTS.

[7] https://reliefweb.int/report/burkina-faso/deadly-heatwave-sahel-and-west-africa-would-have-been-impossible-without-human-caused-climate-change

2. CLIMATE HAZARD ASSESSMENT RESULTS

The screening of the exposure to 8 relevant climate hazards (extreme temperature, extreme precipitation, extreme wind, drought, wildfires, coastal flooding, pluvial flooding, and fluvial flooding) is presented in this section, with the main findings for each one of those climate hazards in each individual subsection. The indicators used in this section have been chosen due to their well-established use for the characterization of the different hazards presented and their impact on infrastructure. For extreme, temperature indicators such as number of days above a given temperature showcase the exposure of infrastructure to critical heat stress that can affect its durability and even lead to infrastructure damage or failure. Typical transport, water and energy infrastructure life-span, between 10 years for maintenance to 25 and 50 years for lineal infrastructure, and 100 years and beyond for high value infrastructure, are used to describe the probability of different hazard thresholds in the form of Return Periods, which represent the frequency of events matching or surpassing a hazard intensity.

2.1 Extreme temperature

The Gambia experiences consistently high temperatures, with mean daily temperatures at 27.8 ºC and 10th and 90th percentiles at 24.7 ºC and 31.4 ºC, respectively. Along the coast, where most of the population resides, the ocean helps moderate the climate. However, temperatures rise significantly further inland. The highest recorded temperature in The Gambia was 46.4ºC, associated with a UTCI (Universal Thermal Climate Index, which describes the synergistic heat exchanges between the thermal environment and the human body) exceeding 50, indicating extreme heat stress. This level of heat disproportionately impacts vulnerable groups, including pregnant women, contributing to maternal heat strain (Bonell et al., 2022). Additionally, the high humidity in the country amplifies heat stress: in Banjul, humidity levels range from 47% to 85%, with an annual average of 68%.

Overall, the temperature distribution exhibits a coastal pattern of lower temperatures and a north-south gradient, with higher temperatures observed in the northern areas. The temperature trend over the 1980–2023 period (Figure 3) shows a clear and consistent rise in annual mean temperatures. During the reference period (1986–2005), annual temperature extremes averaged 40ºC in Banjul, rising to 44ºC in the eastern part of the country (Figure 4, left). Maximum temperatures over a 25-year return period reached 42.5ºC in Banjul and 45ºC in the northern and eastern regions.

Following trends of the recent decades, future projections indicate a consistent warming trend in maximum temperatures across the country. This change is supported by strong model agreement, as shown in Figure 4, where low model agreement areas would be highlighted with grey dots. Extreme temperature events are expected to become more intense, with 25-year return period events increasing by 2050: by 1.7ºC under RCP4.5 and 2.0ºC under RCP8.5 in coastal areas, and by 1.8ºC to 2.5ºC in western regions. Inland areas will see a significant shift, with extreme temperatures that occurred every 25 years during the reference period projected to occur every 2 years by 2050 under the moderate emissions scenario.

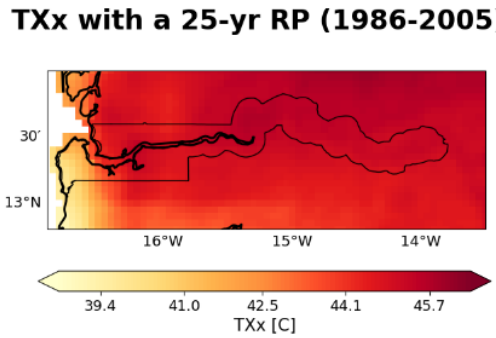

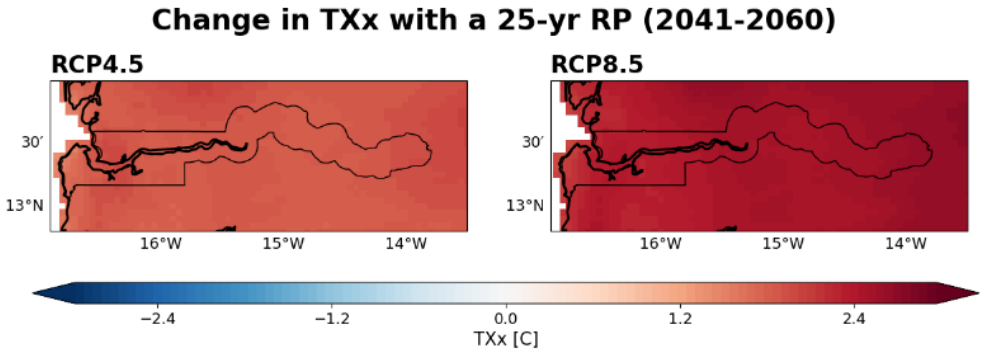

Figure 2-1. Change of projected extreme maximum temperature for a 25-year return period (in degrees Celsius). The left figure represents the reference period, the central figure corresponds to the change for the RCP4.5 climate scenario and the right figure for the RCP8.5. Lack of agreement between models on significative change is indicated with grey dots.

In the future, the number of days exceeding 35ºC is also projected to increase significantly by mid-century (Figure 5), rising from 36 to 50 days along the coast and from 215 to 279 days in the east under RCP4.5, and 70 days on the coast and 290 days in the east under RCP8.5. Under the RCP4.5 scenario, the coastal region is projected to experience an additional 8 days per year with temperatures exceeding 40ºC over a 25-year period, increasing to 13 days under RCP8.5. In the western region, the rise will be even more significant, with 45 additional days per year under RCP4.5 and 75 days under RCP8.5 (Table 2).

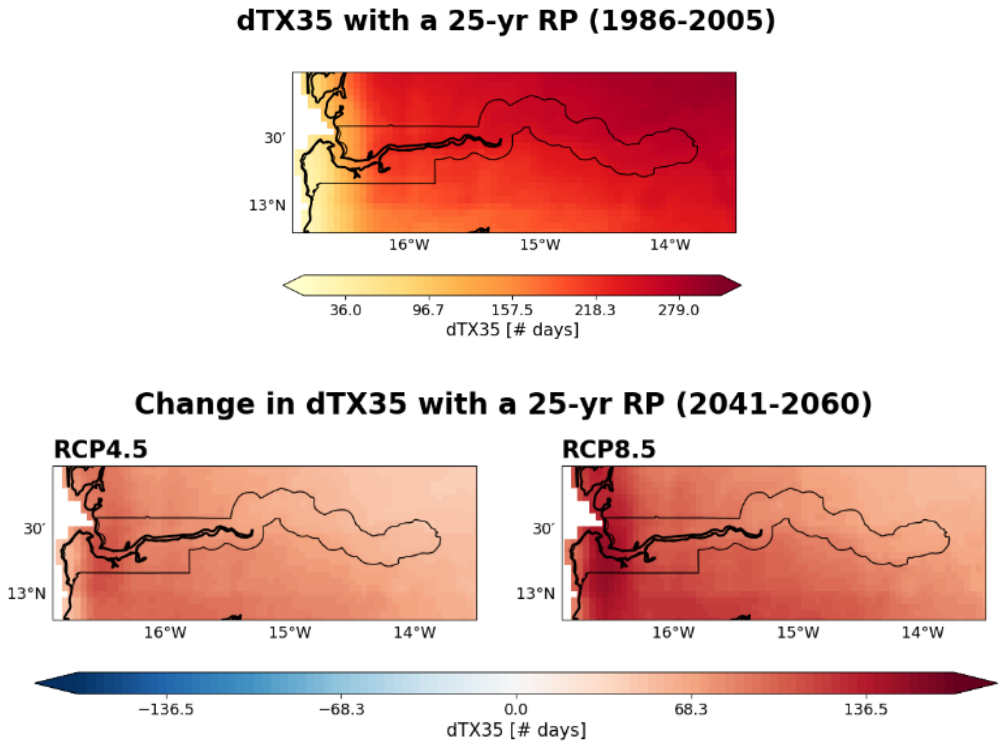

Figure 2-2. Change in the projected number of days exceeding 35ºC with a 25-year return period. The left figure represents the reference period, the central figure corresponds to the change for the RCP4.5 climate scenario and the right figure for the RCP8.5. Lack of agreement between models on significative change is indicated with grey dots.

Interestingly, while the coastal areas are expected to see a greater increase in the average number of days exceeding 35ºC per year by 2050, the northeastern region will experience the largest rise in the frequency of days exceeding 40ºC.

Table 1. Overall maximum of maximum daily temperature (Txx)

	Coastal area (50km from point west)			Inland area (50 km east)		
	Ref period	2050, RCP4.5	2050, RCP8.5	Ref period	2050, RCP4.5	2050, RCP8.5
RP 2 years	40	41.5	41.8	43.8	45.5	45.9
RP 25 years	42.8	44.5	44.8	45.2	47	47.7

Table 2. Number of days with maximum temperature above 40°C (dtx40)

	Coastal area (50km from point west)			Inland area (50 km east)		
	Ref period	2050, RCP4.5	2050, RCP8.5	Ref period	2050, RCP4.5	2050, RCP8.5
RP 2 years	1.6	5.1	7.4	59.7	99.7	114.1
RP 25 years	5.5	13.4	18.5	92.4	137.8	167.7

Table 3. Number of days with maximum temperature above 35°C (dtx35)

	Coastal area (50km from point west)			Inland area (50 km east)		
	Ref period	2050, RCP4.5	2050, RCP8.5	Ref period	2050, RCP4.5	2050, RCP8.5
RP 2 years	63	127.8	157	207	272.6	283.3
RP 25 years	99.1	185	226.5	267	317.5	331.3

2.2 Extreme precipitation

Extreme precipitation is an important issue in The Gambia. In 2022, major precipitation caused the worst flooding recorded in the country, affecting 13,000 households (Reuters[8]). For that event, Banjul International Airport registered 276mm rainfall in one day, surpassing the previous record of 175.4 mm in 1998. Regarding monthly maxima, the highest rainfall ever recorded was observed in August 1999 in Sapu, in the east of the country, with a total of 767 mm (Ceesay and Touray, Geographica Pannonica, 2022).

The analysis of accumulated annual precipitation reveals no significant trends during the reference period (Figure 6). Throughout this timeframe, average annual precipitation varied from approximately 870 mm in the East to around 1,000 mm in the western tip of the country.

By mid-century, under the RCP4.5 scenario, the northwestern region is projected to see a decrease in annual precipitation of 8–8.5%, with models showing no agreement on significant changes in other areas (grey dots in Figure 6). Likewise, under the RCP8.5 scenario, no notable changes in annual precipitation are expected across the entire country.

[8] Reuters

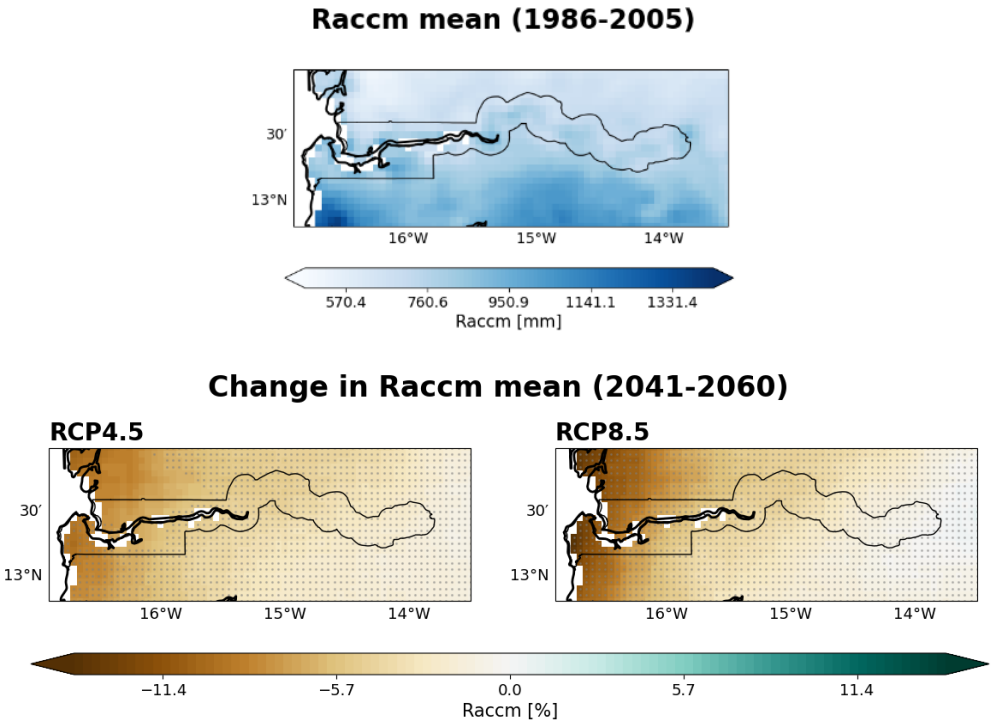

Figure 2-3. Change of projected Mean accumulated precipitation per year. The left figure represents the reference period, the central figure corresponds to the change for the RCP4.5 climate scenario and the right figure for the RCP8.5. Lack of agreement between models on significative change is indicated with grey dots.

To evaluate extreme precipitation in The Gambia, we looked at the maximum 1-day precipitation. During the reference period (1986–2005), the average maximum daily precipitation pattern revealed higher values predominantly in the western region, with extreme daily precipitation averaging around 100mm in Banjul and in the eastern extreme point of the country. In contrast, the central and eastern regions experienced more moderate extremes, averaging approximately 70 mm/day. By 2050, under RCP4.5, extreme daily precipitation is expected to increase by 3% in the west and up to 20% in the east of the country. The eastern region is projected to experience the most significant changes, with extreme one-day precipitation anticipated to rise on average 30% by the end of the century.

For extreme events, a 25-years return period events are also expected to increase significantly, with maximum daily precipitation rises of 17% in the west and 34% in the east under RCP4.5, and 17% in the west and 45% in the east under RCP8.5 (Figure 7). By mid-century, the highest daily precipitation levels are projected to reach 130 mm/day in the eastern tip of the country under both scenarios, while in Banjul, extreme one-day precipitation is forecasted to reach 110 mm/day for both emission scenarios.

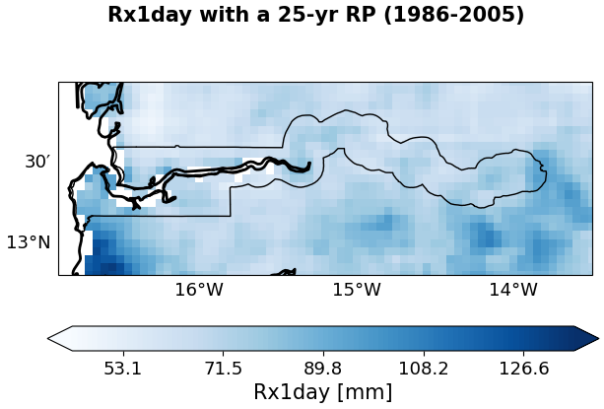

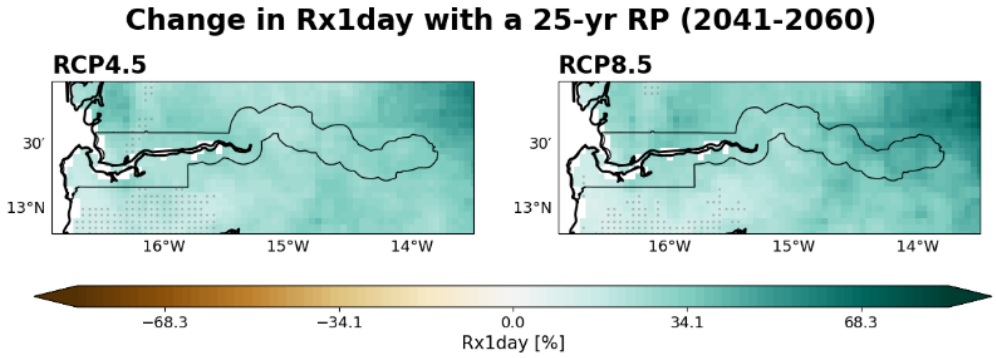

Figure 2-4. Change of projected Maximum total precipitation of consecutive 1-day precipitation for a 25-year return period. The left figure represents the reference period, the central figure corresponds to the change for the RCP4.5 climate scenario and the right figure for the RCP8.5. Lack of agreement between models on significative change is indicated with grey dots.

In addition to assessing the maximum daily precipitation, we also considered what is the total number of days with high precipitation (Figure 8). During the reference period (1986–2005), the number of wet days with precipitation exceeding the 90th percentile of the historical record exhibited a latitudinal gradient, ranging from 12 days in the north to 15 days in the south of the country. In the future, model projections indicate no significant changes in the frequency of days with extreme precipitation. It is important to highlight that model disagreement increases over time for both scenarios, making projections for this indicator highly uncertain.

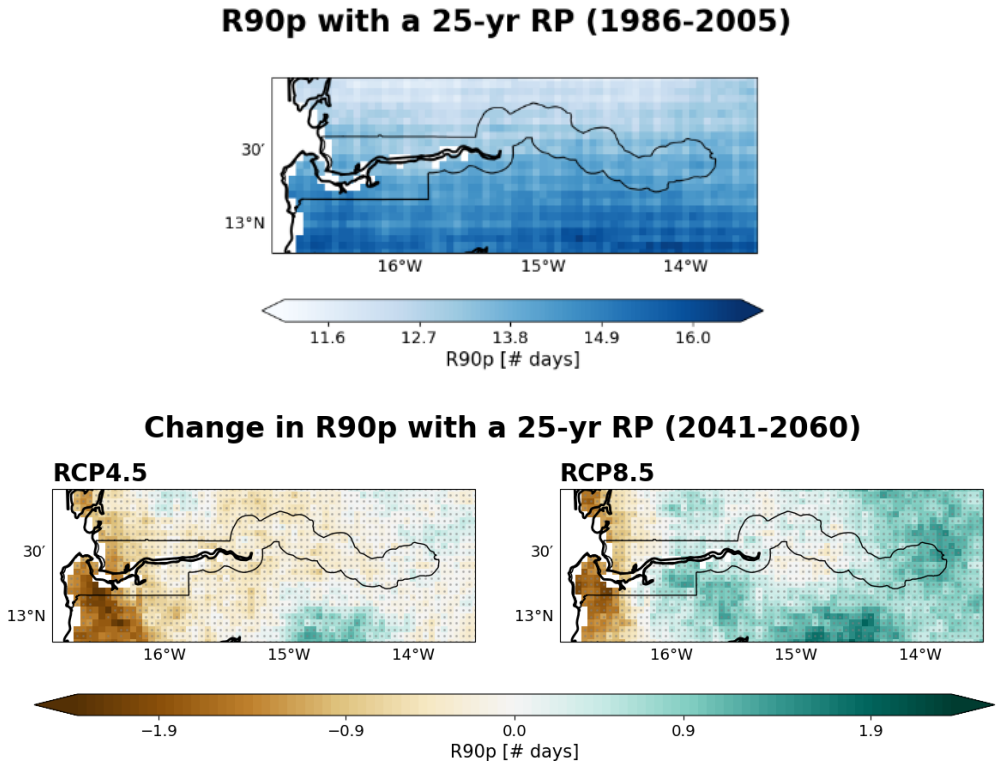

Figure 2-5. Change in number of days with precipitation above the 90th percentile of daily precipitation for a 25-year return period. The left figure represents the reference period, the central figure corresponds to the change for the RCP4.5 climate scenario and the right figure for the RCP8.5. Lack of agreement between models on significative change is indicated with grey dots.

The change in the number of days with precipitation above the 90th percentile is provided also on the table below, differentiating between coastal region and inland. As it can be observed, changes in the number of wet days will not change significantly, as there is between 1 and 2 days difference compared to the historical period, and with high model uncertainty.

Table 4. Number of wet days when precipitation is above the 90th percentile of the historical

	Coastal area (50km from point west)			Inland area (50 km east)		
	Ref period	2050, RCP4.5	2050, RCP8.5	Ref period	2050, RCP4.5	2050, RCP8.5
RP 25 years	14	12	12	14	13	14

2.3 Extreme wind

During the reference period, the highest daily wind gusts were concentrated along the coast, with average gusts of 14.5 m/s, and 25-year return period events reaching up to 17.5 m/s (Figure 9).

Future projections suggest that the average maximum wind gusts will remain largely unchanged across most of the country. Notable changes are observed in the central regions under RCP8.5 by 2050 and under both scenarios by 2070, with increases of up to 2.5 m/s. For 25-year return period events, wind gusts are projected to peak mid-century, with increases of up to 10% under RCP4.5 by 2050 in the central regions between the cities of Bassori and Mansa Konko (Figure 9). After 2050, wind gusts are expected to decrease under RCP4.5, returning to values similar to the reference period under both emissions scenarios.

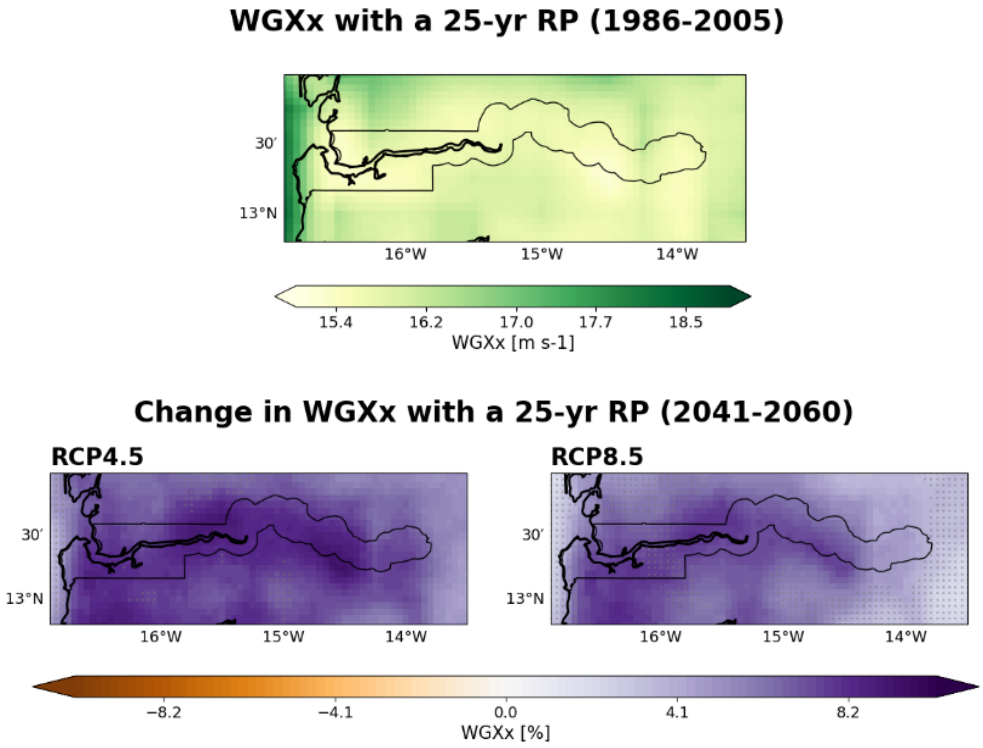

Figure 2-6. Change of projected Maximum daily surface wind gust for a 25-year return period. The left figure represents the reference period, the central figure corresponds to the change for the RCP4.5 climate scenario and the right figure for the RCP8.5. Lack of agreement between models on significative change is indicated with grey dots.

The frequency of days with wind gusts exceeding the 90th percentile is projected to rise in the future, increasing from 36 days during the reference period to an average of 57 by 2050 days under RCP4.5, and 60 days under RCP8.5. Years with extreme wind gust events for a 25-year return period are expected to see up to 90 days of such occurrences (95 days under RCP8.5), see Figure 10.

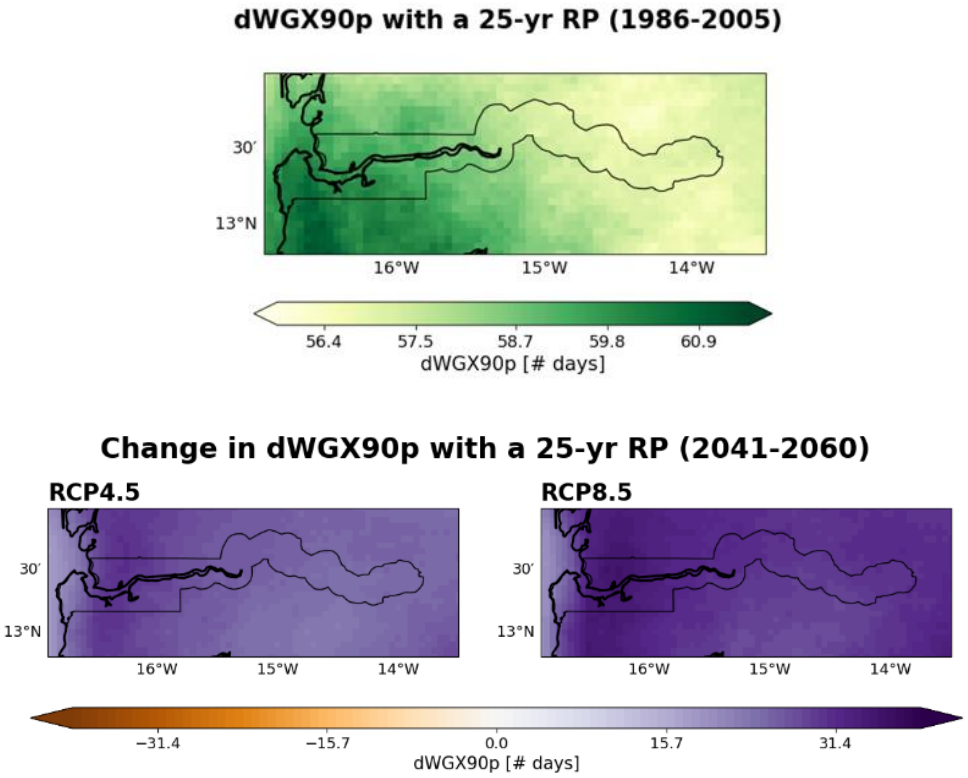

Figure 2-7. Change of projected number of days with above 90th percentile surface wind gusts for a 25-year return period. The left figure represents the reference period, the central figure corresponds to the change for the RCP4.5 climate scenario and the right figure for the RCP8.5. Lack of agreement between models on significative change is indicated with grey dots.

The table below provides more detail on the current and projected number of days above the 90th percentile of surface wind gusts for events with a return period of 25-years, considering coastal versus inland regions.

Table 5. Number of days with daily maximum surface wind gust above 90th percentile [# days]

	Coastal area (50km from point west)			Inland area (50 km east)		
	Ref period	2050, RCP4.5	2050, RCP8.5	Ref period	2050, RCP4.5	2050, RCP8.5
RP 25 years	60.37	81.66	81.20	57.54	80.40	84.82

2.4 Drought

During the reference period (1986-2005), drought has been an important hazard: water scarcity risk in The Gambia is classified as high[9] by the "ThinkHazard" platform developed by the Global Facility for Disaster Reduction and Recovery (GFDRR). In recent decades the region has seen already some trends in accumulated annual precipitation, with a slight decrease in the centre of the country and a small increase east and at the coast, which are not statistically significant.

For this project, drought is evaluated based on the Standardised Potential Evapotranspiration Index, which is a widely used indicator that is designed to take into account both the influence of precipitation and potential evapotranspiration (PET) in determining drought. This indicator captures the main impact of increased temperatures on water demand. Positive SPEI values are given to normal to wet climates, with higher values representing wetter conditions, and negative values given to dry conditions, with the lower

[9] https://thinkhazard.org/en/report/90-the-gambia/DG

values representing dryer conditions. Dryer conditions are expected to affect water availability both for communities and for crops.

Considering a frequent drought risk scenario (2-yr RP) The Gambia can fall under Normal to Moderately dry conditions. For very extreme events, under a 100-yr RP scenario, the country can reach Extremely dry conditions.

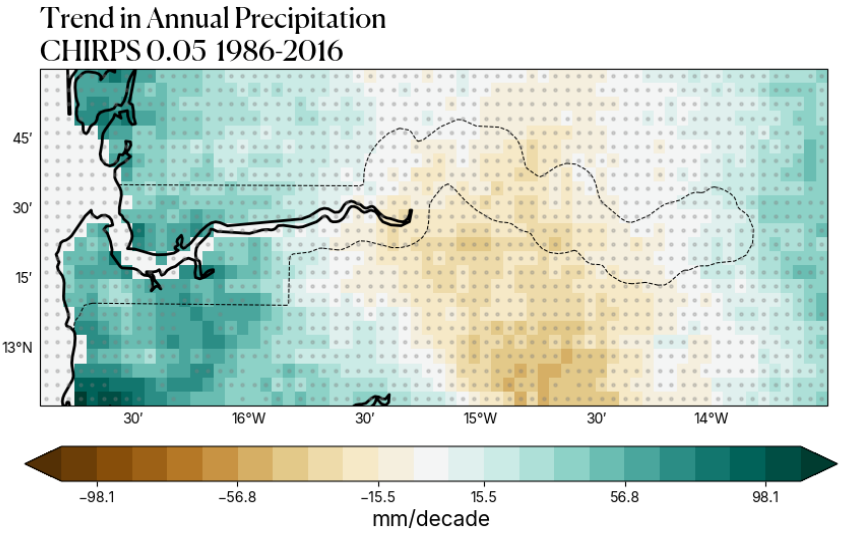

Figure 2-8. *Accumulated annual precipitation trend in the historical period.*

Drought risk is expected to increase consistently over time with differences in the spatial distribution across the country, with a gradient going North (higher negative change) to South (lower negative change). By 2050, biennial droughts across the country are projected to increase in intensity, with a decrease by 0.4 to 0.8 on the SPEI scale, see Figure 13, making the country more likely to go through Moderately dry conditions.

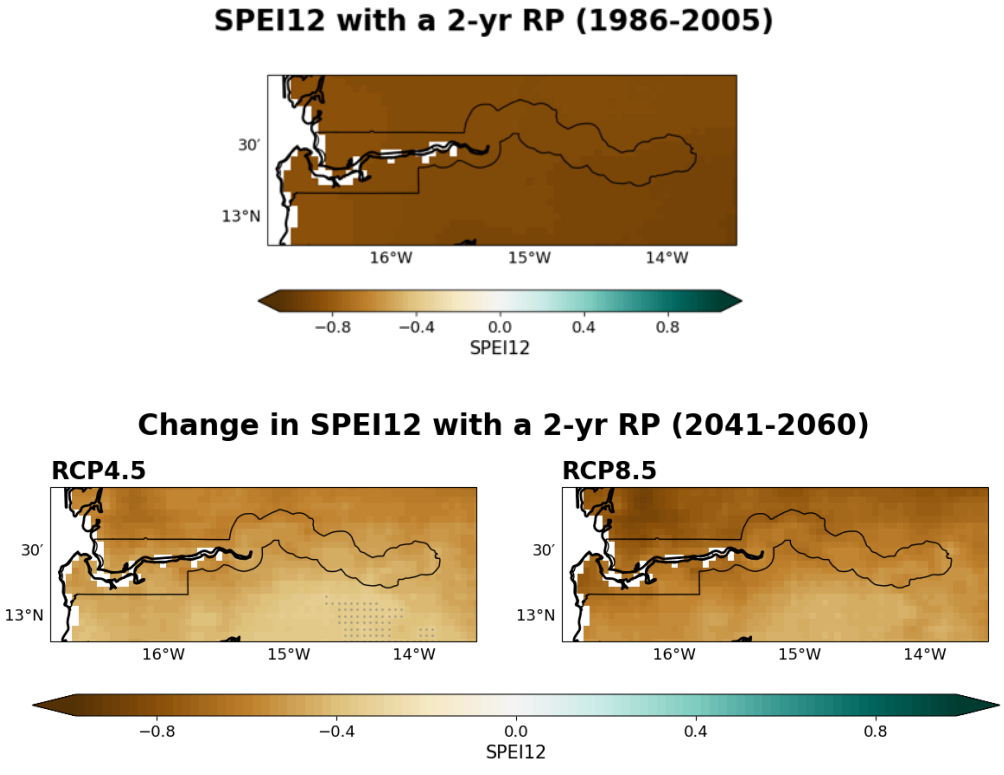

Figure 2-9. Left: Drought conditions represented by the SPEI-12 indicator for a 2-yr RP, considering the historical period (1986-2005). Middle and right figure: Drought conditions represented by the SPEI-12 indicator in the region of interest for a 2-yr RP in 2050 for RCP4.5 (left) and RCP8.5 (right).

By the end of the century the increase trend in drought conditions will lead to most of the country reaching to levels of Severely dry conditions (SPEI < -1.5) under RCP4.5 and reaching in some areas Extremely dry conditions (SPEI < -2) such as the Banjul area (Figure 14). More extreme conditions (100-yr RP), already under the Extremely dry category, will also increase further as temperatures rise during the 21st century. As shown in Figure 14 for the high emissions scenario (RCP8.5), the western region (Koina) is expected to have reach more extreme drought conditions as near the coast (Banjul), with SPEI values reaching beyond -2 values by the end of the century.

Table 6. Standardized Precipitation Evapotranspiration Index 12 [-]

	Coastal area (50km from point west)			Inland area (50 km east)		
	Ref period	2050, RCP4.5	2050, RCP8.5	Ref period	2050, RCP4.5	2050, RCP8.5
RP 2 years	-0.86	-1.44	-1.38	-0.92	-1.36	-1.34

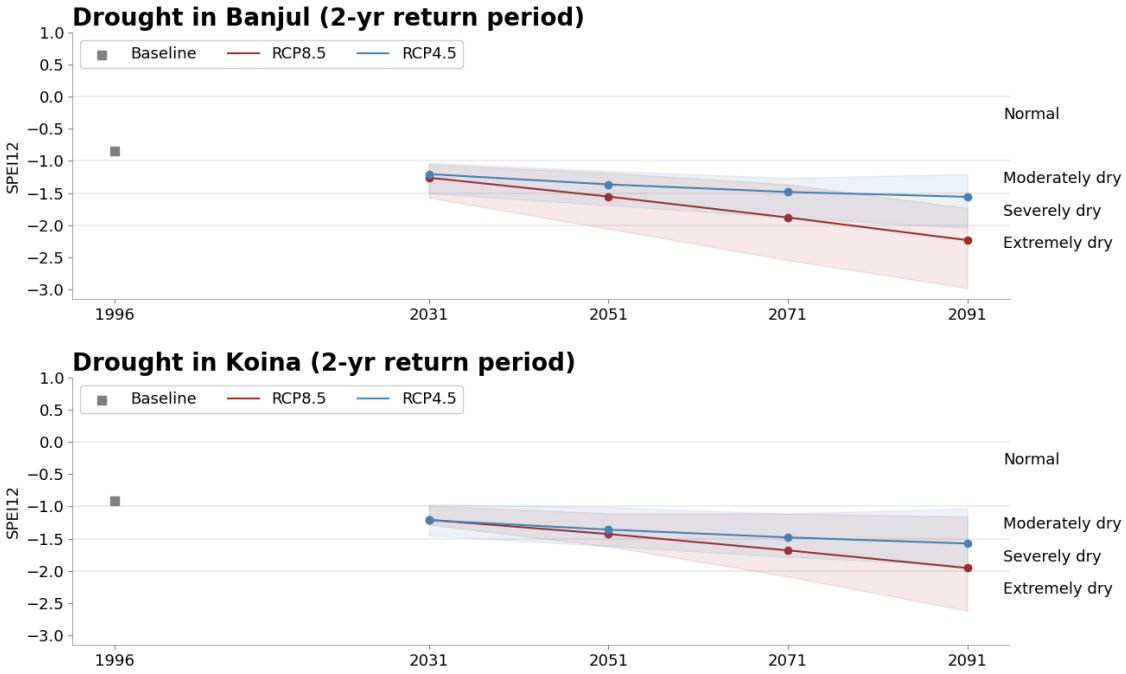

Figure 2-10. Drought conditions represented by the SPEI-12 indicator and its evolution over time at Banjul (top) and Koina (bottom), representing west and east of the country, respectively. Negative SPEI values indicate drought conditions, those being severely dry below -1.5, and extremely dry when they go below -2.

2.5 Wildfires

To effectively understand and mitigate the risks associated with wildfires, scientists and policymakers rely on indicators that combine various climatic factors contributing to fire behaviour. One such crucial metric is the Fire Weather Index (FWI).[10], specifically focusing on the 90th percentile (FWI90p). This percentile is paramount in evaluating fire risk due to its unique ability to capture extreme fire weather conditions. Unlike average values, the FWI90p emphasises the most extreme circumstances, allowing for a comprehensive assessment of the conditions that lead to severe wildfires. A complementary indicator

[10] https://www.nwcg.gov/publications/pms437/cffdrs/fire-weather-index-system

to FWI90p, the number of days exceeding the 90th percentile of historical values (dFWI90p), is also analyzed. This metric identifies the frequency of extreme fire-prone days and provides a comparative framework for assessing how these conditions may evolve under future climate scenarios.

The FWI takes into consideration the different climatic drivers that can trigger the ignition and spread of fires, such as temperature, relative humidity, wind, and precipitation. It is worth noting that this type of index evaluates the meteorological conditions that enhance wildfires. It does not consider the presence of vegetation or materials that could fuel and sustain the fire. Table 4 provides the wildfire risk classifications associated with FWI values, where higher values represent increased risk.

Table 7. Wildfire risk based on the Fire Weather Index scale..11

Risk Level	FWI range
Very Low Danger	< 5.2
Low Danger	Between 5.2 and 11.2
Moderate Danger	Between 11.2 and 21.3
High Danger	Between 21.3 and 38.0
Very High Danger	Between 38.0 and 50.0
Extreme Danger	> 50

Forests and woodlands cover approximately 47% (approximately 423,000 hectares) of The Gambia's total land area. However, according to the Government of The Gambia (GoTG, 2023), over 70% of these forests face some form of degradation, with more than 50% burned annually. Fire incident data from 2012–2022 indicates that bushfires are becoming more frequent, with the highest incidence occurring between January and April (CIFOR-ICRAF).[12]. The underlying cause is due to a combination of human and climate causes. From one side, bushfires are aggravated by human activities such as fuelwood and charcoal production. However, the occurrence of wildfire is more common during dry and hot seasons.

In the baseline period (1986 - 2005), mean FWI values in the 90th percentile ranged between 54 and 71 across the Gambia (Figure 15). Historic FWI levels are classified as extreme exposure risk for wildfires, with locations northeast of The Gambia (e.g. Basse Santa Su) reaching values that breach very extreme risk (Table 4).

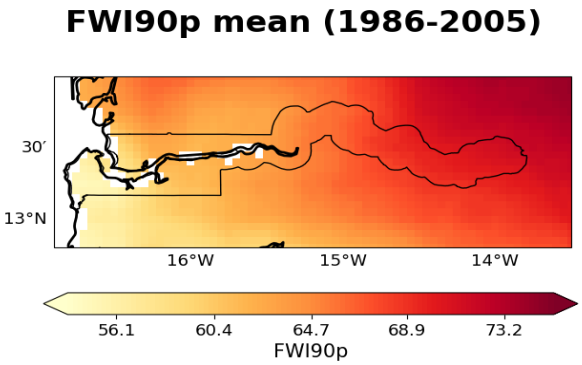

Figure 2-11. 90th percentile of FWI values under mean conditions in the baseline period (1986-2005). Values fall between 54 - 71 and are higher in eastern Gambia.

Future FWI projections under mean conditions show a gradual westward expansion of very extreme risk zones under both RCP 4.5 and RCP 8.5 scenarios (Figure 16). By the mid-21st century, FWI is expected to increase uniformly by 2-3% across The Gambia, with a slightly greater increase under RCP 8.5. This

11 FWI risk level

12 "Reducing forest degradation by managing bushfires in The Gambia." The Center for International Forestry Research and World Agroforestry (CIFOR-ICRAF), https://www.cifor-icraf.org/publications/pdf/briefs/PB24001.pdf.

change is not substantial enough to alter the extreme risk classification for the westernmost regions; however by 2050 as far west as just outside of Janjanbureh will experience very extreme risk. While changes are more apparent under RCP 8.5, deviations from historical FWI levels remain below 5% across all scenarios and time horizons.

An increasing trend in the number of days per year when FWI surpasses the historical 90th percentile (dFWI90p) is projected across The Gambia, indicating a rise in the frequency of high-risk days. Spatial patterns of dFWI90p differ slightly from FWI90p, with the northern regions experiencing the highest number of extreme days (Figure 16), and the southernmost regions the least. By the mid-21st century (2040–2060), dFWI90p is projected to increase by 30-39 days, resulting in 62-72 high-risk days annually. These results indicate The Gambia is expected to experience more frequent high-risk days, with the greatest frequency in the north and east.

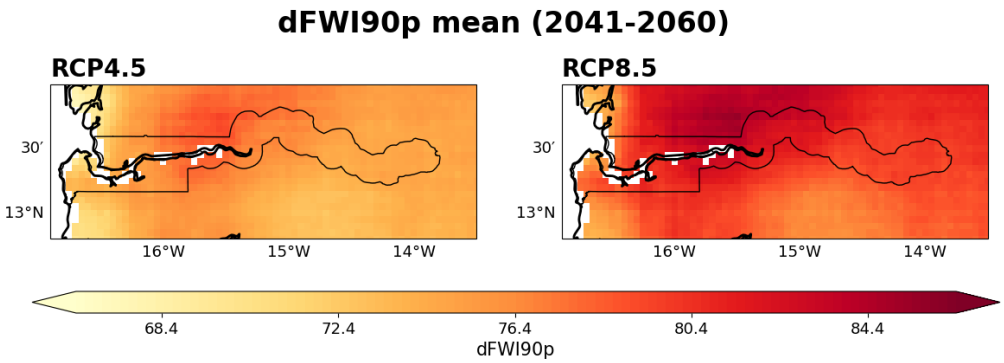

Figure 2-12. Values under mean conditions for number of days above the 90th percentile of the historic period in the mid century future period 2040-2060. Figure shows higher values in the north of The Gambia, and for RCP 8.5 (right).

The following table provides average values across coastal and inland areas for the historical period and future climate change conditions for 2050.

Table 8. Number of days with FWI above the percentile 90th of the historical

	Coastal area (50km from point west)			Inland area (50 km east)		
	Ref period	2050, RCP4.5	2050, RCP8.5	Ref period	2050, RCP4.5	2050, RCP8.5
RP 2 years	33	64	64	33	69	69
RP 25 years	83	137	140	80	128	135

2.6 Flooding

2.6.1 Coastal Flooding

Assessing the maximum ocean water levels for the coastal flood assessment resulted in the values as presented in Table 2-9, where we see a constant storm surge level per return period, an astronomical tide level of 0.83m, and Sea Level Rise projections for both SSP2-4.5 and SSP5-8.5.

Table 2-9: Combined water levels for different return periods and climate scenarios.

Flood Return Period	Time Horizon	Astronomical tide (m)	Sea Level Rise (m) SSP2-4.5	SSP5-8.5	Storm Surge (m)	Max Water Elevation (m) SSP2-4.5	SSP5-8.5
2	*Baseline*	*0.83*	-	-	*0.13*	0.96	0.96
	2030	*0.83*	*0.10*	*0.11*	*0.13*	1.06	1.07
	2050	*0.83*	*0.22*	*0.25*	*0.13*	1.18	1.21
	2070	*0.83*	*0.36*	*0.42*	*0.13*	1.32	1.38

Flood Return Period	Time Horizon	Astronomical tide (m)	Sea Level Rise (m) SSP2-4.5	SSP5-8.5	Storm Surge (m)	Max Water Elevation (m) SSP2-4.5	SSP5-8.5
5	*Baseline*	*0.83*	-	-	*0.14*	0.97	0.97
	2030	*0.83*	*0.10*	*0.11*	*0.14*	1.07	1.08
	2050	*0.83*	*0.22*	*0.25*	*0.14*	1.19	1.22
	2070	*0.83*	*0.36*	*0.42*	*0.14*	1.33	1.39
10	*Baseline*	*0.83*	-	-	*0.17*	1	1
	2030	*0.83*	*0.10*	*0.11*	*0.17*	1.1	1.11
	2050	*0.83*	*0.22*	*0.25*	*0.17*	1.22	1.25
	2070	*0.83*	*0.36*	*0.42*	*0.17*	1.36	1.42
20	*Baseline*	*0.83*	-	-	*0.19*	1.02	1.02
	2030	*0.83*	*0.10*	*0.11*	*0.19*	1.12	1.13
	2050	*0.83*	*0.22*	*0.25*	*0.19*	1.24	1.27
	2070	*0.83*	*0.36*	*0.42*	*0.19*	1.38	1.44
50	*Baseline*	*0.83*	-	-	*0.21*	1.04	1.04
	2030	*0.83*	*0.10*	*0.11*	*0.21*	1.14	1.15
	2050	*0.83*	*0.22*	*0.25*	*0.21*	1.26	1.29
	2070	*0.83*	*0.36*	*0.42*	*0.21*	1.4	1.46
100	*Baseline*	*0.83*	-	-	*0.23*	1.06	1.06
	2030	*0.83*	*0.10*	*0.11*	*0.23*	1.16	1.17
	2050	*0.83*	*0.22*	*0.25*	*0.23*	1.28	1.31
	2070	*0.83*	*0.36*	*0.42*	*0.23*	1.42	1.48

An increase in maximum water levels is visible, which is to be expected considering increasing temperatures. The compound occurrence of these water levels might result in significant flood events.

To quantify changes in flood patterns, difference maps were generated comparing future simulation against the baseline simulation. These difference maps were calculated by subtracting the baseline simulation pluvial flood depths from the future simulation flood depths for each model grid cell. The results were then averaged to show mean differences in flood depths per Local Government Area (LGA), the mean being calculated of only those areas that are flood-prone in either of the two simulations analyzed. Areas displaying darker colors in the difference maps indicate regions where mean pluvial flood depths are predicted to increase most significantly, helping identify potential hotspots for increased flood risk.

Analysis of baseline conditions reveals significant coastal inundation, particularly around Banjul and its surrounding areas. For the 10-year return period event (Figure 2-13), substantial flooding occurs in coastal regions, with notable impacts observed both east and west of Banjul in the estuarine area of the Gambia River. The extensive low-lying mangrove area west of Banjul (Tanbi Wetland) experiences significant inundation, though these natural systems play a crucial role in flood attenuation for inland areas.

The difference maps reveal significant changes in coastal flooding patterns under the SSP5-8.5 climate scenario for 2050. For 10-year return period events (Figure 2-13), the analysis shows:

The Banjul region emerges as the most significantly impacted area. The mangrove regions west of Banjul show substantial increases in inundation depths, though they continue to provide critical flood protection services. Other coastal LGAs show more modest increases, indicating that severe impacts may be concentrated in specific vulnerable locations.

The 100-year return period event under current conditions (Figure 2-14) demonstrates more severe flooding. The inundation extent expands considerably compared to the 10-year event, affecting larger portions of the coastal zone and extending further inland in low-lying areas. This increased extent highlights the vulnerability of coastal regions to extreme events even under current conditions.

For 100-year return period events (Figure 2-14), the changes become more pronounced across all coastal regions. Both Banjul and Brikama LGAs show substantial increases in flood depths. This amplification of extreme event impacts suggests that coastal areas may face significantly greater flood risks under future climate conditions, necessitating robust adaptation strategies.

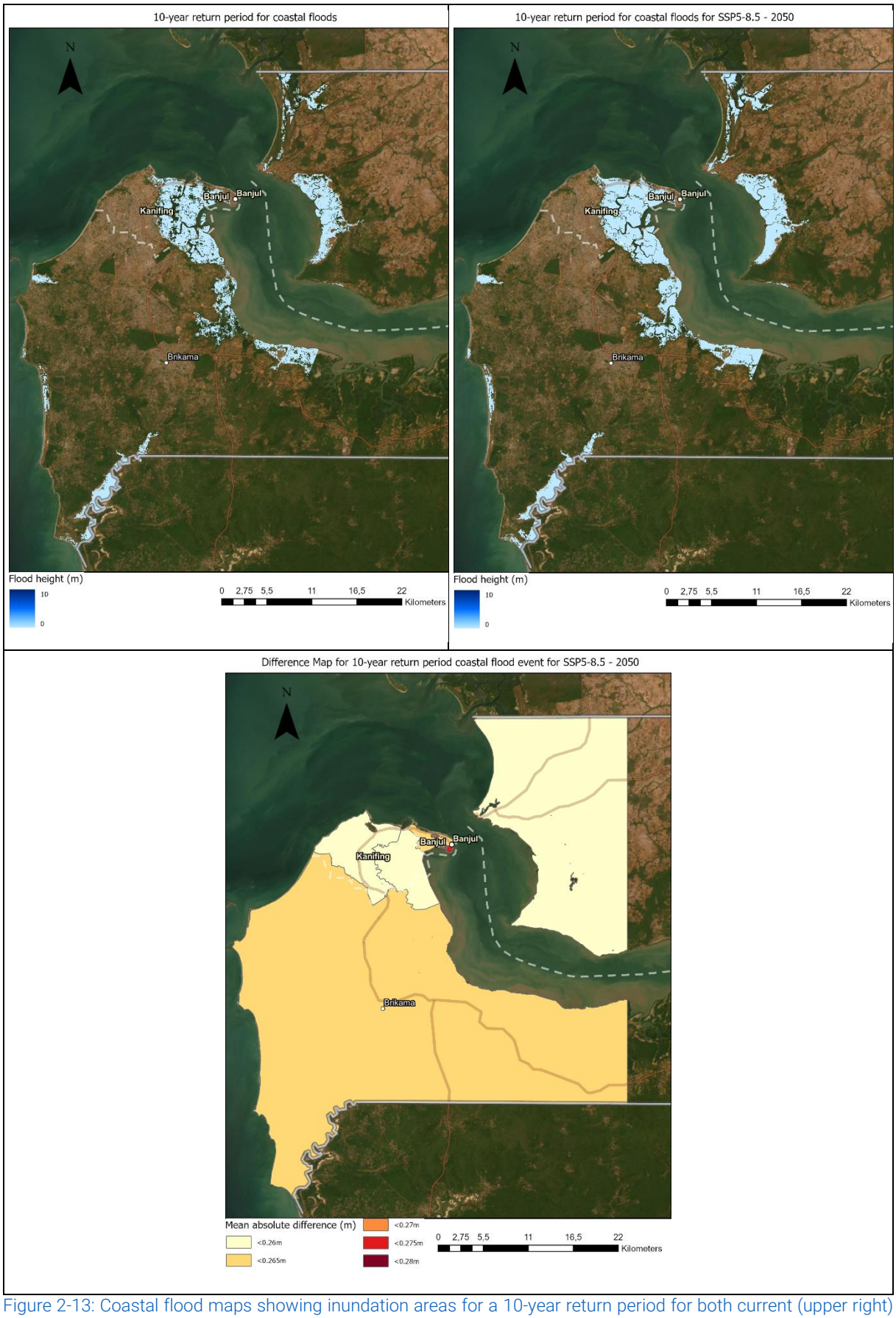

Figure 2-13: Coastal flood maps showing inundation areas for a 10-year return period for both current (upper right) and SSP5-8.5 – 2050 (upper left) simulations. Additionally, a difference map (lower) shows the mean absolute increase in flood height (m) per LGA.

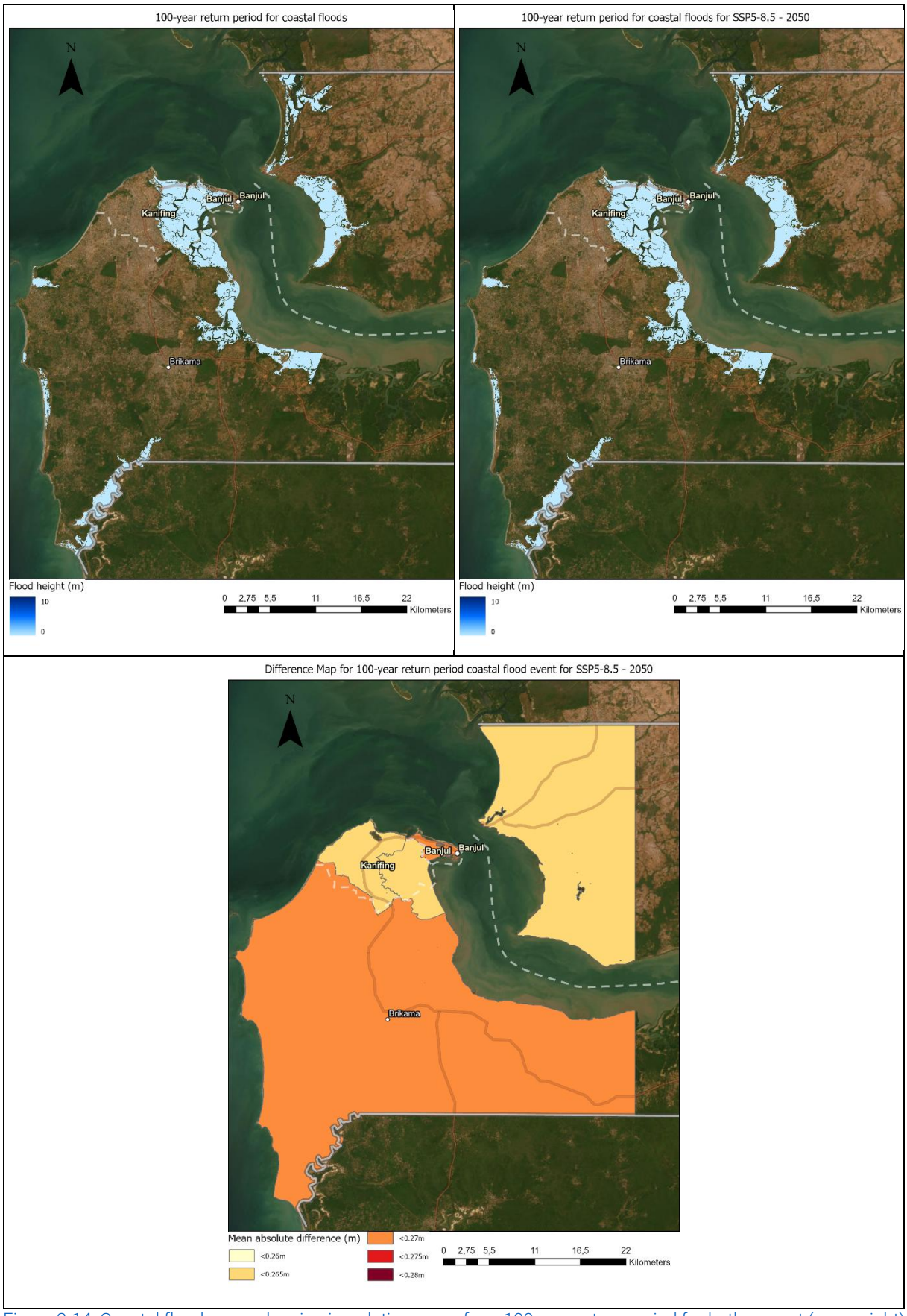

Figure 2-14: Coastal flood maps showing inundation areas for a 100-year return period for both current (upper right) and SSP5-8.5 – 2050 (upper left) simulations. Additionally, a difference map (lower) shows the absolute increase in flood height (m) per LGA.

2.6.2 Pluvial Flooding

Extreme precipitation is an important issue in The Gambia. In 2022, major precipitation caused the worst flooding recorded in the country, affecting 13,000 households (Reuters.[13]). For that event, Banjul International Airport registered 276mm rainfall in one day, surpassing the previous record of 175.4 mm in 1998. Regarding monthly maxima, the highest rainfall ever recorded was observed in August 1999 in Sapu, in the east of the country, with a total of 767 mm (Ceesay and Touray, Geographica Pannonica, 2022).

Figure 2-13 shows the flood maps for the 10-year return period event under current conditions. All regions of The Gambia are affected by pluvial flood events, although seemingly marginally more severe in the eastern regions of the country.

To quantify changes in flood patterns, difference maps were generated comparing future simulation against the baseline simulation. These difference maps were calculated by subtracting the baseline simulation pluvial flood depths from the future simulation flood depths for each model grid cell. The results were then averaged to show mean differences in flood depths per Local Government Area (LGA), the mean being calculated of only those areas that are flood-prone in either of the two simulations analyzed. Areas displaying darker colors in the difference maps indicate regions where mean pluvial flood depths are predicted to increase most significantly, helping identify potential hotspots for increased flood risk.

The difference maps reveal significant changes in pluvial flooding patterns under the SSP5-8.5 climate scenario for 2050. For 10-year return period events, the analysis shows a clear east-west gradient in flood exposure. The eastern regions, particularly Basse, demonstrate the most substantial increases in flood depths. Noticeable is the increase in flood depths in the Kanifing area, and more specifically around Kotu Stream, showing significant localized increases despite its western location, indicating that local topography and urban development play important roles in future flood hazard.

The 100-year return period event under current conditions, as presented in Figure 2-14, shows more severe flooding. The flood extent increases considerably compared to the 10-year event, with deeper flood depths and more extensive inundation areas across all LGAs.

For 100-year return period events the changes become more pronounced across all regions. The east-west gradient becomes more evident. This spatial pattern of change suggests that extreme rainfall events may have particularly severe impacts in eastern regions, while more western areas, though still experiencing increases show relatively lower changes in flood depths. An exception here is the Kanifing area where Kotu Stream plays an essential role in the urban drainage system and simultaneously a significant increase in flood depths is expected.

[13] https://www.reuters.com/world/africa/floods-affect-thousands-gambia-after-heaviest-rainfall-decades-2022-08-03/#:~:text=The%20Gambia%20recorded%20its%20heaviest%20rainfall%20in%20more,Wednesday%2C%20blaming%20climate%20change%20for%20the%20extreme%20weather.

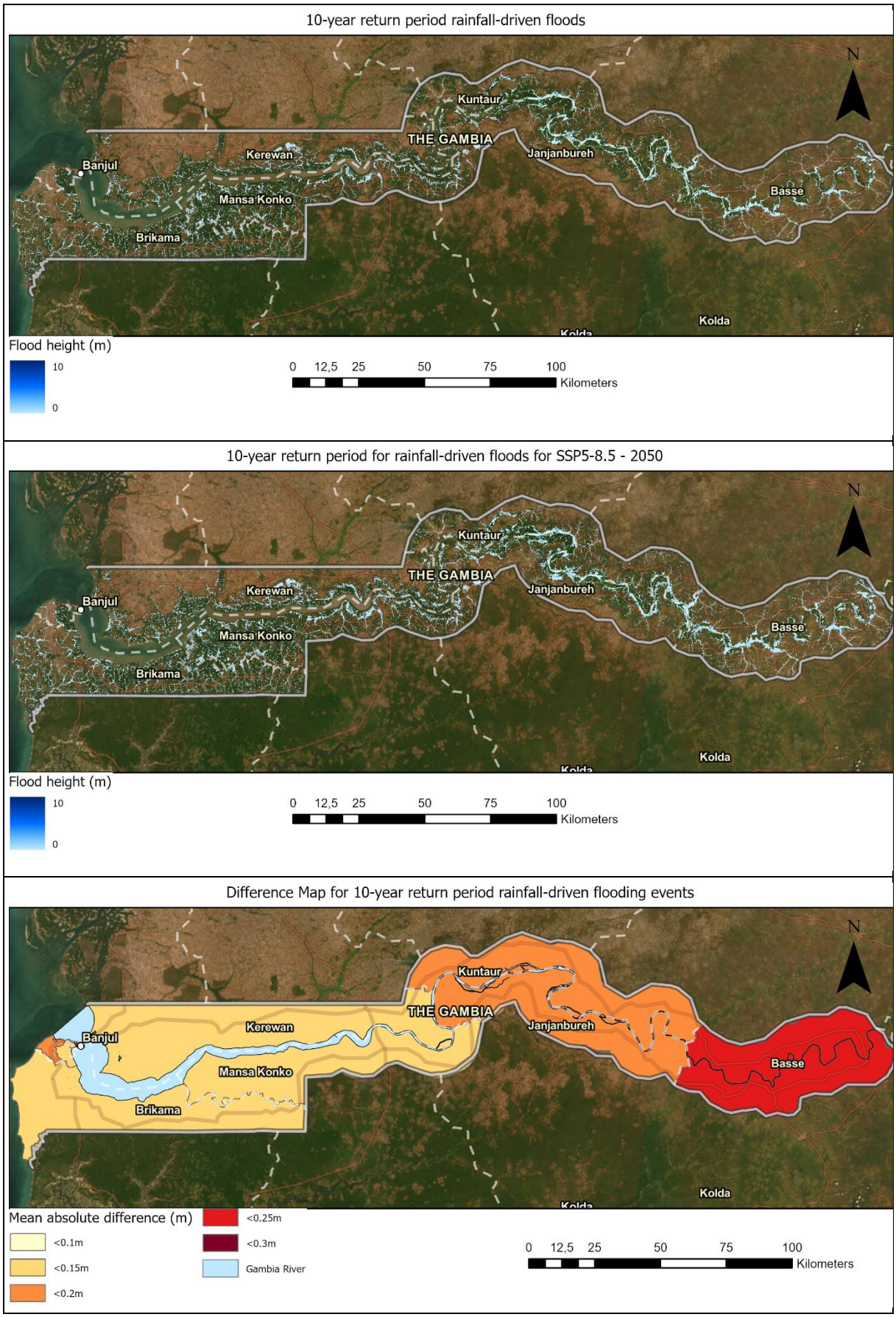

Figure 2-15: Pluvial flood maps showing inundation areas for a 10-year return period for both current (upper) and SSP5-8.5 – 2050 (middle) simulations. Additionally, a difference map (lower) shows the absolute increase in flood height (m) per LGA.

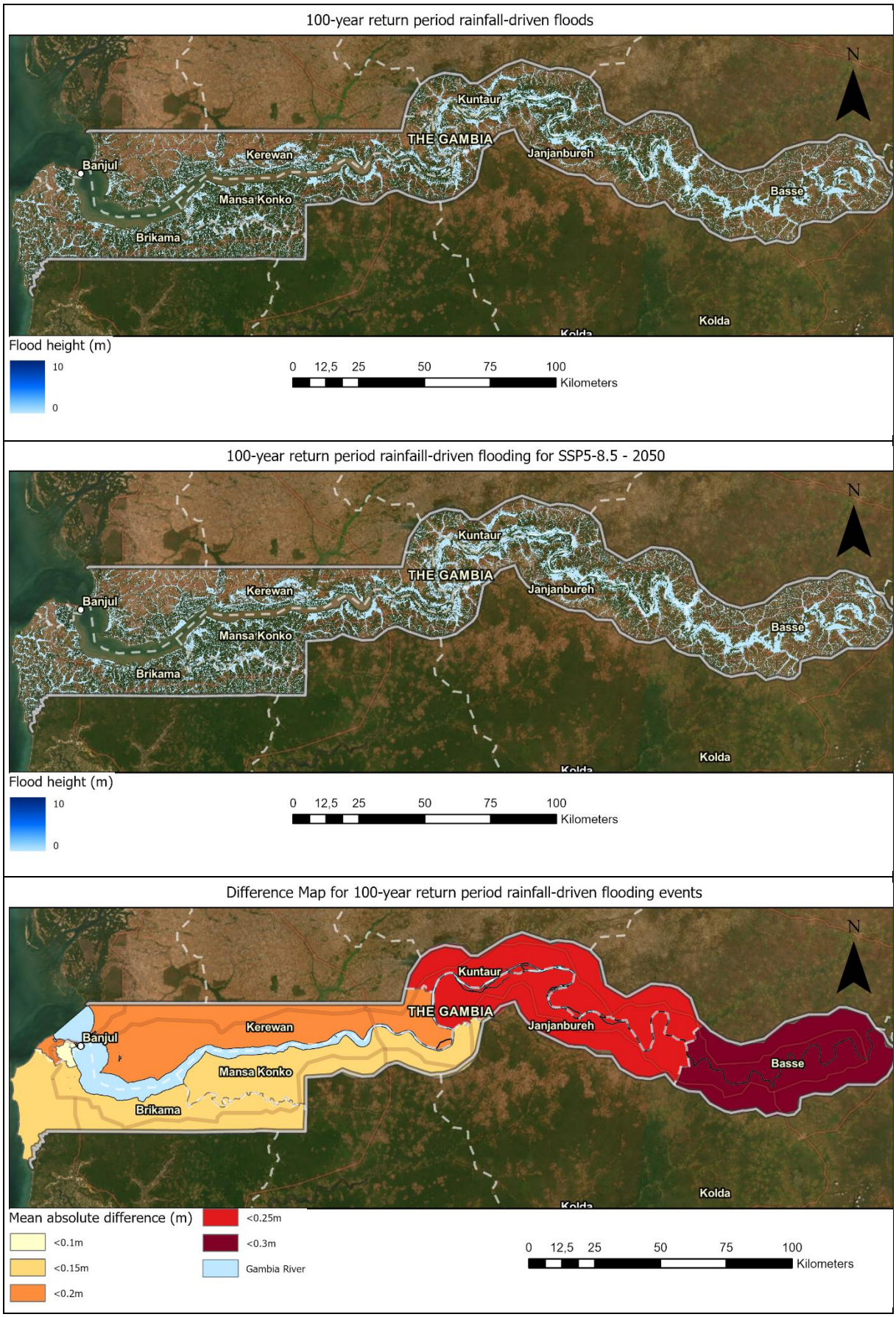

Figure 2-16: Pluvial flood maps showing inundation areas for a 100-year return period for both current (upper) and SSP5-8.5 – 2050 (middle) simulations. Additionally, a difference map (lower) shows the absolute increase in flood height (m) per LGA

2.6.3 Fluvial Flooding

For fluvial flooding, prolonged periods of rainfall are more important than the 1-day extremes that are relevant for pluvial flooding.

The assessment of the 7-day duration precipitation showed similar results as the 1-day duration precipitation, which is decreasing on the long-term. Which itself is consistent with the findings of increasing drought hazard as described in the drought section earlier in this Report.

Analysis of the baseline simulation reveals significant flooding along the Gambia River and its tributaries. Figure 2-15 shows the flood maps for the 10-year return period event under current conditions. Substantial flooding occurs along the main river channel. With especially extensive flooding observed in the flood plains in the region near the Senegambia Bridge.

To quantify changes in flood patterns, difference maps were generated comparing future simulation against the baseline simulation. These difference maps were calculated by subtracting the baseline simulation pluvial flood depths from the future simulation flood depths for each model grid cell. The results were then averaged to show mean differences in flood depths per Local Government Area (LGA), the mean being calculated of only those areas that are flood-prone in either of the two simulations analyzed. Areas displaying darker colors in the difference maps indicate regions where mean pluvial flood depths are predicted to increase most significantly, helping identify potential hotspots for increased flood risk.

The difference maps reveal significant changes in fluvial flooding patterns under the SSP5-8.5 climate scenario for 2050. For 10-year return period events, the analysis shows interesting spatial variations in flood impact. Again, as for pluvial flooding, the Kanifing area exhibits a more significant increase in flood depths than the surrounding LGAs. And also as with pluvial flooding, an east-west gradient of flood depth increases is found, with the most significant increases in the Basse region.

The 100-year return period event under current conditions, as presented in Figure 2-16, shows more severe flooding patterns. The flood extent increases considerably compared to the 10-year event, with deeper flood depths and more extensive inundation zones affecting low-lying areas adjacent to the river system.

For 100-year return period events, the changes become more pronounced with distinct spatial patterns. The middle river regions, particularly Mansa Konko, Kuntaur, and Janjanbureh LGAs, show the largest increases in flood depths. This spatial pattern presents an interesting deviation from the other pluvial and fluvial flooding trends noted above in this assessment.

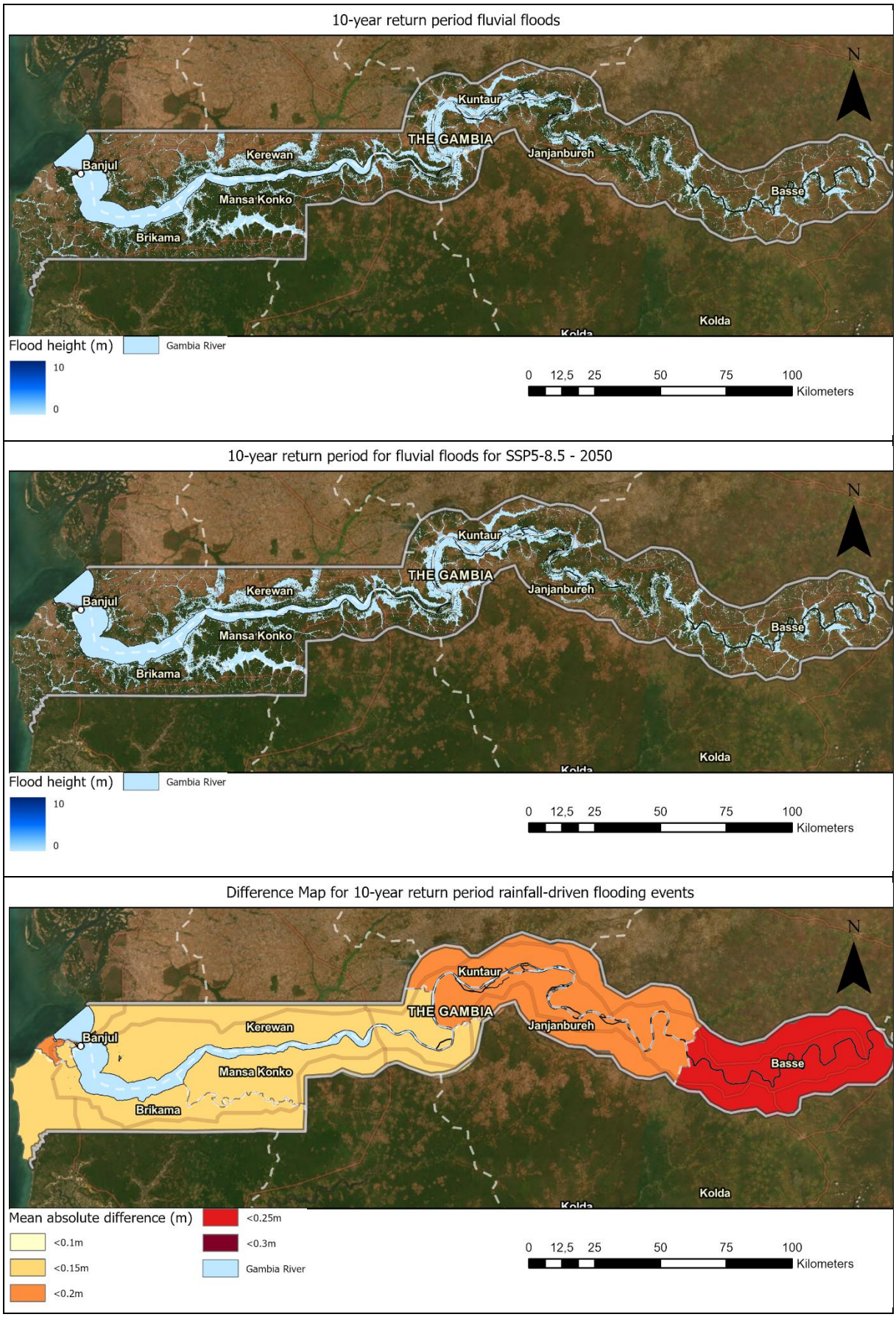

Figure 2-17 : Fluvial flood maps showing inundation areas for a 10-year return period for both current (upper) and SSP5-8.5 – 2050 (middle) simulations. Additionally, a difference map (lower) shows the absolute increase in flood height (m) per LGA.

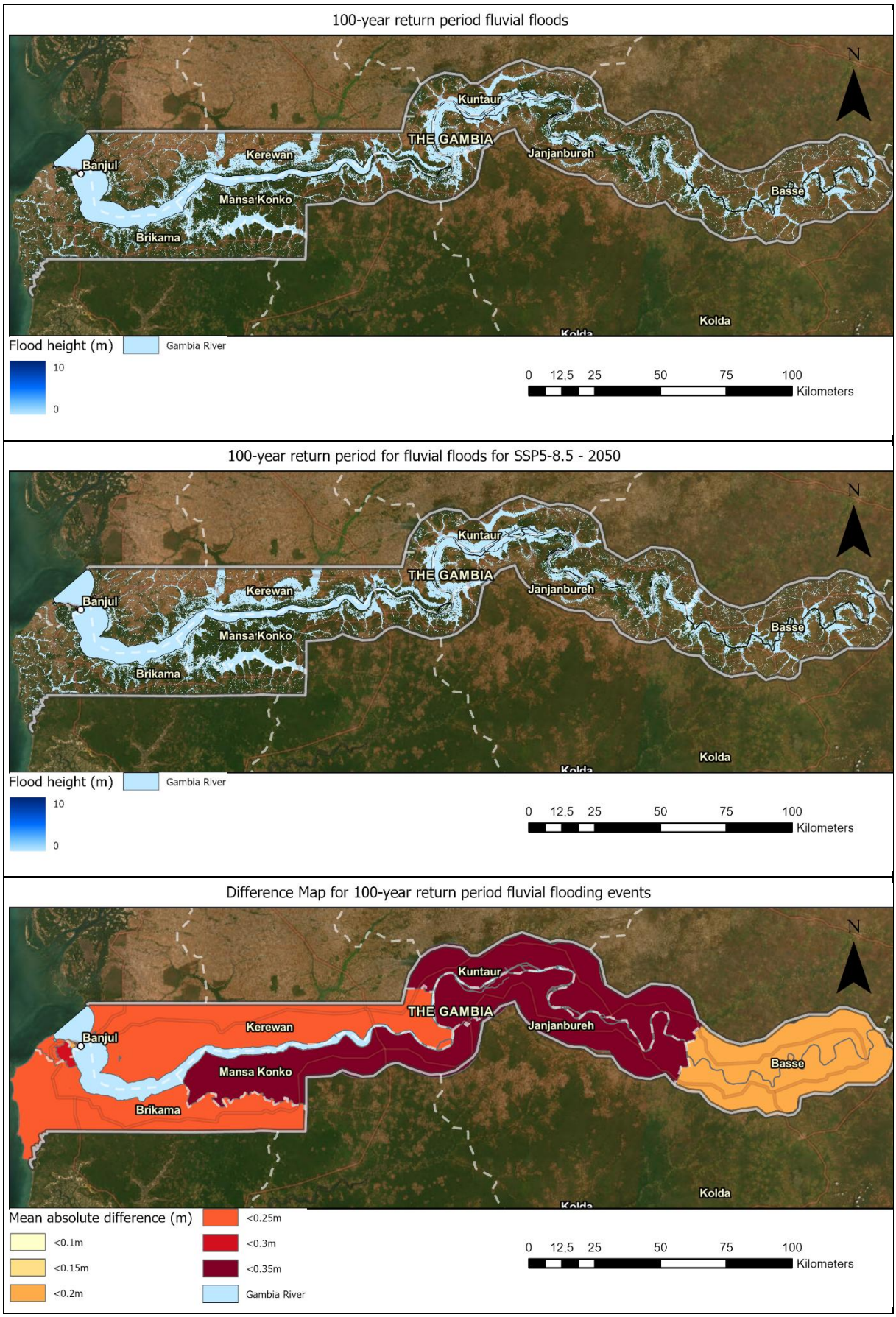

Figure 2-18: Fluvial flood maps showing inundation areas for a 100-year return period for both current (upper) and SSP5-8.5 – 2050 (middle) simulations. Additionally, a difference map (lower) shows the absolute increase in flood height (m) per LGA.

3. METHODOLOGY

3.1 Reference period and future scenarios

Climate projections are model simulations that provide an estimation of the average future climate for a certain period typically between 20 and 30 years. Comparing the simulated climate by the numerical models during the baseline period with the projected climate for the selected future periods we can assess the future change in the occurrence of different climate hazards. We define the reference period as the historical baseline 20-year period between 1986 and 2005 which is a standard reference used by IPCC. Then, we compare it with the climate of the following future horizons: 2021-2040, 2041-2060, 2061-2080, and 2081-2100. However, considering the lifetime of the infrastructures considered, special focus will be dedicated to the intermediate future period between 2041 to 2060. In addition, to obtain a more robust estimation of the observed baseline trends during the baseline analysis in section 3, we use an extended 40-year observational record (from 1981 to 2020).

Two different future scenarios will be considered to reflect the contrasts in the impacts of the different possible futures: The very high-emissions scenario (RCP8.5) represents the upper end of the possible futures with no climate policies implemented worldwide due to enhanced greenhouse gas emissions. The intermediate scenario (RCP4.5) considers significant mitigation efforts within a future world with a notable but irregular reduction in the use of resources and energy together with moderate total population growth.[14]

3.2 Observational baseline

3.2.1 ERA5 reanalysis

The ERA5 global reanalysis from the ECWMF[15] has been used as an observational reference for the historical baseline analysis as well as for correcting the climate projections' biases. A reanalysis, like ERA5, provides a synthetic estimation of the climate state through the combination of a numerical model together with as many observations as possible of the Earth system. Reanalyses are commonly used in climate science, due to the homogeneity and physical consistency of their fields and are usually preferred over observational datasets when observations are scarce in space and time. This is the case of this current analysis where a long-term observational time series of precipitation with the required temporal and spatial resolution is not available. ERA5 provides hourly fields with a spatial resolution of 0.25º (~25km). The resolution of this dataset has been a key factor in deciding to use alternative datasets for important variables such as precipitation and temperature. Only variables such as wind speed and relative humidity are taken from this dataset for this report.

3.2.2 CHIRPS and CHIRTSmax

The Climate Hazards Group Infrared Precipitation (CHIRP) combined with station observations (CHIRPS) is a satellite-based rainfall product with relatively high spatial and temporal resolutions and quasi-global coverage. The generation algorithm integrates three primary data sources: (a) the Climate Hazards group Precipitation climatology (CHPclim), which provides a global precipitation climatology at a resolution of 0.05° latitude/longitude for each month, derived from station data, satellite observations, elevation, latitude, and longitude (b) satellite precipitation estimates based on thermal infrared (TIR) data (IRP); and (c) measurements from rain gauges located on-site. The dataset provides information at both 0.25º and 0.05º. The high resolution has been used as observational data to adjust the climate projections, whereas the lower resolution has been used for the creation of visualisation of precipitation data in the baseline period.

---

[14] The flood hazard assessment considers the SSP2-4.5 and SSP5-8.5 scenarios from the IPCC AR6 report, corresponding to the RCP4.5 and RCP8.5 scenarios respectively.

[15] https://cds.climate.copernicus.eu/cdsapp#!/dataset/reanalysis-era5-single-levels

3.2.3 Observational Data validation

Ground Truth Data

The validation of gridded datasets against ground truth data is critical for assessing their suitability for regional climate analysis. This analysis evaluated precipitation and temperature data considering three sources of ground truth data: NOAA Global Historical Climatology Network daily (GHCNd.[16]), World Meteorological Organization (WMO.[17]), and Global Summary of the Day (GSOD.[18]). Due to Gambia's small size, no GHCNd stations were located within its boundaries. However, a nearby station at Tambacounda, which is inside of The Gambia River basin and just east of the country, was identified and analysed as representative of the eastern region (Figure 17). This station also served to validate consistency across the NOAA, WMO, and GSOD datasets, which all provided overlapping data at this location.

Within The Gambia, GSOD provided data for several stations, but only the Banjul Airport (BJL, Figure 17) station had sufficiently complete records for inclusion. These two stations represent the eastern (Tambacounda) and western (BJL) regions of Gambia, covering key geographic and climatic variability.

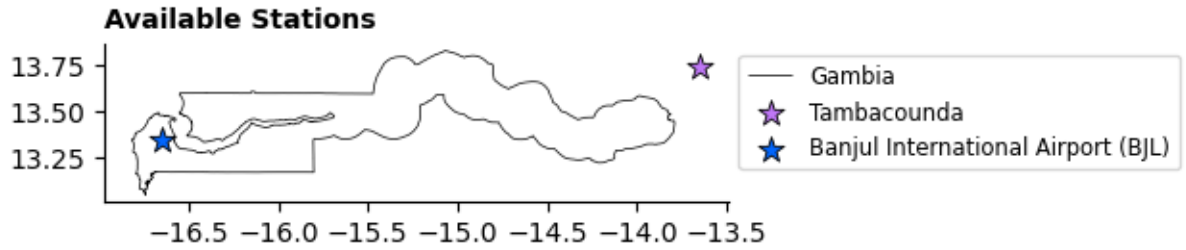

Figure 3-1. Location of the stations in western Gambia, BJL (left), and eastern Gambia river basin, Tambacounda (right) used for Tasmax, Tasmin, and Precipitation.

Precipitation

For analysis of Tambacounda station, Chirps at resolution 0.25 was also added to our analysis. This data was of interest for a coarser resolution analysis of the large area of The Gambia river basin for the water balance model of the basin.

Observed precipitation in the region ranges from 0 to 350 mm daily, with extreme values occurring infrequently. While most gridded datasets underestimate maximum rainfall metrics, cumulative metrics for CHIRPS (0.05) and ERA5 show close agreement with ground truth data (Figure 18) with a below 50% overestimation in the driest years, a below 50% underestimation in the wettest years, and a general agreement in the years with precipitation closer to the average. The extreme precipitation in the gridded models, however, shows a concerning deviation from observations and very extreme values should be provided with a wide range of uncertainty, where precipitation can be expected to be 3 times higher than the modelled values.

[16] https://www.ncei.noaa.gov/products/land-based-station/global-historical-climatology-network-daily
[17] https://www.ncei.noaa.gov/metadata/geoportal/rest/metadata/item/gov.noaa.ncdc:C00838/html
[18] https://www.ncei.noaa.gov/metadata/geoportal/rest/metadata/item/gov.noaa.ncdc:C00516/html

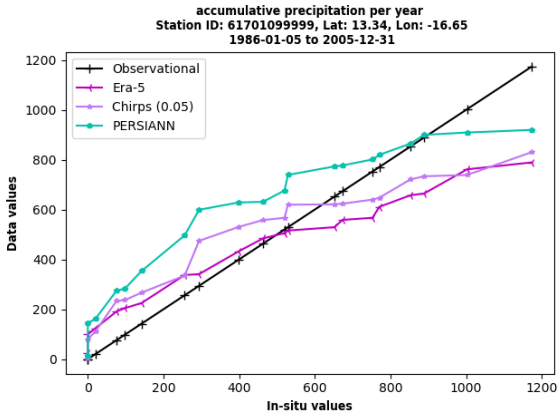

Figure 3-2. Values at BJL of gridded datasets plotted against values of ground truth metrics.

Comparison of interannual time series and seasonal cycles highlighted differences in the performance of gridded datasets. For mean precipitation values in the eastern region, PERSIANN showed closer alignment with ground truth data, though CHIRPS shared the most similar seasonal patterns (Figure 19, top). In contrast, in the western region at Banjul, where gridded datasets tended to overestimate mean precipitation, Chirps provided the closest match to observed values and seasonal cycles. However, all datasets slightly underestimated mean rainfall when analysing seasonal cycles at Banjul, with ERA5 giving the lowest estimates (Figure 19, bottom).

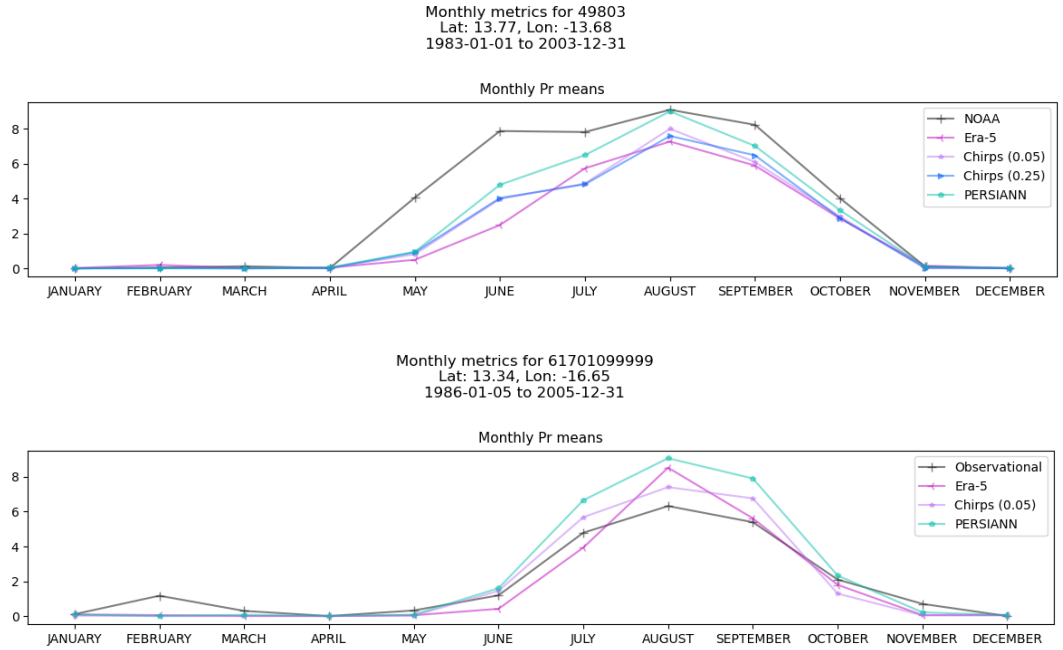

Figure 3-3. Monthly means for daily precipitation values. Comparison of seasonal cycle of gridded datasets and ground truth data in The Gambia. Eastern region, Tabacounda (top), Western region, BJL (bottom).

Regarding data spatial consistency, this analysis revealed limitations in PERSIANN for this region, including data gaps that raised concerns about its reliability. Additionally, spatial resolution of gridded data was critical for this study, given Gambia's small size. For these reasons, Chirps, with its finer 0.05° resolution, was selected as the preferred reference dataset for precipitation.

Temperature

Analysis of temperature values show good agreement between gridded models and observations at the airport and very good agreement in the east at Tambacounda. Across metrics and stations Chirts consistently showed the closest maximum values to ground truth data (Figure 20).

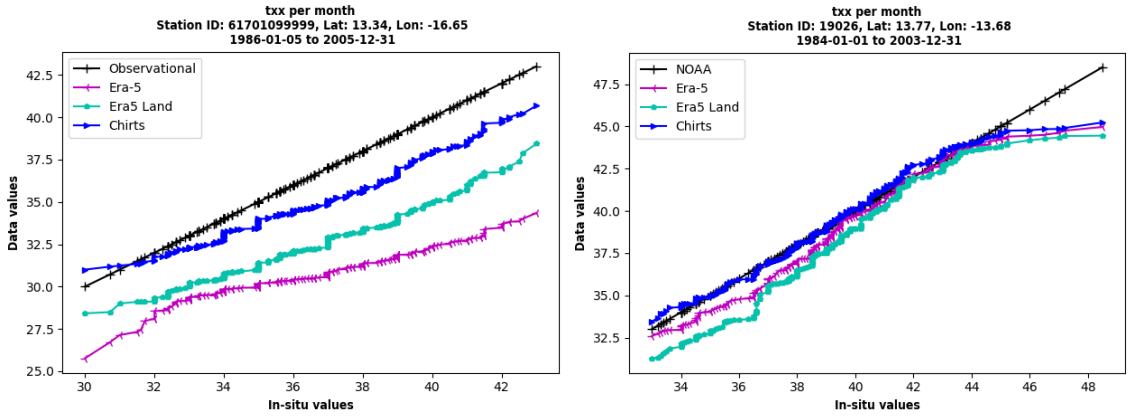

Figure 3-4. Comparison of monthly maximum values of gridded data plotted against ground truth data, indicating that Chirts is the most accurate in both the west (left) and the east (right).

Table 5 gives values for error metrics corresponding to Figure 20. Other maximum metrics showed similar results indicating that Chirts is the gridded dataset with the closest values and seasonal patterns to ground truth.

Table 10. Error for monthly maximum temperature values across stations in The Gambia region.

Source	MSE	RMSE	MAE
Tambacounda (East)			
Era-5	2.37	1.54	0.97
Era5 Land	4.21	2.05	1.47
Chirts	1.59	1.26	0.85
BJL (West)			
Era-5	41.14	6.41	5.91
Era5 Land	19.85	4.45	4.13
Chirts	5.36	2.31	1.83

3.3 Climate Projections

3.3.1 CORDEX

When assessing the climate risks that a specific asset is exposed to, it is essential to work with climate data that can reproduce the climate patterns at the local scale. Features like mountains or coastal areas have a direct impact on the local weather. Moreover, climate hazards like pluvial flooding or storms occur at spatial and temporal scales in the order of a few kilometres and within hours or days. This implies that widely known global projections, like those used in the IPCC report (CMIP) based on global circulation models (GCMs) with typical spatial resolutions smaller than 1° (>100km), cannot be directly used on impact assessments at the asset level. Instead, regional circulation models (RCMs) simulate the climate for a certain part of the globe, usually a continent, with a much higher spatial resolution (~20kms). See the comparison in Figure 21 for the region of The Gambia. This higher resolution allows more accurate reproduction of the small-scale features affecting the local weather and in turn a more reliable estimation of the climate extremes occurring at specific locations on Earth. This is exactly the goal of the international Coordinated Regional Climate Downscaling Experiment (CORDEX) program.[19], to provide

[19] https://cordex.org/

high-resolution climate projections appropriate for climate risk assessments. Still, regional projections require global projections to be used as boundary conditions outside the simulation domain. Thus, each regional climate projection is generated by a RGM coupled with a GCM. The combination of different RCMs and GCMs provides a broad set of plausible future projections. This in turn allows the computation of robust statistics for the estimation of the climate change signal and its corresponding uncertainty.

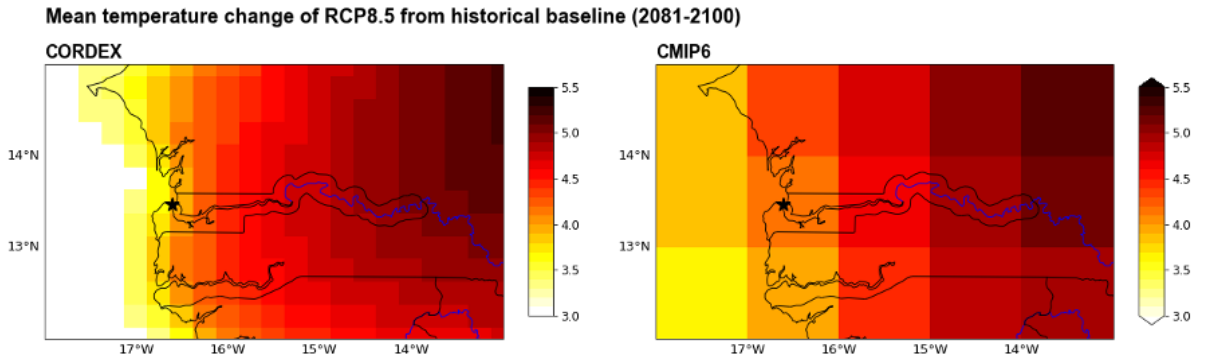

Figure 3-5 - Comparison of an example precipitation field between a CORDEX model (left) and CMIP6 (right). The much higher spatial resolution of CORDEX allows it to resolve climate and meteorological features with a much smaller scale.

Here, we use a multi-model ensemble of 16 regional climate projections from the Africa CORDEX domain combining ten different GCMs with six different RCMs (see Table 6). The spatial resolution of the projections is 0.22° (~22km) with a daily temporal resolution. State-of-the-art CORDEX regional projections use CMIP5 global projections as boundary conditions. The next generation of CORDEX projections using recent CMIP6 global simulations is in development and is still not available.

Table 11 - List of the regional climate models used in this assessment together with the scientific developing institutions. Each climate projection is generated by a specific RCM driven by a specific GCM.

Projection	Driving global circulation model	Regional circulation model
1	NCC-NorESM1-M Norwegian Climate Center, Norway	SMHI-RCA4_v1 Swedish Meteorological and Hydrological Institute, Sweden
2	CCCma-CanESM2 Canadian Centre for Climate Modelling and Analysis, Canada	SMHI-RCA4_v1 Swedish Meteorological and Hydrological Institute, Sweden
3	CCCma-CanESM2 Canadian Centre for Climate Modelling and Analysis, Canada	CCCma-CanRCM4_r2 Canadian Centre for Climate Modelling and Analysis, Canada
4	CNRM-CERFACS-CNRM-CM5 National Centre for Meteorological Research and Centre Européen de Recherche et de Formation Avancée en Calcul Scientifique, France	CLMcom-CCLM4-8-17_v1 Climate Limited-area Modelling Community (CLM-Community)
5	CNRM-CERFACS-CNRM-CM5 National Centre for Meteorological Research and Centre Européen de Recherche et de Formation Avancée en Calcul Scientifique, France	SMHI-RCA4_v1 Swedish Meteorological and Hydrological Institute, Sweden
6	CSIRO-QCCCE-CSIRO-Mk3-6-0 Commonwealth Scientific and Industrial Research Organisation; Queensland Climate Change Centre of Excellence, Australia	SMHI-RCA4_v1 Swedish Meteorological and Hydrological Institute, Sweden

7	ICHEC-EC-EARTH Irish Centre for High-End Computing, Ireland	SMHI-RCA4_v1 Swedish Meteorological and Hydrological Institute, Sweden
8	IPSL-IPSL-CM5A-MR Institut Pierre-Simon Laplace, France	SMHI-RCA4_v1 Swedish Meteorological and Hydrological Institute, Sweden
9	MIROC-MIROC5 National Institute for Environmental Studies and Japan Agency for Marine Earth Science and Technology, JAPÓN	SMHI-RCA4_v1 Swedish Meteorological and Hydrological Institute, Sweden
10	MOHC-HadGEM2-ES MetOffice Hadley Center, UK	KNMI-RACMO22T_v2 Royal Netherlands Meteorological Institute, Netherlands
11		CLMcom-CCLM4-8-17_v1 Climate Limited-area Modelling Community (CLM-Community)
12		SMHI-RCA4_v1 Swedish Meteorological and Hydrological Institute, Sweden
13	MPI-M-MPI-ESM-LR Max Planck Institute for Meteorology, Germany	CLMcom-KIT-CCLM5-0-15 KIT, Karlsruhe, Germany in collaboration with the CLM-Community
14		MPI-CSC-REMO2009_v1 Helmholtz-Zentrum Geesthacht, Climate Service Center, Max Planck Institute for Meteorology, Germany
15		SMHI-RCA4_v1 Swedish Meteorological and Hydrological Institute, Sweden
16	NOAA-GFDL-GFDL-ESM2M The Geophysical Fluid Dynamics Laboratory, NOAA, USA	SMHI-RCA4_v1 Swedish Meteorological and Hydrological Institute, Sweden

3.3.2 CMIP6

Due to the nature of flood hazards as being secondary hazards, the NASA Earth Exchange Global Daily Downscaled Projections - Coupled Model Intercomparison Project Phase 6 (NASA NEX-GDDP-CMIP6) dataset were utilized for the flood hazard assessment. This data provides high-resolution climate projections at a global scale. It includes bias-corrected and statistically downscaled climate projections from 35 CMIP6 GCM models[20]. It downscales CMIP6 climate models to a 0.25-degree (~25 km) spatial resolution, offering daily climate data from 1950 to 2100. For this analysis we have used 10 GCM models to model the future. The list of GCMs used are given in Table 2-5 below.

Table 3-12: Global climate models from CMIP6 used in the flood hazard assessment.

Climate model	Institute	Region
ACCESS-CM2	Australian Community climate and Earth System Simulator	Australia
ACCESS-ESM1-5	Australian Community climate and Earth System Simulator	Australia
BCC-CSM2-MR	Beijing Climate Center (BCC)	China

[20] https://www.nccs.nasa.gov/services/data-collections/land-based-products/nex-gddp-cmip6

CanESM5	Canadian Earth System Model	Canada
CMCC-CM2-SR5	Centro Euro-Mediterraneo sui Cambiamenti Climatici (CMCC)	Italy
CMCC-ESM2	Centro Euro-Mediterraneo sui Cambiamenti Climatici (CMCC)	Italy
MIROC6	Japan Agency for Marine-Earth Science and Technology (JAMSTEC)	Japan
MPI-ESM1-2-HR	Max Planck Institute for Meteorology (MPI-M)	Germany
MPI-ESM1-2-LR	Max Planck Institute for Meteorology (MPI-M)	Germany
MRI-ESM2-0	Meteorological Research Institute (MRI)	Japan

3.3.3 General bias adjustment

Long-term climate records allow us to test the performance of climate simulations. The fact that models are able to reproduce the major climate features observed during the last decades to last centuries grants us confidence in their skills for predicting future climate. This skill is based on their ability to correctly reproduce the main physics driving the climate dynamics and thus the corresponding relative changes occurring. However, the number of required simplifications that are introduced in these models to reproduce the highly complex relations of the climate system led to systematic biases between the simulated and the observed climate. All this means that a climate model may be able to correctly reproduce the climate change signal in precipitation for a certain region during the coming decades, but it may struggle to accurately predict the exact amount of precipitation of a given climatological month. It is for this reason that an essential initial part of any climate assessment is the bias adjustment of the different climate simulations. Only after correcting the bias of each of the projections, we will be able to compare them, and we will also be sure that the projected absolute quantities are realistic.

In this study, we implement the Quantile Delta Mapping bias correction method described by Cannon et al. 2015[21] which assures the correct adjustment of all the quantiles of the distribution (i.e., including extreme values) while preserving the climate change signal of the raw simulations (Figure 22). Regional maps of any indicator always show climate data with ERA5 as a reference, and thus, possible bias might exist.

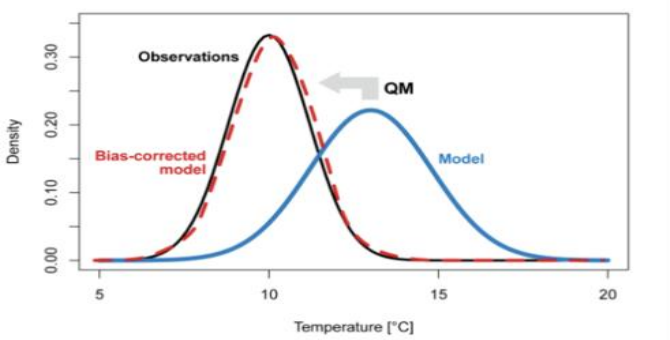

Figure 3-6 - Illustrative description of a quantile mapping bias correction for a conceptual representation of temperature. The figure shows the statistical distribution of all the possible temperature values from an observational dataset (black) and from a model (blue), which do not accurately match in general. Only after applying an appropriate bias adjustment (red), the model representation of the reality matches the observational world.

3.4 Climate change signal

Change in the different climate indicators can be expressed as a relative or absolute change between the corresponding future period and the reference period used as the baseline. Relative changes are

[21] Cannon, A. J., Sobie, S. R., & Murdock, T. Q. (2015). Bias Correction of GCM Precipitation by Quantile Mapping: How Well Do Methods Preserve Changes in Quantiles and Extremes? Journal of Climate, 28(17), 6938-6959.

commonly used for 0-based variables like precipitation or wind, while absolute changes are typically used for temperatures. Both are computed according to the following expressions:

$$Relative\ change\ [\%]\ = 100\ \cdot\ \frac{(Projected\ \ Value - Baseline\ Value)}{Baseline\ Value}$$

$$Absolute\ Value = Projected\ \ value - Observed\ \ value$$

3.5 Uncertainty estimation

The climate system presents an inherent unpredictability due to its internal variability that must be considered in any impact assessment. Following a common practice in the IPCC, we represent the uncertainty of the climate projections for a given result (e.g., a projected change) as the percentage of models that agree on that particular outcome. We, therefore, consider each of the 16 climate projections as independent plausible futures which combined altogether allow us to provide a probabilistic estimation of any of our results. The probabilistic estimation is expressed as percentiles where the median or percentile 50th represents the central estimation, meaning that 50% of the models predict a higher estimate and the other 50% a lower estimate. Percentiles 10th and 90th are always included and they represent the lower and higher bounds of the estimation thus accounting for the uncertainty of the predicted value. When for example percentile 10th of an estimated change for a future period is higher than 0, it means that more than 90% of the models agree on a future positive change. The use of percentiles is convenient when working with predictions with high uncertainty as is the case of climate projections since it allows to account for this uncertainty in the consecutive estimations of a risk assessment[22].

3.6 Hazard frequency analysis

The intensity of any hazard is intimately related to its frequency of occurrence. For any type of hazard, intense events happen on average less frequently, i.e., within longer temporal windows, than weaker events. This frequency is usually represented by return periods which refer to the span of time required on average for a specific hazard to happen with a certain intensity. These intensities, also called return levels, are computed for each hazard for the different return periods in a two-step process. First, a time series with the yearly maximum (or minimum) values are obtained for each hazard indicator and each temporal period. Then, the return levels are calculated for the prescribed return periods after fitting the corresponding indicator yearly time series to an appropriate statistical distribution. We use the Probability Weighted Moments method since it provides more robust results than standard maximum likelihood algorithms. Selected return periods are 2, 5, 10, 20, 50 and 100 years. Note that a given return period is also related to an annual probability of occurrence. For example, an event with a 20-year return period has a probability of occurrence in a given year of 5% since in a 100-year period, on average, 5 different 20-year events would happen. Then, in 1 year, 100 times less, i.e., 5%.

[22] This uncertainty estimation applies to hazard assessment of extreme temperature, extreme precipitation, drought, extreme winf\d and wildfires.

4. HAZARDS CONSIDERED

The intensity and frequency of occurrence of each hazard will be estimated for both the historical reference period, considered as the baseline, and for the future climate projections. Hazards are characterized next by the listed appropriate indicators.

4.1 Extreme temperature

Events with extreme temperatures will be described using the commonly used indicator TXx which refers to the maximum daily temperature within a year (ETCCDI[23]). Additional indicators to describe extreme temperatures are TX35 and TX40, which provides the number of days in a year with maximum daily temperatures above 35ºC and 40ºC. TX35 provides an interesting indicator of more moderate but still extreme conditions that already happen in the area but will happen much more frequently in the future posing a serious threat to sustained outdoor activities or labour productivity. Daily extreme temperatures time series will be estimated from the CHIRTS observational dataset for the baseline period and from the CORDEX projections for future periods.

4.2 Extreme precipitation

Episodes of extreme precipitation will be estimated using the indicator RX which refers to the maximum precipitation accumulated within different temporal windows. In this study, we use the temporal windows of 1 day, referred to as RX1day. Extreme precipitation will be estimated from the CHIRPS observational dataset for the baseline period and from the CORDEX projections for future periods. Additional indicators such as number of days above 20 mm and 50 mm have been considered also in this analysis. Other indicators, such as Raccm and dr90p, referring to mean accumulated precipitation and days with precipitation above the 90th percentile of daily rain, have also been used for adding context to the hazard and its potential future changes.

4.3 Extreme Wind

Extreme winds are notoriously difficult to simulate accurately by climate models, and long-time records of in-situ wind data are always required to adjust the numerical simulations. At the time of this analysis, ground-based observations were not available with the required precision, and no adjustment has been possible. However, we use ERA5 daily maximum wind gusts as a reference for the baseline period and employ a statistical correction to derive maximum wind gusts from the CORDEX daily wind mean. A careful validation of this methodology has been carried out leading to a neglectable absolute bias (error centred in 0) and an averaged normalised error (nRMSE) below 10%. This means that even though our estimation may not be suited for accurate quantitative analysis, it provides a reliable qualitative estimate of the projected future changes.

Table 13 – description of wind levels according to the Beaufort scale.24

Beaufort number	Description	Wind speed	Land conditions
0	Calm	0.2 m/s	Smoke rises vertically
1	Light air	0.3–1.5 m/s	Direction shown by smoke drift but not by wind vanes
2	Light breeze	1.6–3.3 m/s	Wind felt on face; leaves rustle; wind vane moved by wind
3	Gentle breeze	3.4–5.4 m/s	Leaves and small twigs in constant motion; light flags extended

[23] http://etccdi.pacificclimate.org/list_27_indices.shtml

[24] https://www.weather.gov/mfl/beaufort

4	Moderate breeze	5.5–7.9 m/s	Raises dust and loose paper; small branches moved
5	Fresh breeze	8–10.7 m/s	Small trees in leaf begin to sway; crested wavelets form on inland waters
6	Strong breeze	10.8–13.8 m/s	Large branches in motion; whistling heard in telegraph wires; umbrellas used with difficulty
7	High wind, moderate gale, near gale	13.9–17.1 m/s	Whole trees in motion; inconvenience felt when walking against the wind
8	Gale, fresh gale	17.2–20.7 m/s	Twigs break off trees; generally impedes progress
9	Strong/severe gale	20.8–24.4 m/s	Slight structural damage (chimney pots and slates removed)
10	Storm,[12] whole gale	24.5–28.4 m/s	Seldom experienced inland; trees uprooted; considerable structural damage
11	Violent storm	28.5–32.6 m/s	Very rarely experienced; accompanied by widespread damage
12	Hurricane-force	≥ 32.7 m/s	Devastation

4.4 Drought

Droughts or periods with a sustained deficit of precipitation will be quantified by the annual accumulation of precipitation. In this case, to quantify the intensity of drought events, we will look at two indicators. On the one hand, the minimum annual accumulation of precipitation will provide a general description of changes in annual precipitation. On the other hand, the multivariate SPEI (Standardized Precipitation Evapotranspiration Index. The drought indicator accounts for the contribution not only of a deficit in precipitation but also the expected warmer temperatures and a corresponding increase in evapotranspiration. SPEI values greater than 2 are considered extremely wet, 1.5-2 are considered very wet, 1-1.5 moderately wet, − 1 to 1 normal, − 1.5 to − 1 moderately dry, − 2 to − 1.5 severely dry, and values below − 2 extremely dry. We also include an even more extreme category that is below -2.5 which will represent an unprecedented intense drought not seen in the historical record. Required variables will be obtained from the ERA5 observational dataset for the baseline period and from the CORDEX projections for future periods.

Table 14: Drought levels based on the SPEI Index scale.

Risk Level	SPEI range
Extremely wet	>2
Very wet	Between 1.5 and 2
Moderately wet	Between 1 and 1.5
Normal	Between -1 and 1
Moderately dry	Between -1.5 and -1
Severely dry	Between -2 and -1.5
Extremely dry	< -2

4.5 Wildfires

The risk for the occurrence of wildfires will be represented by the Fire Weather Index (FWI).[25] which represents an estimation of the meteorological conditions that favour the ignition of wildfires. FWI specifically considers the deficit in precipitation and instantaneous temperature, humidity, and wind values. FWI is a non-dimensional variable with larger values representing a higher probability of fire ignition. FWI values from 21.3 to 38 indicate a high risk of ignition, values from 38 to 50 indicate very high risk and values above 50 indicate conditions with extreme risk of fire ignition. We will look at the percentile 90th of the FWI, named FWI90p, to select the most favourable conditions for a fire to occur. Daily time series for the 4 meteorological variables required for computing FWI are extracted from the previously described observational dataset for the baseline period and analyzed jointly with the indicators derived from the CORDEX projections for future periods.

Table 15: Wildfire risk based on the Fire Weather Index scale.

Risk Level	FWI range
Very Low Danger	< 5.2
Low Danger	Between 5.2 and 11.2
Moderate Danger	Between 11.2 and 21.3
High Danger	Between 21.3 and 38.0
Very High Danger	Between 38.0 and 50.0
Extreme Danger	> 50

4.6 Flooding

Flooding represents a significant climate hazard that can manifest in different forms based on the source and mechanisms of inundation. For this assessment, three distinct types of flooding are considered: coastal, pluvial, and fluvial. Each flooding type requires specific modeling approaches and data inputs to accurately represent current conditions and project future changes. Different modeling tools are employed for different flood types: RHDHV's Global Flood Risk Tool (GFRT) for coastal flooding, and the FastFlood model developed by Fast Hazard for both fluvial and pluvial flooding. The setup of the models for each of the flood types is described in more detail in the Flood Hazard Report, attached to this Hazard Assessment Report in Annex 1.

4.6.1 Coastal flooding

Coastal flooding will be assessed using RHDHV's inhouse developed Global Flood Risk Tool (GFRT). The GFRT has been developed by Royal HaskoningDHV as a cloud-based platform that facilitates comprehensible flood-risk analyses along with analysis of recommendations for adaptation measures. The GFRT can be applied to any location globally, including data-scarce environments, and can incorporate global or local datasets as appropriate.

The assessment of coastal flooding requires consideration of several processes that contribute to extreme water levels. The maximum water elevation for a flood event is typically calculated through the combination of different components following the equation: Maximum Water Level = Mean High Water Spring (MHWS) + Sea Level Rise (SLR) + Storm Surge. In this assessment, the influence of waves is not included to account for uniformity within the Gambia River estuary, which results in a slight underestimation of flooding in areas directly facing open ocean where waves can exacerbate flooding.

The methodology assumes that MHWS level will coincide with storm surge events given that maximum tidal levels occur approximately twice a day, spring tide occurs approximately once every 14 days, and storm surge events can last multiple days. The incremental Sea Level Rise for specified climate scenarios and time horizons is then added to the equation for each storm surge recurrence period event. The Mean High Water Spring levels are derived from measured data from the IHO Banjul tidal station, SLR is sourced from NASA Sea Level projections based on CMIP6, and storm surge levels are obtained from the global reanalysis work CODEC.

[25] https://www.nwcg.gov/publications/pms437/cffdrs/fire-weather-index-system

4.6.2 Pluvial flooding

Pluvial flooding will be assessed using the FastFlood model developed by Fast Hazard. This model is a web-based simulation platform that combines industry standard methodologies developed in the LISEM model since 1993 (Bout & Jetten, 2018), with recent innovations in flood modelling (Bout et al., 2023). Using this rapid flood modelling tool, a simulation framework is applied that allows for efficient assessment and analysis of flash floods resulting from intense rainfall events.

The extreme precipitation analysis is used to determine the current precipitation intensities and future trends in the region. The model specifically extracts short duration-high intensity precipitation events to form the input for the flash flood simulations. The identified trends in precipitation events are then used to determine the characteristics of future extreme events under various climate scenarios, allowing for comprehensive assessment of how pluvial flooding patterns may change over time. This approach enables detailed analysis of areas susceptible to surface water flooding resulting from rainfall that exceeds the capacity of drainage systems or infiltrates into the ground.

4.6.3 Fluvial flooding

Fluvial flooding will also be assessed using the FastFlood model, the same web-based simulation platform used for pluvial flooding assessment. The fluvial flood simulation focuses specifically on river flooding by incorporating the discharge boundary conditions as derived from the catchment-scale model. For each combination of return period, climate scenario, and time horizon, a different discharge boundary will be used to represent climate change impacts on river flow regimes.

One limitation of the current model is that it allows for only one discharge boundary condition, which works well on a more local scale but presents challenges for larger systems where the entire river basin should be accounted for. To address this limitation for the Gambia River, which has multiple side streams, the model combines both discharge boundary conditions and long-duration catchment rainfall to simulate the flows of the main river and its tributaries more accurately.

Furthermore, a downstream boundary condition is applied representing the current sea levels and future sea level rise projections. This downstream boundary incorporates the maximum water levels in line with the coastal flood modelling methodology (calculated as Maximum Water Level = Mean High Water Spring + Sea Level Rise + Storm Surge), ensuring consistency between the different flood modelling approaches. This integrated approach allows for comprehensive assessment of how river flooding patterns may evolve under changing climatic conditions throughout the river system.

1 ANNEX: FLOOD HAZARD ASSESSMENT REPORT

EXECUTIVE SUMMARY

The Gambia, with its low-lying coastal regions, extensive river system, and varying topography, faces significant flooding challenges that threaten critical infrastructure across its transport, energy, and water resource sectors. These sectors are vital for the nation's socio-economic stability, yet they are increasingly vulnerable to flood hazards including coastal inundation, pluvial flooding from intense rainfall, and fluvial flooding along the Gambia River system. The impacts of these flood events disrupt mobility, trade, and access to essential services, posing risks to livelihoods and economic development.

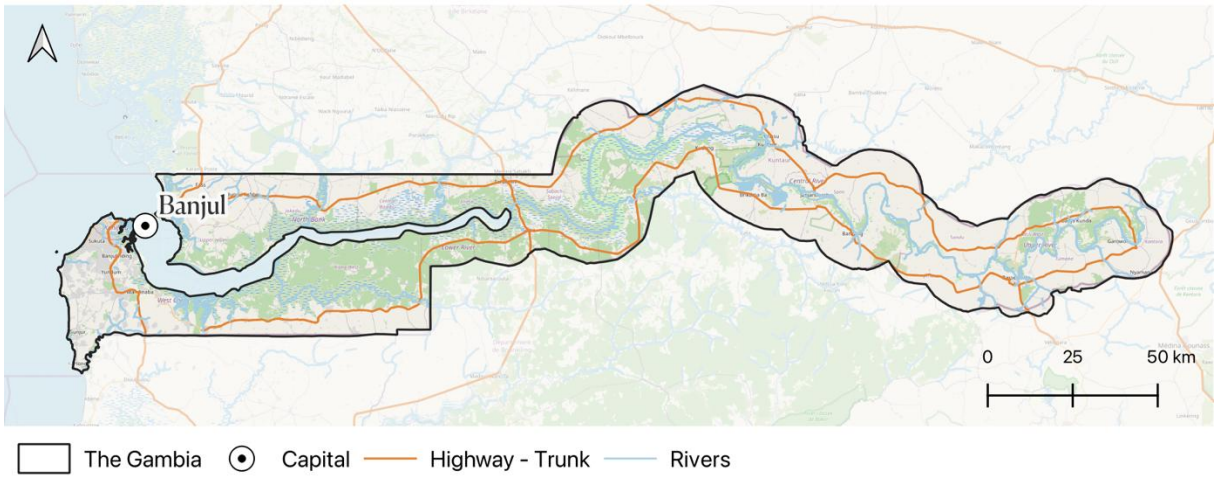

The Gambia's flood vulnerability is shaped by its unique hydrological and geographical characteristics. The country is dominated by the Gambia River Basin, which exhibits a tropical hydrological regime defined by distinct wet and dry seasons. Annual precipitation varies significantly across the basin, ranging from 1,700 mm in southern highlands to less than 700 mm in northern Sahelian areas. This variation, combined with the river's large tidal range and extensive flood plains, creates complex flood dynamics that require careful assessment.

This flood hazard assessment covers three flood types identified to be relevant in the country:

- coastal flooding influenced by sea level rise and storm surge;
- pluvial flooding from extreme rainfall events; and
- fluvial flooding along the Gambia River system.

The assessment combines modelling techniques with extensive data analysis to understand both current and future flooding under various climate scenarios. The methodology integrates climate change projections, hydrological modelling and hydraulic simulations to provide a thorough understanding of flood hazards across different temporal and spatial scales. This assessment aims to provide a solid foundation for informed decision-making in addressing flood risks.

An analysis framework was defined that takes account of the three afore-mentioned types of flooding, three climate scenarios (historical, SSP2-4.5 and SSP5-8.5), four time horizons (current, 2030, 2050 and 2070) and six flood return periods (2, 5, 10, 20, 50 and 100 year) such that a range of hydraulic flood simulations (126 no. in total) are subsequently undertaken that provide a 'band-width' of possible flood hazard outcomes spatially and temporally for consideration in flood risk mitigation.

This flood hazard assessment utilises multiple input datasets chosen to provide the most accurate representation of The Gambia's environmental conditions. Where possible, higher-quality local datasets are employed. When local data is not available, global datasets supplement the collected information.

To assess flood hazard, multiple modelling tools were used. For coastal flooding, the Global Flood Risk Tool (GFRT) was utilised, whereas pluvial and fluvial flooding were assessed using the FastFlood modelling platform.

Results per flood hazard type are summarised below:

Coastal Flooding: The coastal flood assessment reveals particular hazard in the Greater Banjul Area and the Gambia River estuarine area. Current coastal floods are concentrated in low-lying areas around Banjul, with significant inundation during extreme water level events. Mangrove areas west of Banjul show high inundation levels, underlining their crucial role and potential in flood attenuation. Sea level rise will amplify coastal flood risks, with projected increases in flood depths under the SSP5-8.5 climate scenario of 0.25 meters by 2050 and 0.42m by 2070. The combination of sea level rise and storm surge creates compound effects that will increasingly challenge coastal infrastructure. Banjul and Brikama regions show the highest projected increases in flood depths for extreme events between the current and 2050 time horizons. These findings suggest an urgent need for coastal adaptation strategies, particularly for critical infrastructure in the Greater Banjul Area.

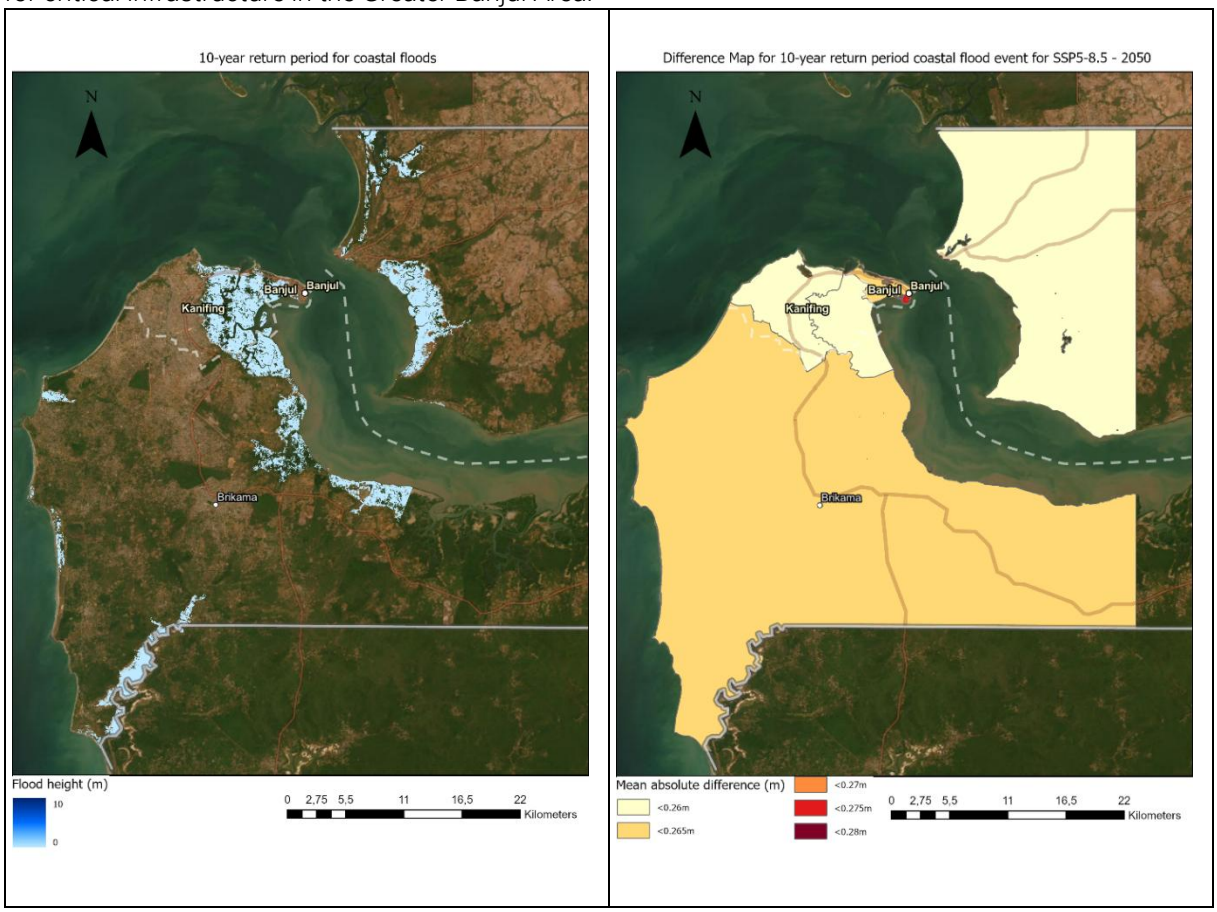

Pluvial Flooding: The analysis of rainfall-driven flooding reveals widespread pluvial flood hazard across The Gambia, with distinct spatial patterns. Eastern regions, particularly Basse, show the highest susceptibility to pluvial flooding and the largest projected increases in flood depth under future climate scenarios. Urban areas demonstrate particular vulnerability to local flash flooding, with Kanifing showing significant localized impacts around Kotu Stream. Short-duration, high-intensity rainfall events are projected to increase in frequency and severity under future climate scenarios, leading to increased flooding. The east-west gradient in increased flood exposure suggests the need for regionally differentiated adaptation strategies. These patterns highlight the importance of improving urban drainage systems and localized flood management strategies.

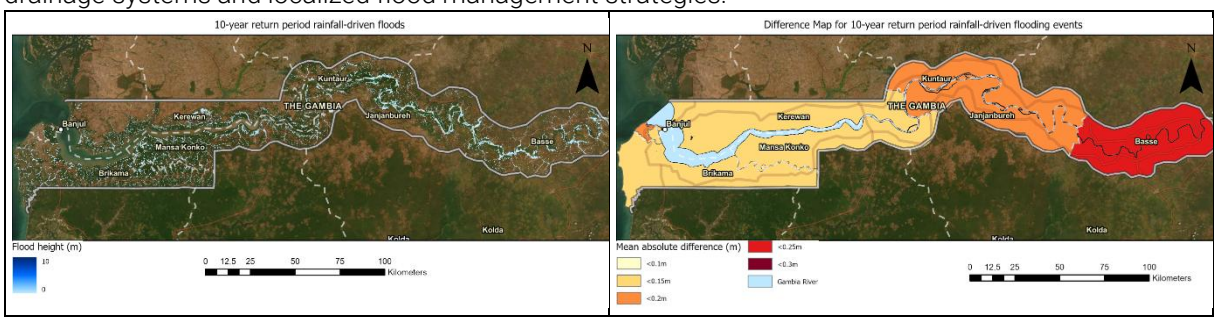

Fluvial Flooding: The assessment of riverine flooding reveals complex interactions between river dynamics and flood exposure. The Gambia River and its tributaries have extensive flood plains, particularly in middle river regions (Mansa Konko, Kuntaur, and Janjanbureh) which also show the most significant fluvial flood hazard. Under future climate scenarios, the effect of increased sea levels is transmitted up the Gambia River as far as the tidal effect, resulting in increased flooding in the lower river regions under these scenarios. Up to 2050, the 7-day precipitation change ratio for future climate scenarios is positive, reflecting increased long-duration rainfall; however after 2050 it then reflects a pronounced decline in total cumulative rainfall under the high-emission scenario SSP5-8.5. This shift points to a strong decrease in long-duration extreme precipitation, and thus in the magnitude of fluvial floods between 2050 and 2070. The spatial pattern of fluvial flood hazard contrasts with pluvial hazard patterns requiring integrated flood management. The validation against 2007 flood events demonstrates the model's capability to capture major flood patterns with sufficient accuracy for the purposes of this assessment.

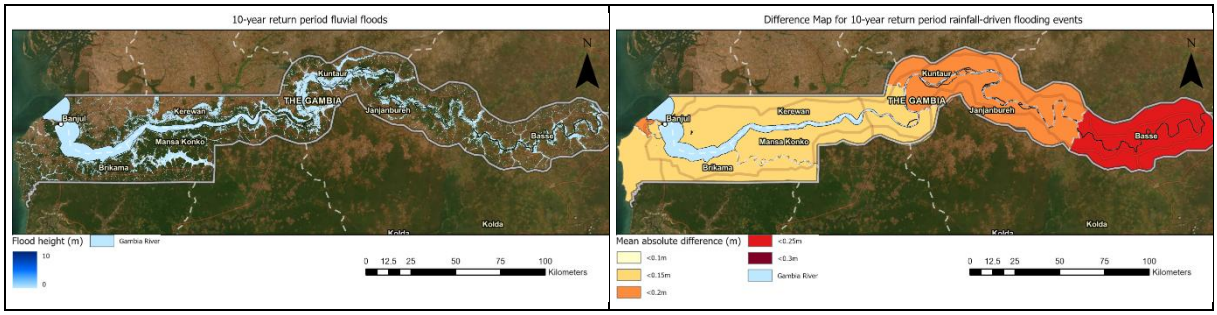

In summary, the results of this flood hazard assessment offer a robust foundation for flood risk management while highlighting areas where future research and more detailed modelling could enhance understanding of flood hazard in The Gambia.

1. INTRODUCTION

1.1 Country context

The Gambia, with its low-lying coastal regions, extensive river system, and varying topography, faces significant flooding challenges that threaten critical infrastructure across its transport, energy, and water resource sectors. These sectors are vital for the nation's socio-economic stability, yet they are increasingly vulnerable to flood hazards including coastal inundation, pluvial flooding from intense rainfall, and fluvial flooding along the Gambia River system. The impacts of these flood events disrupt mobility, trade, and access to essential services, posing risks to livelihoods and economic development.

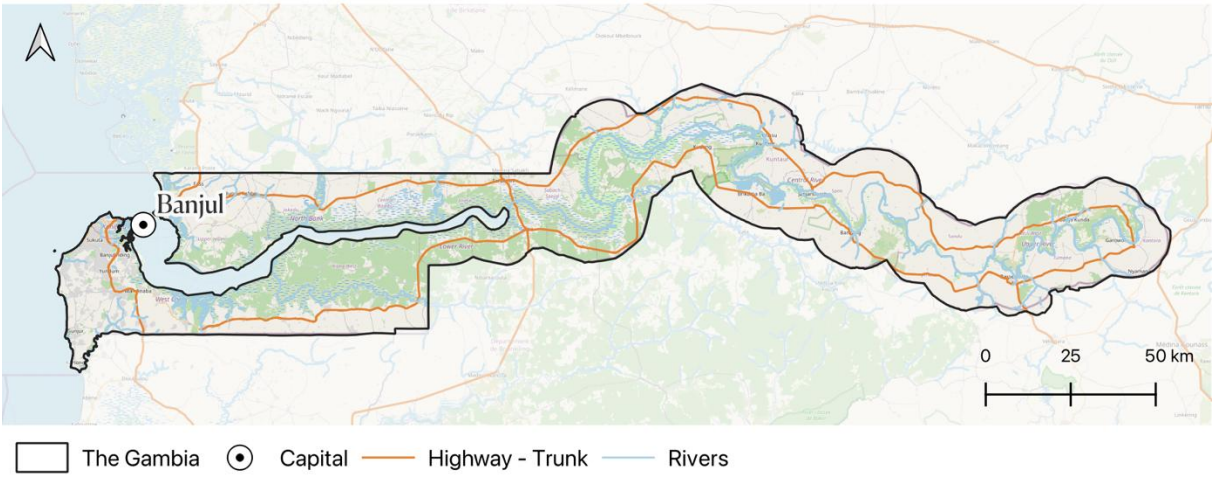

Figure 1-1: The Gambia - country context

1.2 This Report

Climate hazards of Extreme Temperature, Extreme Precipitation, Extreme Wind, Drought and Wildfires for the country of The Gambia are assessed in the Climate Hazard Assessment Report dated 27 January 2025. This Addendum to the Climate Hazard Assessment assesses the climate hazard of Flooding.

This assessment aims to define flood hazard within the country of The Gambia. Three distinct flood types are considered, namely:

- Pluvial flooding from local rainfall events,
- Fluvial flooding associated with the Gambia River, and
- Coastal flooding as influenced by sea level rise and storm surge.

This assessment combines modelling techniques with extensive data analysis to understand both current and future flooding under various climate scenarios. The methodology integrates climate change projections, hydrological modelling and hydraulic simulations to provide a thorough understanding of flood hazards across different temporal and spatial scales. This assessment aims to provide a solid foundation for informed decision-making in addressing flood risks.

The following Section 1.3 of this Report introduces the hydrological setting; Section 2 then sets out the analysis framework; Section 3 lists the key input datasets used; Section 4 sets out the modelling set-up and methods applied to assess flooding hazard; whilst Section 5 provides the results of the flood hazard assessment and Section 6 provides conclusions.

1.3 Hydrological setting

From a hydrological perspective the country of The Gambia is dominated by the Gambia River Basin. The Gambia River Basin exhibits a tropical hydrological regime, defined by two distinct seasons: a wet season from June to October and a dry season from November to May. Annual precipitation across the basin varies significantly, ranging from 1,700 mm in the southern highlands to less than 700 mm in the northern Sahelian areas, according to WorldClim 2.1 data. These climatic gradients affect river discharge and

groundwater recharge, with downstream regions heavily reliant on upstream conditions. The basin has been the subject of earlier hydrological modelling, using the GR4J model[26], which captures runoff dynamics by accounting for rainfall, evapotranspiration, and storage components at various sub-catchments, including Make, Simenti, and Gouloumbou, where rainfall patterns are notably different[27].

Flood hazards present a major challenge throughout the basin, especially in low-lying areas and regions experiencing rapid urban expansion, such as the West Coast Region. Geospatial assessments have identified that up to 26.9% of the country's surface area faces a high to very high flood risk. In particular, flooding disrupts essential infrastructure, including road networks and health facilities, concentrated near urban areas[28]. The social cost of flooding events can also be very significant, both in terms of lives lost and disruption of livelihoods, as well as indirect socio-economic impacts.

Climate change projections suggest that, under high-emission scenarios, annual streamflow in the basin could decline by 22% to 26%, complicating water management; whilst the frequency of intense floods increases[29]. These earlier results are confirmed by the analysis carried out for this Climate Hazard Assessment Report and Addendum.

The risk of pluvial flooding intensifies during the rainy season when sudden increases in discharge overwhelm stream and river channels; with the effects of flooding exacerbated by rapid urbanisation and minimal flood management systems. The Gambia has experienced numerous devastating rainfall-driven floods, such as the rainfall-driven floods of 1988, 1999, 2002, 2007, 2020, and 2022.

Figure 1-2 shows the extent of the Gambia river basin that was simulated for fluvial flooding. This river has a large tidal range, representing the transitional hydrological zone where the tidal influences from the Atlantic Ocean interact with riverine flows. The Gambia has experienced numerous devastating riverine floods, such as the floods of 2007, 2010, 2020, and 2022.

Furthermore the Gambia has experienced numerous devastating coastal floods, caused by different factors, and often as a compound effect of storm surge and high tides, such as during the floods of 2002, 2010, 2016, 2020, and 2022, particularly affecting its low-lying coastal areas and estuarine regions and compounded by coastal erosion and inadequate coastal flood defense systems.

The complex hydrodynamics of this system underscore the importance of integrated flood management strategies, combining river discharge monitoring, tidal forecasts, and catchment scale rainfall monitoring.

Figure 1-2: The Gambia River basin (image from Wikidata).

[26] https://webgr.inrae.fr/eng/tools/hydrological-models/daily-hydrological-model-gr4j

[27] https://enveurope.springeropen.com/articles/10.1186/s12302-024-00848-2

[28] https://link.springer.com/article/10.1007/s00267-024-02059-0

[29] https://www.mdpi.com/2306-5338/5/1/21

2. ANALYSIS FRAMEWORK

This section describes the analysis framework for which flood hazard results are produced and reported on in Section 5.

The analysis framework takes account of various climate scenarios, time horizons and flood return periods, such that a range of hydraulic flood simulations are subsequently undertaken that provide a 'bandwidth' of possible flood hazard outcomes for consideration in flood risk mitigation.

2.1 Climate Scenarios

2.1.1 Historical (Observational) Baseline

The first climate scenario is defined to be a historical baseline reflecting observed data. The historical climatology is assessed for the period 1995-2014, a standard reference period used by the Intergovernmental Panel on Climate Change (IPCC) to define climate conditions that generally reflect recent history before noticeable anthropogenic effects start appearing in the observations.

This historical period is used as the baseline for comparison with future climate projections to assess the changes in climate across return periods and time horizons. For convenience, this period is sometimes referred to as 'current climate'.

2.1.2 Climate Projections

Climate projections are provided by the Coupled Model Intercomparison Project Phase 6 (CMIP6) simulations, developed by IPCC and published in the latest Sixth Assessment Report AR6 (IPCC AR6, 2022). CMIP6 includes different Shared Socioeconomic Pathways (SSPs), which describe future socio-economic conditions and corresponding greenhouse gas (GHG) concentrations. This flood hazard assessment considers the following two climate change scenarios, each aligned with a specific SSP:

- SSP2-4.5 – Stabilization scenario: Intermediate scenario assumes a gradual transition towards cleaner and more efficient technologies, but without significant transformative changes.
- SSP5-8.5 – Business-as-usual: Most severe scenario assumes a continuation of current trends with high population growth, fossil fuel-dependent energy systems, and limited environmental regulations.

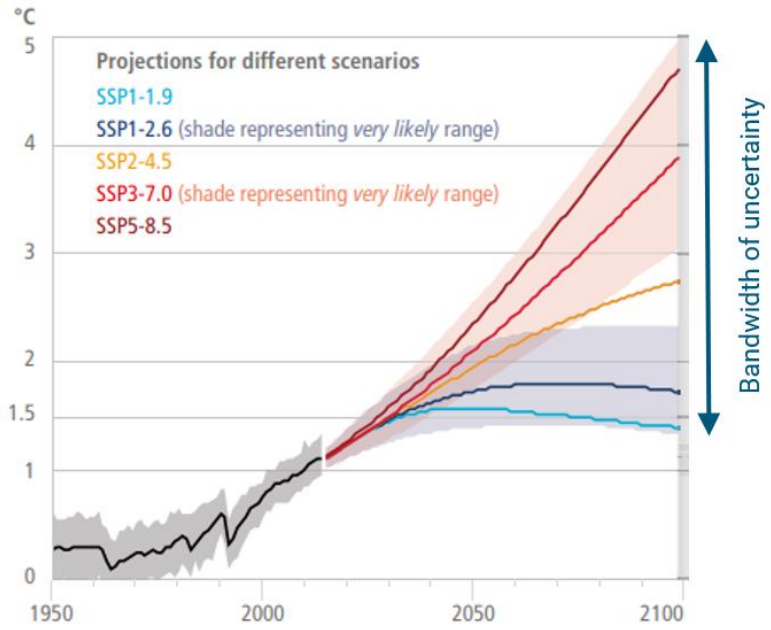

Figure 2-1: Climate projections for different scenarios (IPCC AR6 Work Group II, 2022).

These projections are the foundation for predicting future changes to rainfall patterns, however they are relatively coarse (~110km) which can lead to indicating the same climate for a wide area. Thus to capture local differences accurately, the downscaled climate projections developed by NASA's Earth Exchange Global Daily Downscaled Projections (NEX-GDDP-CMIP6) (Thrasher, et al., 2022) are used, which are based on the same global circulation models (GCMs) used for IPCC AR6. NEX-GDDP-CMIP6 data offers a downscaled resolution of approximately 28km available on a daily timescale. This finer resolution provides a more detailed representation of climate variability across diverse landscapes, including mountainous regions, coastal areas, and arid zones. This is crucial for understanding localized climate impacts, such as changes in rainfall patterns.

The NASA dataset comprises outputs from 35 GCM models. The inclusion of multiple models ensures a robust estimation of projection uncertainty through model agreement. By considering the collective results of these models, the dataset provides a comprehensive understanding of the potential range of future climate conditions. The intensity of the climate variables is analysed for each model before a median value is taken as input for the hazard frequency analysis. This approach assesses the uncertainty in intensity values associated with climate projections, considering variations across different models and their agreement on project outcomes.

2.2 Time Horizons

In this assessment, the climate projections considered above are applied to three future time horizons to understand trajectory of possible future climate. For this assessment, a rolling 20-year window is used to evaluate changes in future climate from 2021 to 2080, encompassing the following time horizons:

- 1995-2014 (historical baseline, referred to henceforth in this Report as current 2025);
- 2021-2040 (reference year 2030);
- 2041-2060 (reference year 2050); and
- 2061-2080 (reference year 2070).

The climate projection data are considered for within the country boundaries as well as for the broader Gambia River catchment area to allow for inclusion of climate changes across all catchments that affect flooding within the country of The Gambia.

2.3 Flood Return Periods

Frequency analysis is a statistical method used to estimate the probability of certain climate hazard events occurring within a given period. By analysing historical data and fitting a probability distribution, the likelihood of different event magnitudes can be determined.

The return period, or recurrence interval, represents the average time between occurrences of an event of a specific magnitude. For example, a 100-year return period event has a 1% chance of occurring in any given year. However, it is important to note that such an event could happen multiple times within a century or not at all. Climate change can influence these patterns, potentially increasing the frequency and intensity of hazard events.

For this assessment, return periods of 2, 5, 10, 20, 50, and 100 years are considered. To calculate return levels for each hazard and return period, a two-step process is employed. First, a time series of annual maximum (or minimum) values is created for each hazard indicator and period. Then, return levels are calculated by fitting the time series to an appropriate statistical distribution. The Gumbel method is used for its robustness.

Table 2-1 provides an overview of the return period analysis framework with the different return periods applied in this flood hazard assessment, the annual probability of occurrence and the analysis method.

Table 2-1: Return Period Analysis Framework.

Return Period (years)	Annual Probability	Analysis Method
2	50%	Annual Maximum Series
5	20%	Gumbel Distribution
10	10%	Gumbel Distribution
20	5%	Gumbel Distribution
50	2%	Gumber Distribution
100	1%	Gumbel Distribution

2.4 Summary of Analysis Framework

Considering the possible permutations when the above climate scenarios, time horizons and flood return periods are combined, 42 simulations result. Given that coastal, pluvial, fluvial flooding are each simulated separately (as described in the following Section 4), a total of 126 hydraulic simulations are thus undertaken in this flood hazard assessment (refer list in Annex 1). The figure below illustrates these permutations.

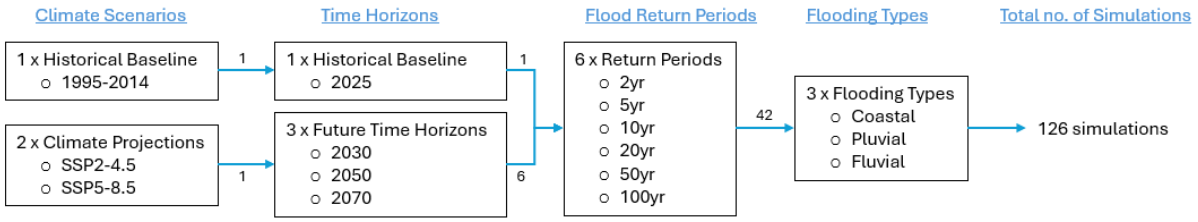

Figure 2-2: Summary of Analysis Framework

3. INPUT DATASETS

This flood hazard assessment utilises multiple input datasets chosen to provide the most accurate representation of The Gambia's environmental conditions. The quality of flood simulations depends predominantly on the input data quality. Where possible, higher-quality local datasets are employed. When local data is not available, global datasets supplement the collected information. **Error! Reference source not found.** provides an overview of datasets used and their data sources. The use of these datasets is further contextualised in the following Section 4.

Table 3-1: Overview of datasets used for flood type simulations and their data sources.

Parameter	Data source	Fluvial	Pluvial	Coastal
Terrain Elevation	Copernicus[30]	X	X	
Coastal Elevation	DeltaDTM[31]			X
Tidal Data	Banjul IHO Tidal Station[32]	X		X
Storm Surge	CODEC[33]	X		X
Sea level Data	NASA CMIP6 Projections[34]	X		X
Precipitation	ERA5[35] / NASA CMIP6	X	X	
River Discharge	GLOFAS[36]	X		
Land Cover	WORLDCOVER[37]	X	X	
Soil Properties	SoilGRIDS[38]	X	X	

The origin and use of these datasets are described further in Sections 2, 4 and 5. Those datasets not further described therein are briefly described below:

Terrain Elevation: The analysis uses Copernicus 20m resolution digital elevation model, providing detailed topographic information essential for accurate flood modelling. This high-resolution dataset enables precise delineation of flood-prone areas and accurate calculation of flood depths.

River Discharge: River discharge information comes from GLOFAS (Global Flood Awareness System), offering reliable streamflow data for the Gambia River. This data undergoes rigorous quality control to ensure accuracy in representing both normal flows and extreme events.

Land Cover: WORLDCOVER data provides detailed land use classification, crucial for understanding surface runoff patterns and flood vulnerability. This dataset helps account for variations in surface permeability and flood response across different terrain types.

[30] https://dataspace.copernicus.eu/explore-data/data-collections/copernicus-contributing-missions/collections-description/COP-DEM

[31] https://www.nature.com/articles/s41597-024-03091-9

[32] Department of Water Resources of The Gambia

[33] https://research.vu.nl/en/datasets/codec-dataset-data-underlying-the-paper-a-high-resolution-global-

[34] https://www.nccs.nasa.gov/services/data-collections/land-based-products/nex-gddp-cmip6

[35] https://cds.climate.copernicus.eu/datasets/reanalysis-era5-single-levels?tab=overview

[36] https://global-flood.emergency.copernicus.eu/

[37] https://esa-worldcover.org/en

[38] https://soilgrids.org/

4. MODEL SETUP

For assessment of the different flood types, different modelling tools and approaches are used.

- For coastal flooding RHDHV's inhouse developed Global Flood Risk Tool is utilized.
- For fluvial and pluvial flooding, the FastFlood model developed by Fast Hazard is applied.

The setup of the models for each of the flood types is described below.

4.1 Global Flood Risk Tool for coastal flooding

4.1.1 Tool Introduction

The Global Flood Risk Tool (GFRT) has been developed by Royal HaskoningDHV as a cloud-based platform[39] that facilitates comprehensible flood-risk analyses along with analysis of recommendations for adaptation measures. The GFRT can be applied to any location globally, including data-scarce environments, and can incorporate global or local datasets as appropriate.

4.1.2 Methodology for determination of Maximum Water Level

The assessment of coastal flooding requires consideration of several processes that contribute to extreme water levels. The maximum water elevation for a flood event is typically calculated through the combination of different components:

Maximum Water Level = Mean High Water Spring (MHWS) + Sea Level Rise (SLR) + Storm Surge + Waves

In this assessment the influence of waves is not included to account for uniformity within the Gambia River estuary. This means that there is a slight underestimation of flooding in the areas directly facing open ocean where waves can slightly exacerbate flooding. The maximum water elevation in this assessment is thus calculated through:

Maximum Water Level = Mean High Water Spring (MHWS) + Sea Level Rise (SLR) + Storm Surge

While each component of the water elevation follows its own probability of occurrence, the analysis combines the components based on the following logic to determine maximum water levels used in the coastal flood assessment:

- Given that the maximum tidal levels occur approximately twice a day and spring tide occurs approximately once every 14 days, and that storm surge events can be multiple days in duration, the methodology assumes that MHWS level will coincide with storm surge events. Therefore MWHS is added to the storm surge level determined for each storm surge recurrence period event.
- As Sea Level Rise is a long-duration event spanning decades, the incremental Sea Level Rise for specified climate scenarios and time horizons is then also added to the equation for each storm surge recurrence period event.

The Mean High Water Spring levels are derived from measured data from the IHO Banjul tidal station. SLR is sourced from the NASA Sea Level projections, which are based on the CMIP6 projections. Lastly, storm surge levels resulting from the global reanalysis work CODEC are used.

4.1.3 Digital Terrain Model

The Digital Terrain Model used in the assessment is DeltaDTM, a specialized dataset providing corrected elevation data particularly suited for coastal areas. This high-resolution topographic information is appropriate for broad-scale coastal flood hazard assessment. The dataset has undergone specific corrections for vertical datum inconsistencies common in coastal regions. The horizontal resolution of 5 meters enables detailed representation of coastal topography affecting flood propagation. It should be

[39] https://www.royalhaskoningdhv.com/en/services/global-flood-risk-tool

noted that the extents of flooding determined in the assessment is very sensitive to the elevation data used. The DeltaDTM does not include fine-scale topographic features such as specific flood protection measures or specific road elevations, which might lead to an overestimation of floods in the model. Given the relatively low state of development of infrastructure in The Gambia however, this short-coming is not considered to be significant.

4.2 FastFlood Model for pluvial and fluvial flooding

4.2.1 Model introduction

The FastFlood model is a web-based simulation platform, that combines industry standard methodologies developed in the LISEM model since 1993 (Bout & Jetten, 2018), with recent innovations in flood modelling (Bout et al., 2023). It features Interactive speed, easy-to-use model setup and simulation, and the accuracy of industry-standard methods. The model integrates hydrological and hydraulic components to provide comprehensive flood simulations across multiple scales and flooding mechanisms.

Using this rapid flood modelling tool, a simulation framework is applied that allows for efficient assessment and analysis within a confined period. At the core of this modelling setup is the FastFlood simulation method, a rapid simulation technique based on direct estimation of peak variables[40]. The FastFlood Model operates through three distinct simulation modes, each designed to capture specific flood behaviour, as bulleted below and reflected in the modelling flowchart in Figure 4-1:

- Local flash flood simulation: High-detail simulation of hydrology/flooding for local rainfall-induced flooding.
- Catchment-scale hydrology/flood simulation: Using rainfall and snowmelt input for larger river basins, usually at lower resolution, with 1D-2D linked setup to account for river dynamics.
- Fluvial flood simulation: Simulation of local fluvial floods using a discharge boundary condition to provide water inflow into the simulation. The discharge value might be obtained from observations or the regional catchment-scale model. For larger river basins with multiple side streams, a combination of both discharge boundary and catchment rainfall might be used to simulate the flows of the side streams of the main river in the catchment.

[40] https://www.sciencedirect.com/science/article/pii/S1364815223001731

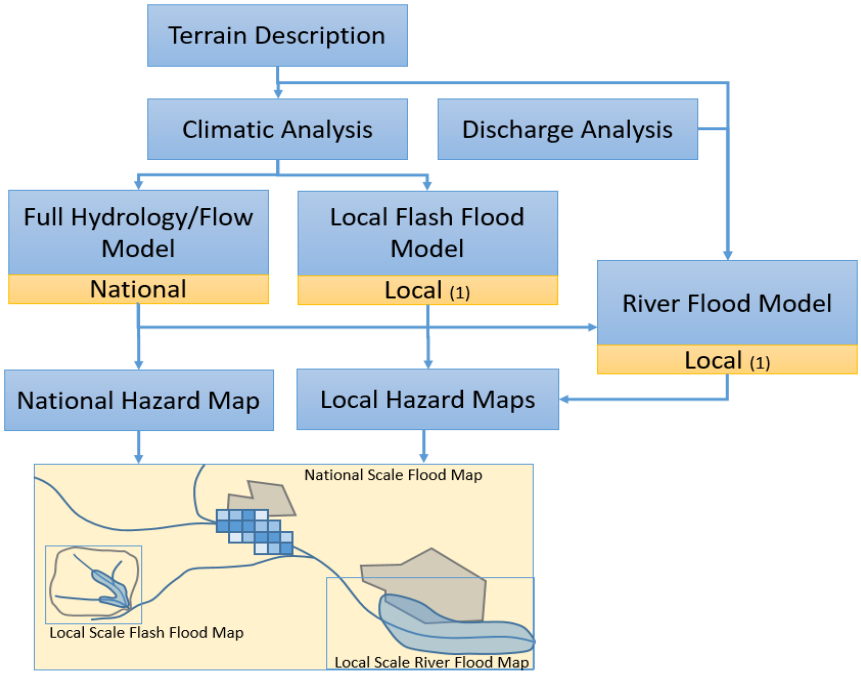

Figure 4-1: Flowchart of the modelling setup.

The set-up of the above-mentioned models for this assessment are described in the following sections.

4.2.2 Set-up for local flash flood modelling

Local flash flood modelling provides higher-detail simulation specifically focused on local rainfall-induced flooding. The implementation uses a resolution of 30 meters, making it particularly suitable for analysing pluvial flooding in urban areas and locations with critical infrastructure. The model incorporates detailed terrain data from Copernicus, land cover patterns from WORLDCOVER, and soil characteristics from SoilGRIDS to represent the physical environment affecting flood development.

An extreme precipitation analysis is conducted to determine the current precipitation intensities and future trends. The current precipitation intensities are presented in the form of an IDF-curve showing for each return period a curve representing the intensity of rainfall for specific time durations. In this manner, the short duration-high intensity precipitation events are extracted to form the input for the flash flood model. A trend analysis is then conducted using future precipitation projections. Subsequently, these trends are analysed and for each combination of climate scenario, return period, and time horizon, a rainfall multiplier is applied to account for climate change. Refer to Sections 5.2.1 and 5.2.1.2 for the results of the precipitation analysis.

4.2.3 Set-up for catchment-scale hydrology/flow modelling

A catchment-scale model is used to model the broader watershed dynamics. As this model focuses on the whole catchment, a resolution of 300 meters is sufficient. The model employs a 1D-2D linked setup to account for river dynamics across the Gambia River basin. This setup allows for efficient simulation of both channel flows and overbank flooding, which are essential for understanding the basin's response to precipitation events.

For the catchment-scale modelling the extreme precipitation analysis focusses on long-duration rainfall. The current extreme precipitation values can be extracted from the same IDF-curve as the short-duration extremes, and for future time horizons, climate projections are used to define rainfall multipliers similarly as for local flash flood modelling.

Long-duration rainfall events have a more representative effect on river dynamics and the subsequent floods. From this model, peak discharges are derived per combination of climate scenario, return period, and time horizon. These peak discharges are used in the fluvial flood model as boundary conditions.

4.2.4 Fluvial flood modelling

The fluvial flood simulation focuses specifically on river flooding by incorporating the discharge boundary conditions as derived from the catchment-scale model. For each combination of return period, climate scenario, and time horizon a different discharge boundary will be used to represent climate change. However, one limitation of the current model is that the current model allows for only one discharge boundary condition, which works well on a more local scale. For bigger systems the whole river basin should be accounted for. Hence, for the Gambia River, which has multiple side streams, the model combines both discharge boundary conditions and long-duration, catchment rainfall to simulate the flows of the main river and its tributaries.

Furthermore, a downstream boundary condition is applied representing the current sea levels and future sea level rise. This downstream boundary incorporates the maximum water levels in line with the coastal flood modelling (calculated as *Maximum Water Level = Mean High Water Spring (MHWS) + Sea Level Rise (SLR) + Storm Surge)*.

4.2.5 Model calibration procedure

In order to calibrate and validate the model, data on historical flood events is required. Since no field observation or discharge data was available for The Gambia at the time of assessment, flood extent data of the 2007 floods created by The United Nations Satellite Centre (UNOSAT)[41] was used for calibration.

The flood simulations are calibrated using a gradient descent algorithm (see Figure 4-2Figure 4-2). The physical parameters used in calibration are based on established practices in flood modelling; for instance, Manning's surface roughness, saturated hydraulic conductivity and initial soil moisture, as well as other parameters that are related to the model hydrology. Parameter values are limited between 50 and 150 % of their original values to remain within physically realistic limits and to obtain convergence.

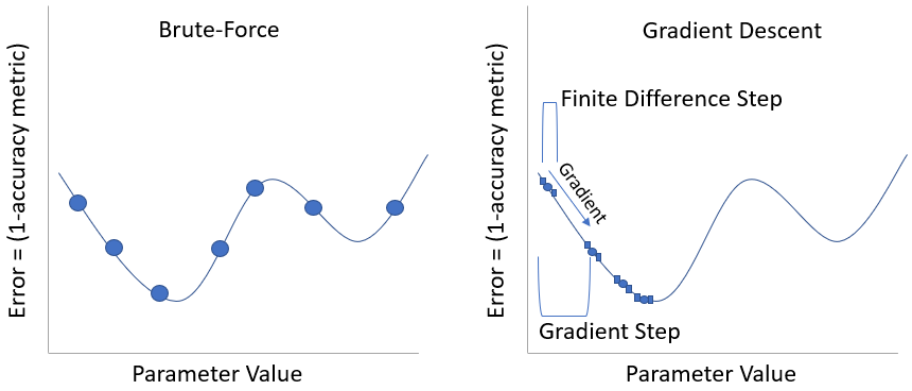

Figure 4-2 The two different calibration procedures that are used in combination in this assessment. Brute-force is more robust and slower, but Gradient descent is less stable but more efficient when working correctly.

The flood models assume that there are no structural flood protection measures or man-made drainage structures since data on these were unavailable at time of assessment. Incorporating such information into the flood model would provide a more accurate outcome at a local scale, but is not deemed significant at a national scale.

[41] https://reliefweb.int/map/gambia/flood-water-identification-central-gambia-18-sep-2007

5. FLOOD HAZARD RESULTS

In this section the results of the flood hazard assessment are presented, per each of the three distinct types of flooding namely:

- Coastal flooding.
- Pluvial (or rainfall-driven) flooding.
- Fluvial (or riverine) flooding.

For purposes of report presentation, the 10yr and 100yr return period flood maps for the historical baseline and SSP5-8.5 climate scenarios for current and 2050 time horizons are presented as illustrative of the nature of the flood maps and the flood patterns arising. Difference maps are also presented that reflect the extent of flood depth changes between the time horizons, agglomerated per Local Government Area (LGA), such that it is more easily visualisable where the biggest changes are forecast to take place.

Error! Reference source not found. provides a full list of the 124 no. flood hazard raster maps produced in this assessment, in accordance with the multiple combinations of climate scenarios, time horizons and flood return periods that have been assessed, as described in Section Error! Reference source not found. This full set of maps has not been incorporated into the Report due to the extreme size of the data; cloud-based access to the map data is available.

5.1 Coastal Flooding

Indicator: Flood Depth

The results of the coastal flooding assessment are presented below in two parts; firstly, the oceanographic analysis of the water levels as per the model set-up described in Section 4.1.2 is presented; and then secondly, the flood extents and depths resulting from the calculated water levels as imposed on the coastal topography are presented and discussed.

5.1.1 Maximum water levels

As described in Section 4.1.2, maximum water levels are calculated as:

Maximum Water Level = Mean High Water Spring (MHWS) + Sea Level Rise (SLR) + Storm Surge

The derivation of each component in this equation is described below, followed by the resulting Maximum Water Levels.

5.1.1.1 Tidal levels

In The Gambia, the tidal pattern is semi-diurnal, characterized by two high tides and two low tides per day. Based on tidal timeseries from the IHO Banjul Tidal Station, tidal levels are defined as presented in Table 5-1. The mean tide of The Gambia is approximately 1.21m and the tidal range for spring tide is approximately 1.69m. For the computation of coastal flooding, the Mean High Water Spring tidal levels is used, which refers to the average high tide level during spring tides, occurring twice a month (when the gravitational forces of the moon and sun align).

Table 5-1: Tidal levels derived from IHO Banjul tidal station

Tidal Level	Relative to Gambia Datum (GD) (m)
HAT	0.97
MHWS	0.83
MHHW	0.64
MHW	0.57
MSL	0
MLW	-0.64
MLLW	-0.67
MLWS	-0.86
LAT	-1.00

5.1.1.2 Storm Surge

Wind-induced surge is a key component of extreme water levels. The extreme water levels in the coastal waters surrounding The Gambia have been taken from the global reanalysis work CODEC. The results of this analysis specific to the Gambian coastal region are shown in Table 5-2.

Table 5-2: Maximum storm surge levels at the coast of The Gambia

Storm surge return period	Surge levels (m)
1 yr	+0.12
2 yrs	+0.13
5 yrs	+0.14
10 yrs	+0.17
20 yrs	+0.18
50 yrs	+0.21
100 yrs	+0.23

5.1.1.3 Sea Level Rise

Sea Level Rise (SLR) represents the projected increase in sea levels over time due to factors such as melting ice caps and thermal expansion of seawater. Table 5-3 shows the projected sea level rises under the two future climate scenarios for the three future time horizons applied in this assessment, based on the IPCC projections.

Table 5-3: IPCC sea level rise projections for two future climate scenarios.

Time Horizon	Sea level rise (m) under SSP2-4.5	Sea level rise (m) under SSP5-8.5
2030	0.10	0.11
2050	0.22	0.25
2070	0.36	0.42

5.1.1.4 Maximum Water Levels

Table 2-9 presents the combined results of the maximum water levels for the different climate scenarios, time horizons and return periods considered in this assessment. These maximum water levels are then added to Mean Sea Level in the Global Flood Risk Tool (GFRT) to determine flood extents and depths, as discussed further in Section 5.1.2.

Table 5-4: Combined water levels for different return periods and climate scenarios.

Flood Return Period	Time Horizon	Astronomical tide (m)	Sea Level Rise (m) SSP2-4.5	SSP5-8.5	Storm Surge (m)	Max Water Elevation (m) SSP2-4.5	SSP5-8.5
2	*Baseline*	*0.83*	-	-	*0.13*	0.96	0.96
	2030	*0.83*	*0.10*	*0.11*	*0.13*	1.06	1.07
	2050	*0.83*	*0.22*	*0.25*	*0.13*	1.18	1.21
	2070	*0.83*	*0.36*	*0.42*	*0.13*	1.32	1.38
5	*Baseline*	*0.83*	-	-	*0.14*	0.97	0.97
	2030	*0.83*	*0.10*	*0.11*	*0.14*	1.07	1.08
	2050	*0.83*	*0.22*	*0.25*	*0.14*	1.19	1.22
	2070	*0.83*	*0.36*	*0.42*	*0.14*	1.33	1.39
10	*Baseline*	*0.83*	-	-	*0.17*	1	1
	2030	*0.83*	*0.10*	*0.11*	*0.17*	1.1	1.11
	2050	*0.83*	*0.22*	*0.25*	*0.17*	1.22	1.25
	2070	*0.83*	*0.36*	*0.42*	*0.17*	1.36	1.42
20	*Baseline*	*0.83*	-	-	*0.19*	1.02	1.02
	2030	*0.83*	*0.10*	*0.11*	*0.19*	1.12	1.13
	2050	*0.83*	*0.22*	*0.25*	*0.19*	1.24	1.27
	2070	*0.83*	*0.36*	*0.42*	*0.19*	1.38	1.44
50	*Baseline*	*0.83*	-	-	*0.21*	1.04	1.04

Flood Return Period	Time Horizon	Astronomical tide (m)	Sea Level Rise (m) SSP2-4.5	SSP5-8.5	Storm Surge (m)	Max Water Elevation (m) SSP2-4.5	SSP5-8.5
	2030	*0.83*	*0.10*	*0.11*	*0.21*	1.14	1.15
	2050	*0.83*	*0.22*	*0.25*	*0.21*	1.26	1.29
	2070	*0.83*	*0.36*	*0.42*	*0.21*	1.4	1.46
100	*Baseline*	*0.83*	*-*	*-*	*0.23*	1.06	1.06
	2030	*0.83*	*0.10*	*0.11*	*0.23*	1.16	1.17
	2050	*0.83*	*0.22*	*0.25*	*0.23*	1.28	1.31
	2070	*0.83*	*0.36*	*0.42*	*0.23*	1.42	1.48

5.1.2 Coastal flooding results

5.1.2.1 Presentation of Results

The coastal flood assessment results presented here are for both current conditions and future simulations, focused on the 10-year and 100-year return period events. The results specifically illustrate the SSP5-8.5 climate scenario for the 2050 time horizon, to understand potential future impacts under high-emission conditions. To quantify changes in flood patterns, difference maps were generated comparing this future simulation against the baseline simulation.

These difference maps were calculated by subtracting the baseline simulation coastal flood depths from the future simulation flood depths for each model grid cell. The results were then averaged to show mean differences in flood depths per Local Government Area (LGA), the mean being calculated of only those areas that are flood-prone in either of the two simulations analyzed. Areas displaying darker colors in the difference maps indicate regions where mean coastal flood depths are predicted to increase most significantly, helping identify potential hotspots for increased flood risk.

5.1.2.2 Current Coastal Flooding

Analysis of baseline conditions reveals significant coastal inundation, particularly around Banjul and its surrounding areas. For the 10-year return period event (Figure 2-13), substantial flooding occurs in coastal regions, with notable impacts observed both east and west of Banjul in the estuarine area of the Gambia River. The extensive low-lying mangrove area west of Banjul (Tanbi Wetland) experiences significant inundation, though these natural systems play a crucial role in flood attenuation for inland areas.

The 100-year return period event under current conditions (Figure 2-14) demonstrates more severe flooding. The inundation extent expands considerably compared to the 10-year event, affecting larger portions of the coastal zone and extending further inland in low-lying areas. This increased extent highlights the vulnerability of coastal regions to extreme events even under current conditions.

5.1.2.3 Projected Future Coastal Flooding

The difference maps reveal significant changes in coastal flooding patterns under the SSP5-8.5 climate scenario for 2050. For 10-year return period events (Figure 2-13), the analysis shows:

The Banjul region emerges as the most significantly impacted area. The mangrove regions west of Banjul show substantial increases in inundation depths, though they continue to provide critical flood protection services. Other coastal LGAs show more modest increases, indicating that severe impacts may be concentrated in specific vulnerable locations.

For 100-year return period events (Figure 2-14), the changes become more pronounced across all coastal regions. Both Banjul and Brikama LGAs show substantial increases in flood depths. This amplification of extreme event impacts suggests that coastal areas may face significantly greater flood risks under future climate conditions, necessitating robust adaptation strategies.

The quantitative analysis of these changes provides crucial insights for flood risk management and adaptation planning, particularly in highly vulnerable areas like Banjul and its surrounding regions.

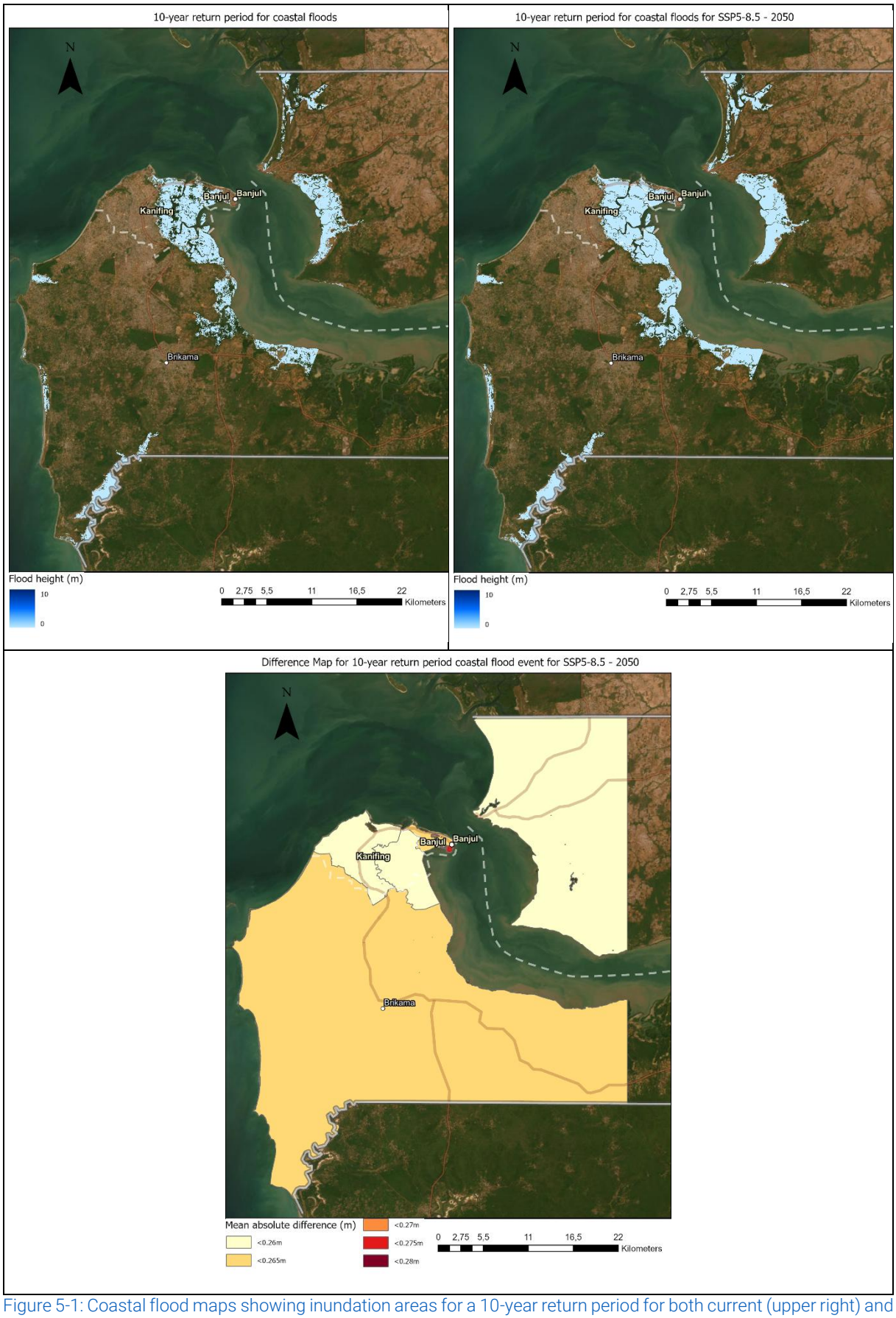

Figure 5-1: Coastal flood maps showing inundation areas for a 10-year return period for both current (upper right) and SSP5-8.5 – 2050 (upper left) simulations. Additionally, a difference map (lower) shows the mean absolute increase in flood height (m) per LGA.

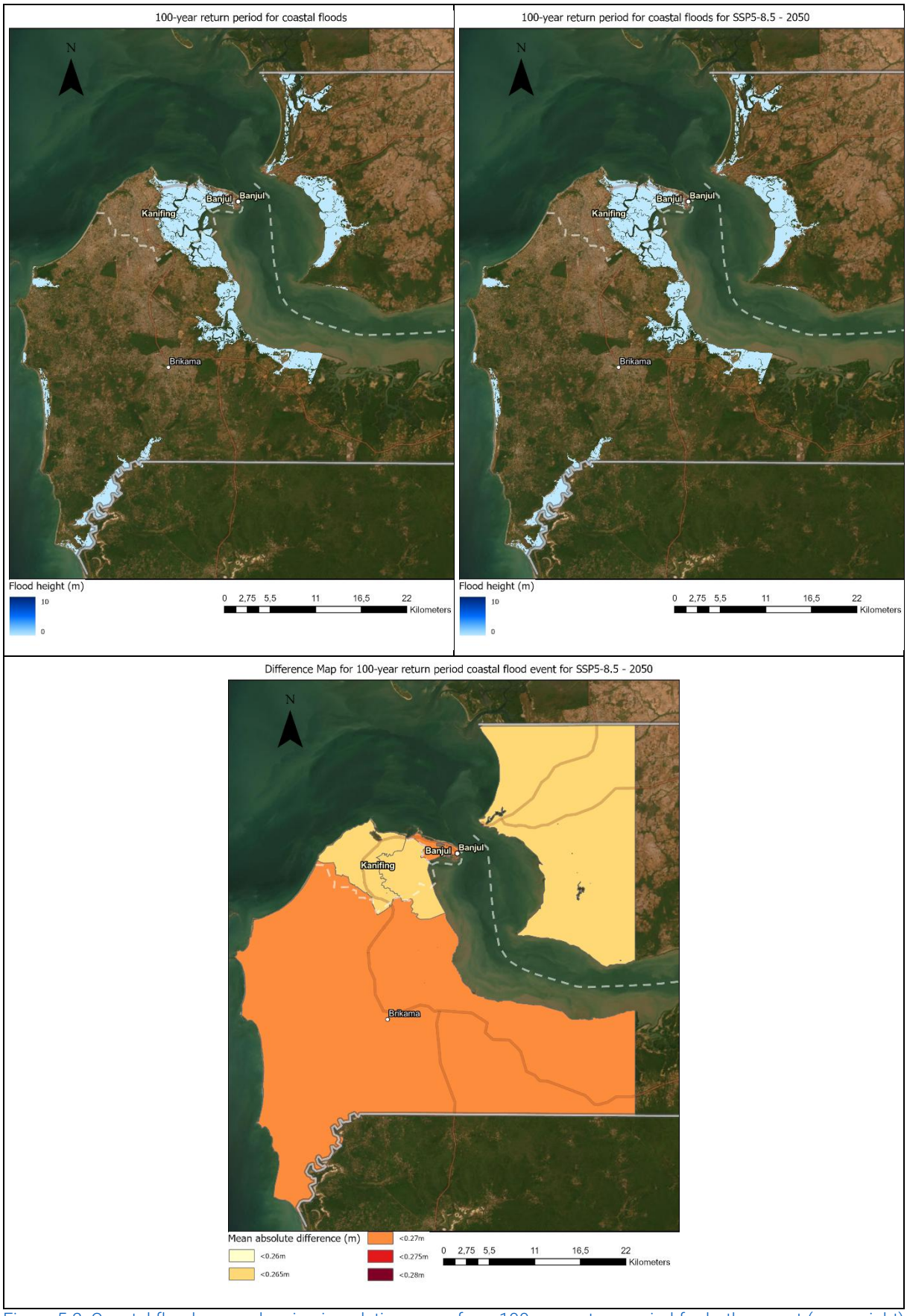

Figure 5-2: Coastal flood maps showing inundation areas for a 100-year return period for both current (upper right) and SSP5-8.5 – 2050 (upper left) simulations. Additionally, a difference map (lower) shows the absolute increase in flood height (m) per LGA.

5.1.3 Coastal flood duration analysis

Understanding flood duration provides crucial information for emergency response and infrastructure planning. The water depths in the flood maps are the result of the assumptions of a constant high-water level, ignoring time-varying water levels. A large contribution to the flood water levels is the MHWS of 0.83 m. This water level is related to the tide and thus the semidiurnal characteristics (i.e. 2 high water levels per day). The other factors of discharge and surge typically span over multiple days, and SLR is, of course, indefinite. Therefore, it is possible to estimate the flood duration based on tidal variations.

The analysis considers the temporal characteristics of different flooding components:

Tidal Influence: With a tidal range of 1.69 meters during spring tides, water levels rise and fall at approximately 28 cm per hour. This creates varying flood durations depending on water depth.

Storm surge and extreme weather effects typically persist for multiple days, potentially causing repeated flooding cycles as tides rise and fall. This combination of short-term tidal flooding and longer-duration surge effects creates complex patterns of coastal inundation that require careful consideration in flood risk management.

Since the surge and wave effects can last for multiple days, more than one flooding event can be expected as the tide rises again. The tidal range at MHWS near the coast is 1.69 m, thus the water rises and falls at about 28 cm/hour. In other words, a flooding with maximum water depth of 28 cm lasts for 2 hours (i.e. from 0cm up to 28cm and back down to 0cm).

Table 5-5: Flood durations for specific water levels for coastal floodings.

Water depth (cm)	Duration
10	43 min
20	1 h 28 min
40	2 h 56 min
60	4 h 24 min
80	5 h 52 min

5.2 Pluvial Flooding

Indicator: Flood Depth

The pluvial flood assessment focuses on how intense rainfall events generate fairly local short-duration surface water flooding.

The results of the pluvial flooding assessment are presented below in three parts; firstly, precipitation extremes for both current and future simulations are presented and discussed; and then secondly, the flood extents and depths resulting from these rainfall events as applied in the model are presented and discussed.

5.2.1 Analysis of Precipitation Extremes

5.2.1.1 Current Precipitation Extremes

The rainfall analysis for pluvial flooding utilizes 80 years of historical precipitation records from ERA5-LAND re-analysis data, a state-of-the-art global gridded dataset, which undergo thorough validation to ensure local applicability. These records enable the development of Intensity-Duration-Frequency (IDF) curves that show the relationship between rainfall intensity and storm duration for return periods ranging from 2 to 1,000 years. The curves demonstrate how short, intense storms tend to be more frequent, while longer-duration events typically deliver lower intensities.

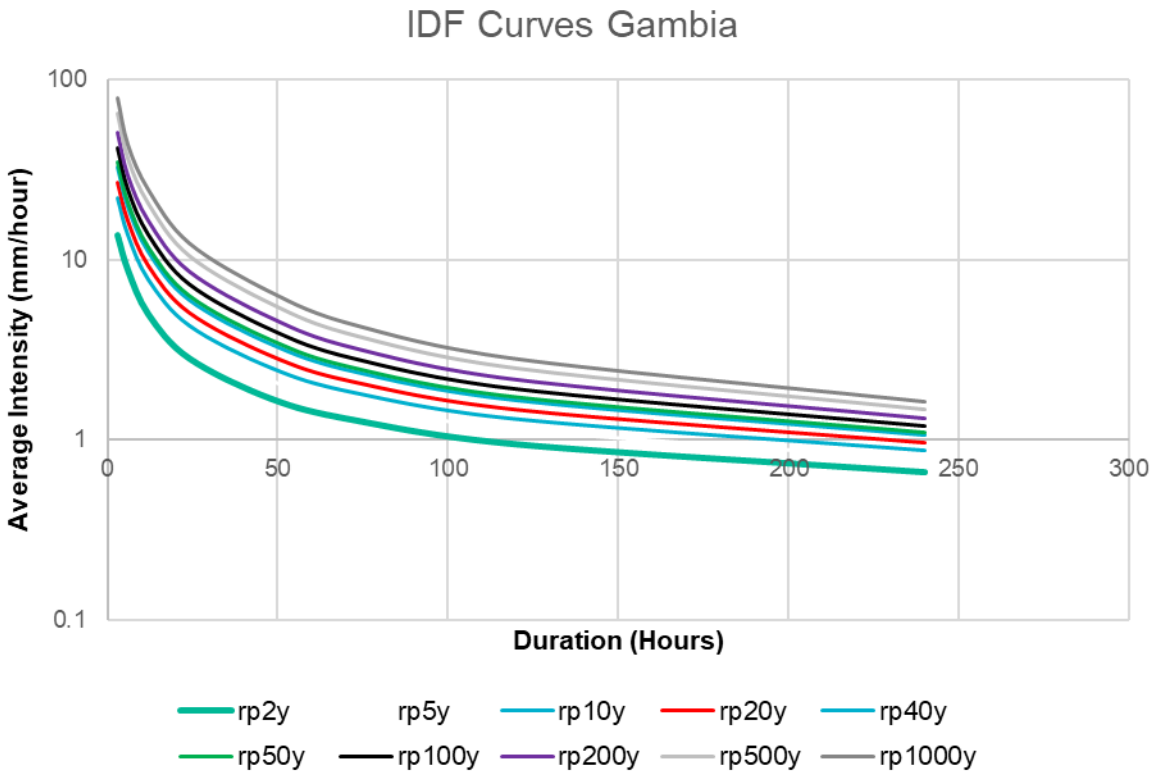

Figure 5-3: IDF Curves for Gambia, focusing on local precipitation extremes, based on 80 years of ERA5-LAND data.

Intensity-Duration-Frequency (IDF) curves enable hydrologists and engineers to anticipate and design against floods, ensuring critical infrastructure like bridges, roads, and urban drainage systems can withstand both frequent and extreme weather events. The presented IDF curves (Figure 5-3) for the Gambia River Basin display the relationship between the average rainfall intensity in (mm/hour) and storm duration for return periods ranging from 2 to 1,000 years. The curves exhibit a declining trend in rainfall intensity as the storm duration increases, consistent with hydrological behaviour where short, intense storms are more frequent, while long-duration events tend to deliver lower intensities. This behaviour underscores the critical need for accounting for both short and long-duration precipitation events when

designing flood control infrastructure, as short bursts of intense rain are more likely to trigger flash floods, while prolonged rainfall can cause riverine flooding through sustained runoff accumulation.

The return periods depicted in the figure, ranging from 2 to 1,000 years, provide a probabilistic understanding of extreme rainfall events. For example, higher intensity values are associated with shorter return periods (e.g., 2 or 5 years), indicating that these events are more common, while longer return periods (e.g., 200 or 1,000 years) correspond to rarer, extreme events. The use of IDF curves is essential for planning resilient infrastructure in the Gambia River Basin.

5.2.1.2 Future Precipitation Extremes

Figure 5-4 shows projected median precipitation change ratios for 1-day rainfall events across various SSP scenarios. Under SSP2-4.5 and SSP5-8.5, The Gambia is expected to experience increasing trends in short-duration extreme rainfall by 2080. These projections suggest a heightened risk of flash floods, which could directly impact critical infrastructure such as roads and bridges, especially during the wet season. The increase in intense rainfall confirms findings from other regional studies indicating that West African countries will likely see more frequent extreme weather events driven by climate variability. If unaddressed, these trends could accelerate road erosion and structural deterioration of transport networks and other infrastructure.

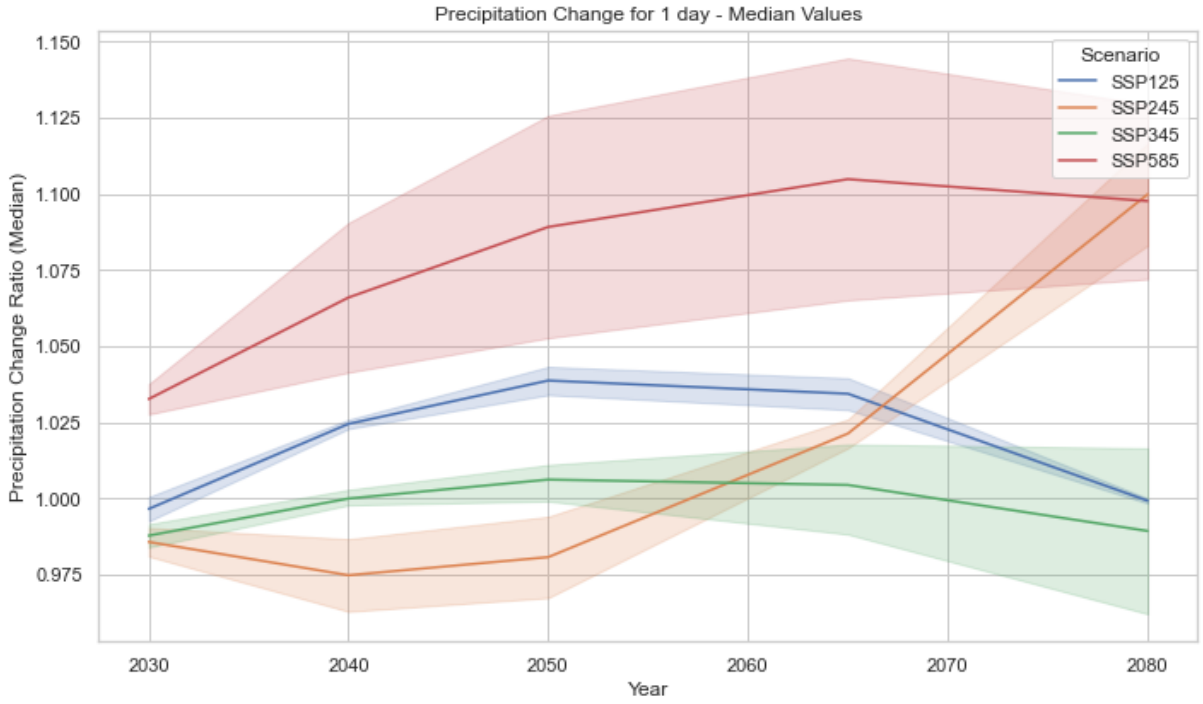

Figure 5-4 Climate change analysis results: Relative changes in extreme precipitation for 1-day rainfall events for various climate scenarios

5.2.2 Pluvial flooding results

5.2.2.1 Presentation of Results

The pluvial flood assessment results presented here are for both current conditions and future simulations, focused on the 10-year and 100-year return period events. The results specifically illustrate the SSP5-8.5 climate scenario for the 2050 time horizon, to understand potential changes in rainfall-driven flooding under high-emission conditions. To quantify changes in flood patterns, difference maps were generated comparing this future simulation against the baseline simulation.

These difference maps were calculated by subtracting the baseline simulation pluvial flood depths from the future simulation flood depths for each model grid cell. The results were then averaged to show mean differences in flood depths per Local Government Area (LGA), the mean being calculated of only those areas that are flood-prone in either of the two simulations analyzed. Areas displaying darker colors in the

difference maps indicate regions where mean pluvial flood depths are predicted to increase most significantly, helping identify potential hotspots for increased flood risk.

5.2.2.2 Current Pluvial Flooding

Analysis of baseline conditions reveals distinct patterns of pluvial flooding across The Gambia, with significant regional variations in flood susceptibility.

Figure 5-5 shows the flood maps for the 10-year return period event under current conditions. All regions of The Gambia are affected by pluvial flood events, although seemingly marginally more severe in the eastern regions of the country.

The 100-year return period event under current conditions, as presented in Figure 5-6, shows more severe flooding. The flood extent increases considerably compared to the 10-year event, with deeper flood depths and more extensive inundation areas across all LGAs.

5.2.2.3 Projected Future Pluvial Flooding

The difference maps reveal significant changes in pluvial flooding patterns under the SSP5-8.5 climate scenario for 2050. For 10-year return period events (Figure 5-5), the analysis shows a clear east-west gradient in flood exposure. The eastern regions, particularly Basse, demonstrate the most substantial increases in flood depths. Noticeable is the increase in flood depths in the Kanifing area, and more specifically around Kotu Stream, showing significant localized increases despite its western location, indicating that local topography and urban development play important roles in future flood hazard.

For 100-year return period events (Figure 5-6), the changes become more pronounced across all regions. The east-west gradient becomes more evident. This spatial pattern of change suggests that extreme rainfall events may have particularly severe impacts in eastern regions, while more western areas, though still experiencing increases show relatively lower changes in flood depths. An exception here is the Kanifing area where Kotu Stream plays an essential role in the urban drainage system and simultaneously a significant increase in flood depths is expected.

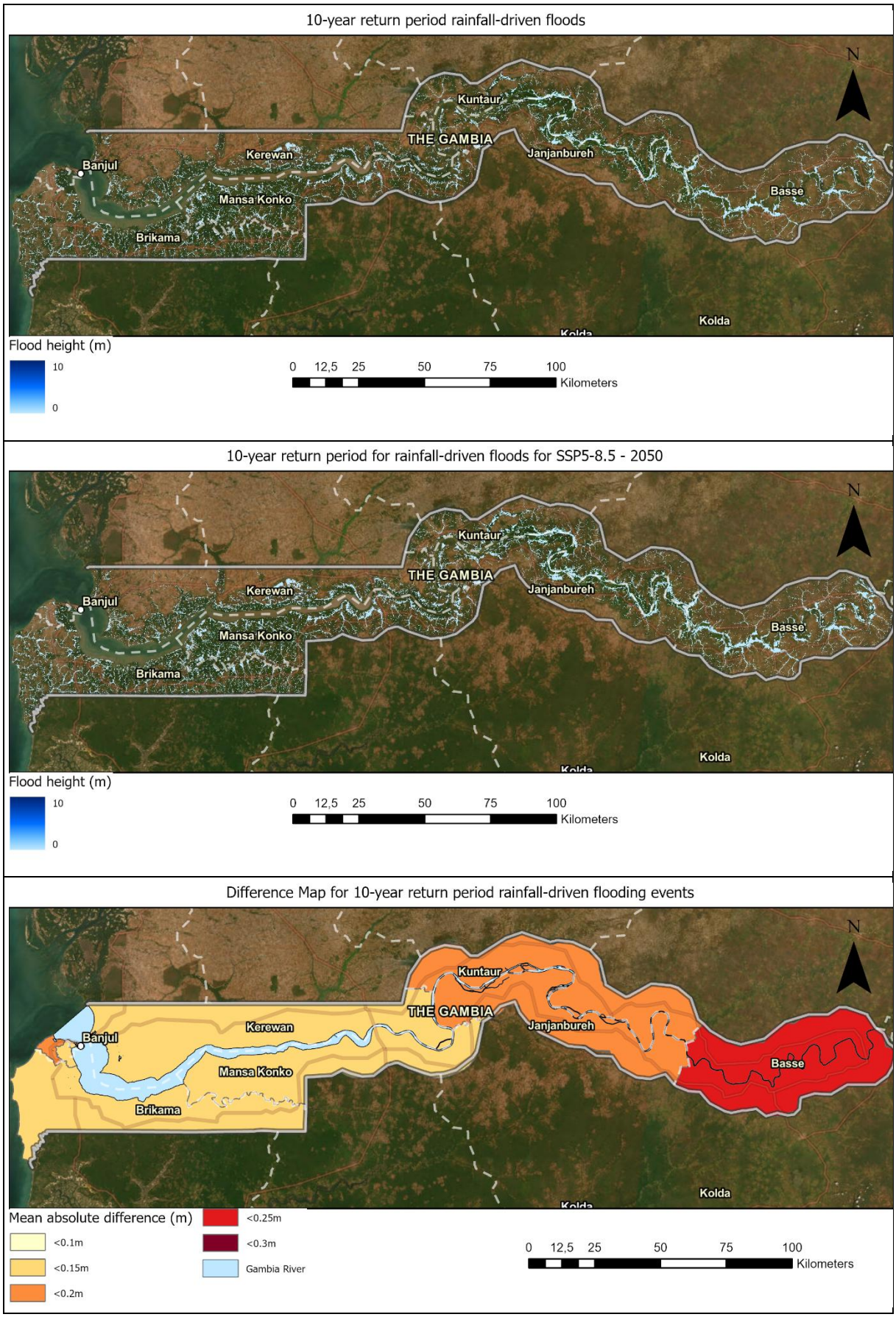

Figure 5-5: Pluvial flood maps showing inundation areas for a 10-year return period for both current (upper) and SSP5-8.5 – 2050 (middle) simulations. Additionally, a difference map (lower) shows the absolute increase in flood height (m) per LGA.

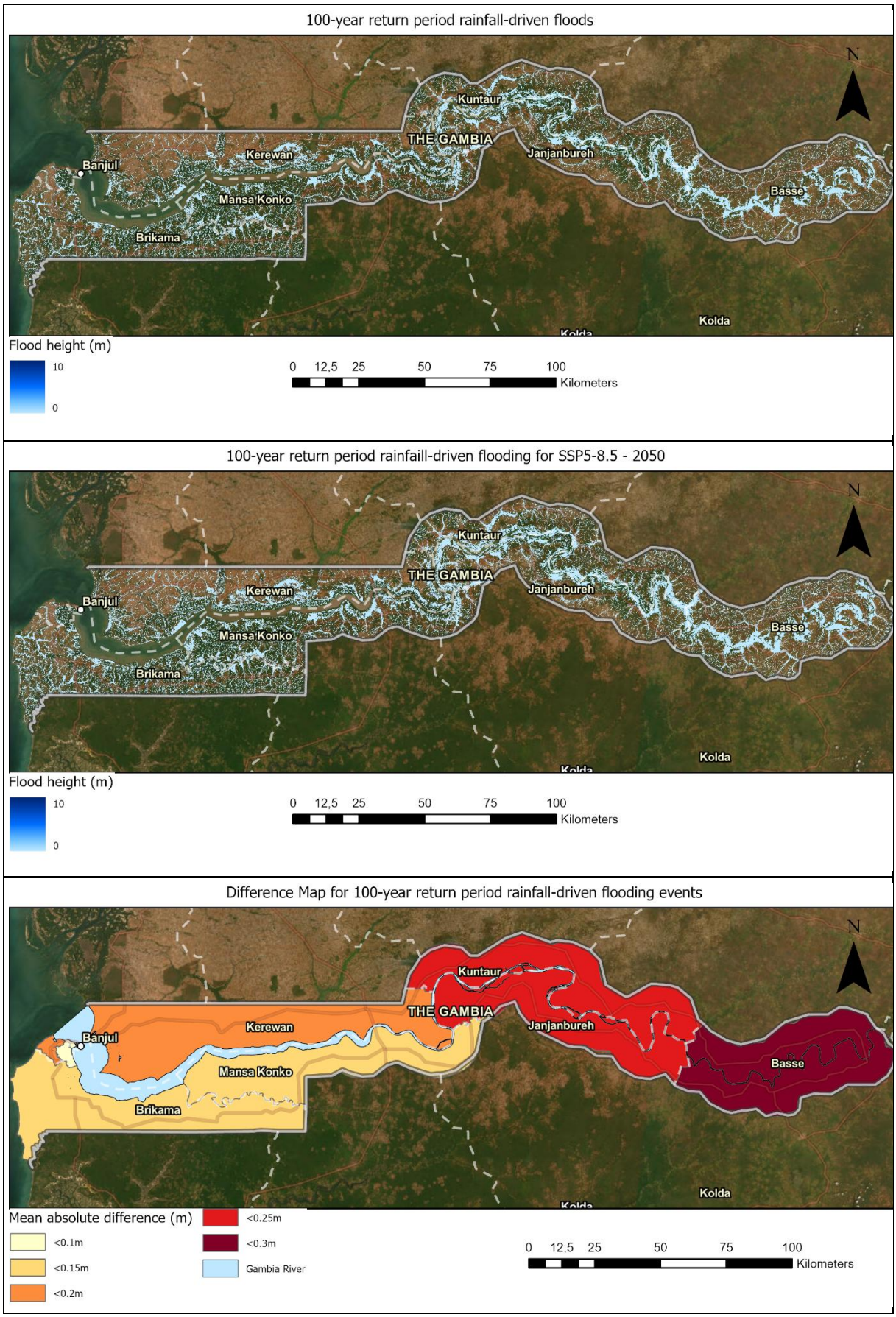

Figure 5-6: Pluvial flood maps showing inundation areas for a 100-year return period for both current (upper) and SSP5-8.5 – 2050 (middle) simulations. Additionally, a difference map (lower) shows the absolute increase in flood height (m) per LGA.

5.3 Fluvial Flooding

Indicators: Flood Depth

The fluvial flood assessment was conducted taking long duration catchment-scale rainfall events into account that lead to fluvial flood events.

The results of the fluvial flooding assessment are presented below in three parts; firstly, precipitation extremes for future simulations are presented and discussed; secondly, reference is made to the determination of the maximum sea water levels used as the downstream boundary condition in the model; and then thirdly, the flood extents and depths resulting from the rainfall events and boundary conditions as applied in the model are presented and discussed.

5.3.1 Catchment-scale precipitation

The analysis of extreme events for fluvial flooding focuses on catchment-averaged precipitation, which differs from localized extremes. Using 80 years of ERA5-LAND data, the analysis employs a Gumbel distribution to characterize extreme values in the Gambia River basin. This approach accounts for the fact that catchment rainfall extremes require separate analysis from localized events, as they drive the occurrence of fluvial flooding through large precipitation systems in the region. Figure 5-7 provides an overview of the precipitation change for a 7-day precipitation event.

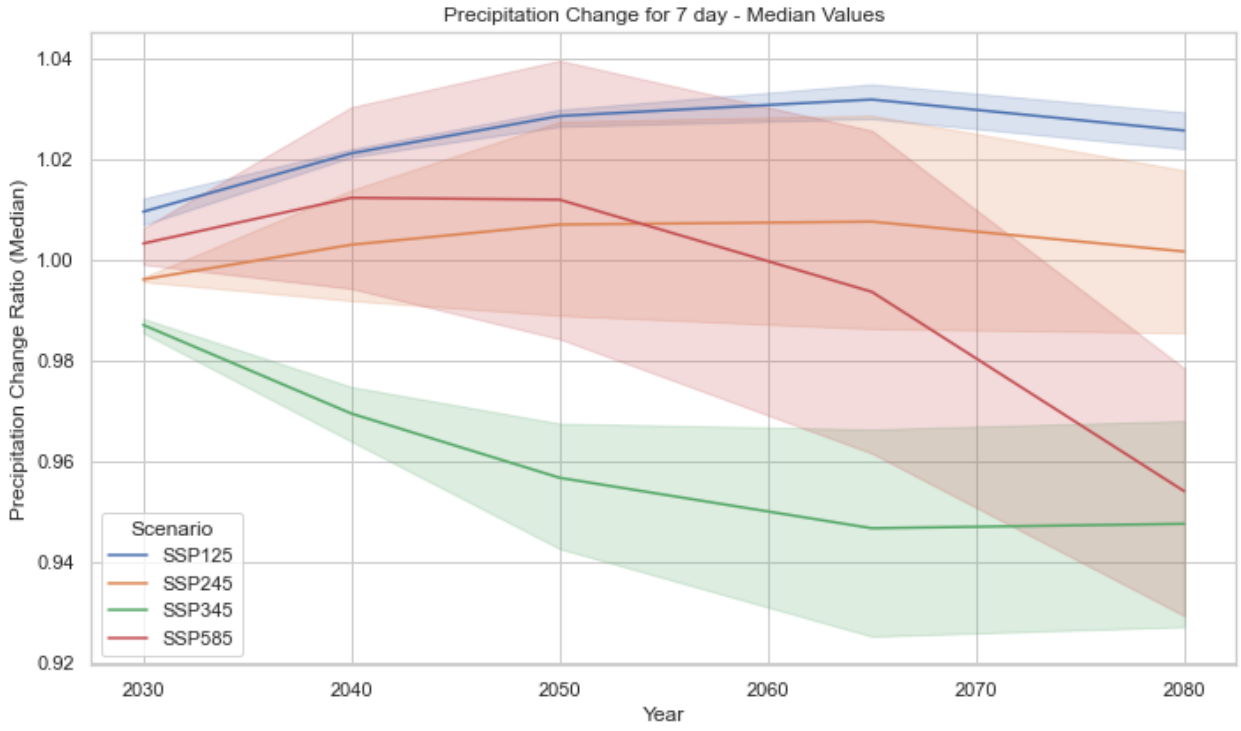

Figure 5-7: Climate change analysis results: Relative changes in extreme precipitation for 7-day rainfall events for various climate scenarios

The 7-day precipitation changes show similar increasing trends as the 1- day extreme precipitation until 20250. However the 7-day precipitation change ratio then reflects a **pronounced decline in total cumulative rainfall under the high-emission scenario SSP5-8.5**. This shift points to a strong decrease in long-duration extreme precipitation, and thus in the magnitude of fluvial floods. This potentially indicates an increasing likelihood of seasonal droughts, exacerbating water scarcity in both urban and rural areas of Gambia. Long-term reductions in rainfall could also strain infrastructure and transport services through lower normal and flood-event river levels; e.g. stranded ferry crossing berths. These insights support findings from hydrological studies suggesting that fluctuating precipitation patterns could complicate water resource management across the basin, reinforcing the need for adaptive infrastructure planning to mitigate both fluvial flood and drought risks.

5.3.2 Maximum sea water levels

Another critical aspect of the fluvial flood assessment is incorporation of tidal influences creating a transitional hydrological zone where tidal effects interact with riverine flows. Hence, an assessment on extreme sea levels has been conducted (similarly as for coastal flooding) and used as a downstream boundary condition in modelling the fluvial floods.

As storm surges and fluvial flooding are statistically distinct events, the influence of storm surge levels were not included in the boundary condition. The boundary condition of maximum sea water level was thus computed as:

Maximum sea water level = Mean High Water Spring (MHWS) + Sea Level Rise (SLR)

Please refer to Section 5.1.1 for the derivation of these levels.

5.3.3 Fluvial flooding results

Presentation of Results

The fluvial flood assessment results presented here are for both current and future flooding along the main Gambia River system, focused on the 10-year and 100-year return periods. The results specifically illustrate the SSP5-8.5 climate scenario for the 2050 time horizon, to understand potential changes in riverine flooding under high-emission conditions. To quantify these changes, difference maps were generated comparing this future simulation against the baseline simulation.

These difference maps were calculated by subtracting the baseline simulation fluvial flood depths from the future simulation flood depths for each model grid cell. The results were then averaged to show mean differences in flood depths per Local Government Area (LGA), the mean being calculated of only those areas that are flood-prone in either of the two simulations analyzed. Areas displaying darker colors in the difference maps indicate regions where mean fluvial flood depths are predicted to increase most significantly, helping identify potential hotspots for increased flood risk.

5.3.3.1 Current Fluvial Flooding

Analysis of the baseline simulation reveals significant flooding along the Gambia River and its tributaries. Figure 5-8 shows the flood maps for the 10-year return period event under current conditions. Substantial flooding occurs along the main river channel. With especially extensive flooding observed in the flood plains in the region near the Senegambia Bridge.

The 100-year return period event under current conditions, as presented in Figure 5-9, shows more severe flooding patterns. The flood extent increases considerably compared to the 10-year event, with deeper flood depths and more extensive inundation zones affecting low-lying areas adjacent to the river system.

These flooding extents highlight that the Gambia River system is prone to sever flooding even under current conditions.

5.3.3.2 Projected Future Fluvial Flooding

The difference maps reveal significant changes in fluvial flooding patterns under the SSP5-8.5 climate scenario for 2050. For 10-year return period events (Figure 5-8), the analysis shows interesting spatial variations in flood impact. Again, as for pluvial flooding, the Kanifing area exhibits a more significant increase in flood depths than the surrounding LGAs. And also as with pluvial flooding, an east-west gradient of flood depth increases is found, with the most significant increases in the Basse region.

For 100-year return period events (Figure 5-9), the changes become more pronounced with distinct spatial patterns. The middle river regions, particularly Mansa Konko, Kuntaur, and Janjanbureh LGAs, show the largest increases in flood depths. This spatial pattern presents an interesting deviation from the other pluvial and fluvial flooding trends noted above in this assessment.

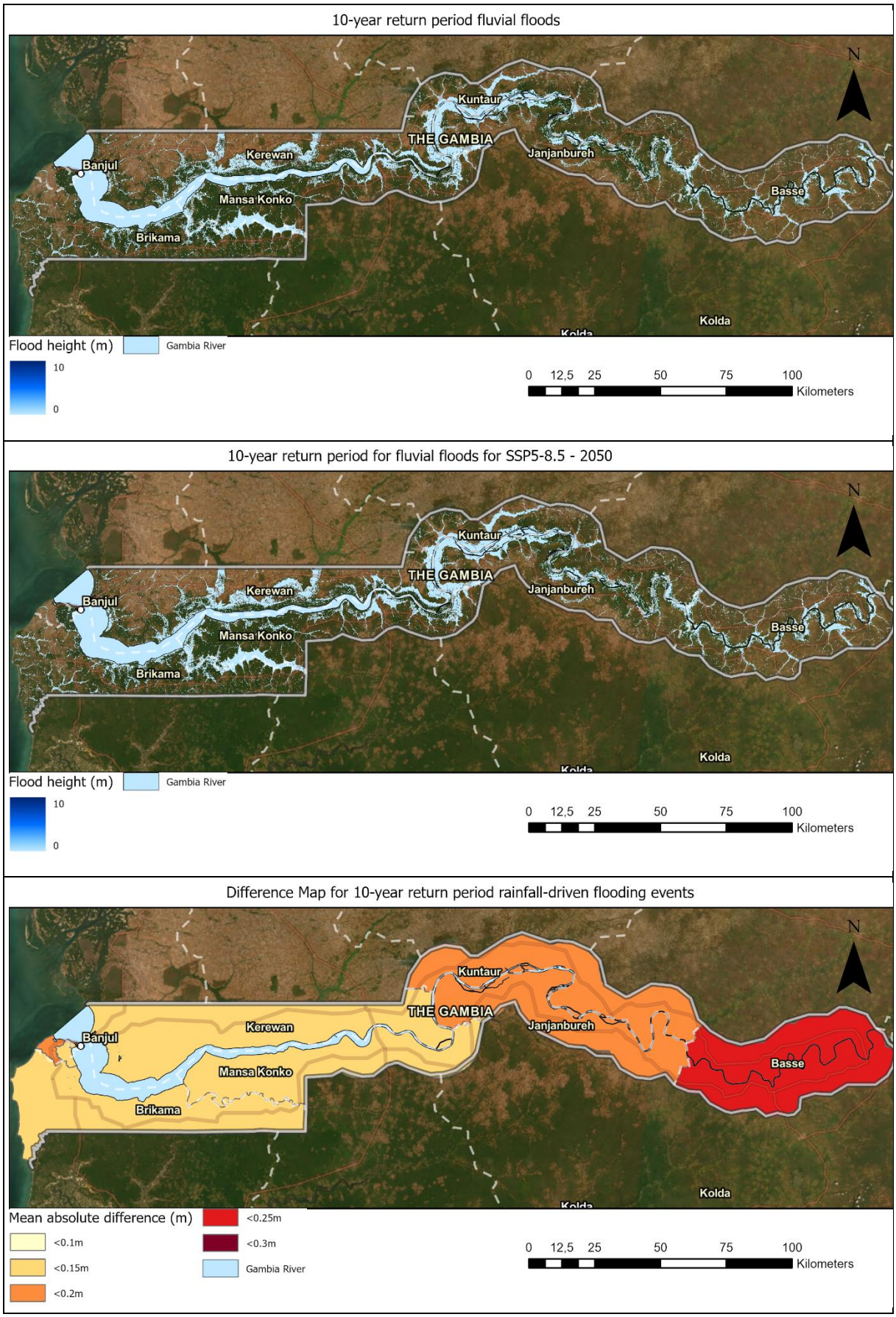

Figure 5-8: Fluvial flood maps showing inundation areas for a 10-year return period for both current (upper) and SSP5-8.5 – 2050 (middle) simulations. Additionally, a difference map (lower) shows the absolute increase in flood height (m) per LGA.

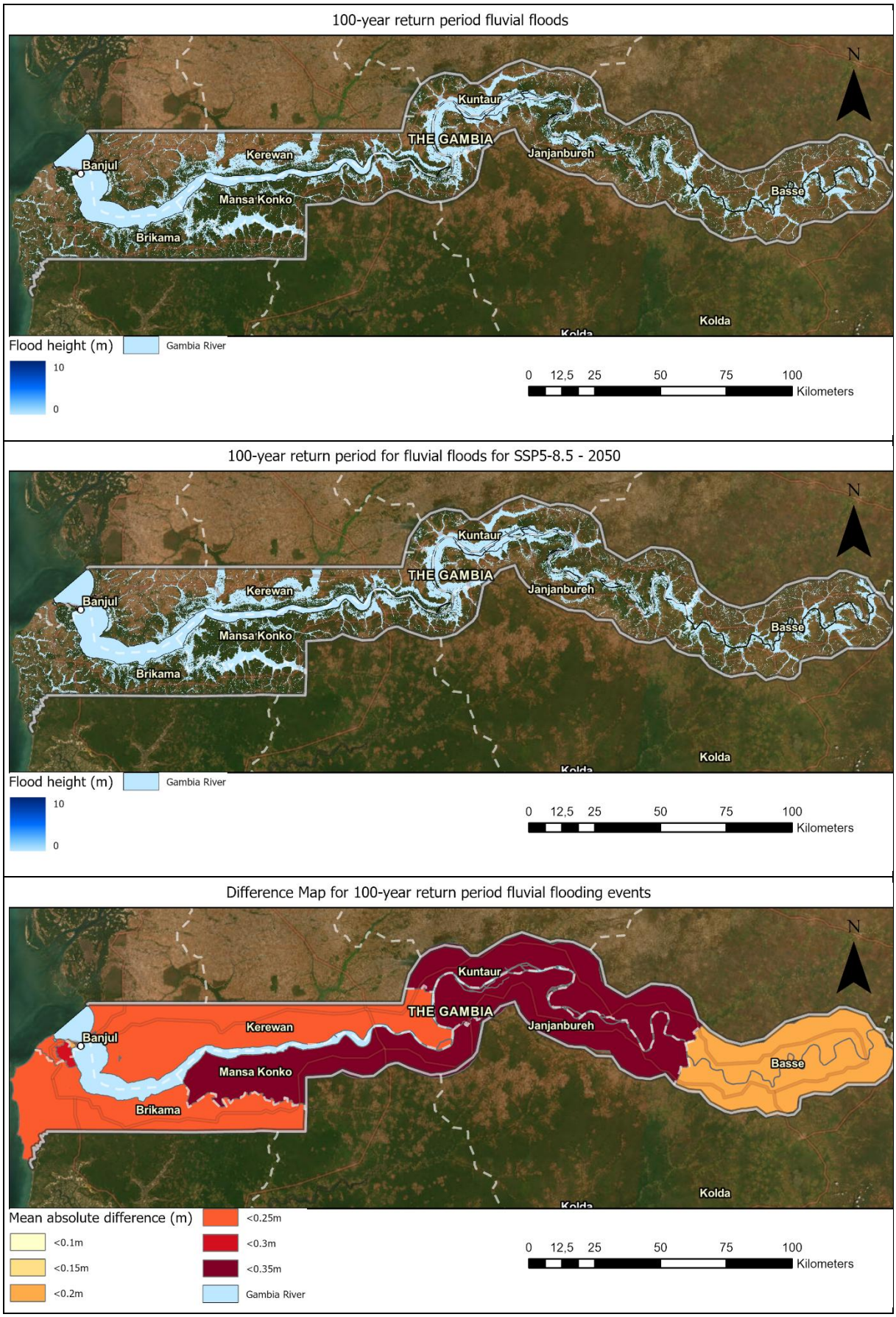

Figure 5-9: Fluvial flood maps showing inundation areas for a 100-year return period for both current (upper) and SSP5-8.5 – 2050 (middle) simulations. Additionally, a difference map (lower) shows the absolute increase in flood height (m) per LGA.

5.3.4 Calibration and Validation

To calibrate the model, flood maps produced by UNOSAT for 2007 floods were used. In that year, The Gambia experienced severe flooding as a result of heavy rains, causing both local flash (pluvial) floods and riverine (fluvial) flood events. The flood extent maps were derived from satellites and therefore is limited to areas that were not covered by clouds[42].

Figure 5-10 shows the comparison of the observed flood extent of 2007 with the modelled baseline flood 10-year event. The calibration demonstrates a generally strong agreement between simulated and observed flood extents. Despite the complex hydrological processes at play, especially the dominance of flash floods in the region, the model captures most of the inundation patterns visible in the satellite imagery. This suggests that key parameters – such as channel roughness, rainfall-runoff characteristics, and topographic data – have been well represented in the modelling framework.

Noticeable, is the area on the lower left side of the flood map, where the difference between the observed flood extent and modelled flooding is the largest. This area represents a change in land cover, from low canopy to high canopy woodland. This land use type may result in differences in elevation between actual and modelled, possibly giving rise to the differences in this area.

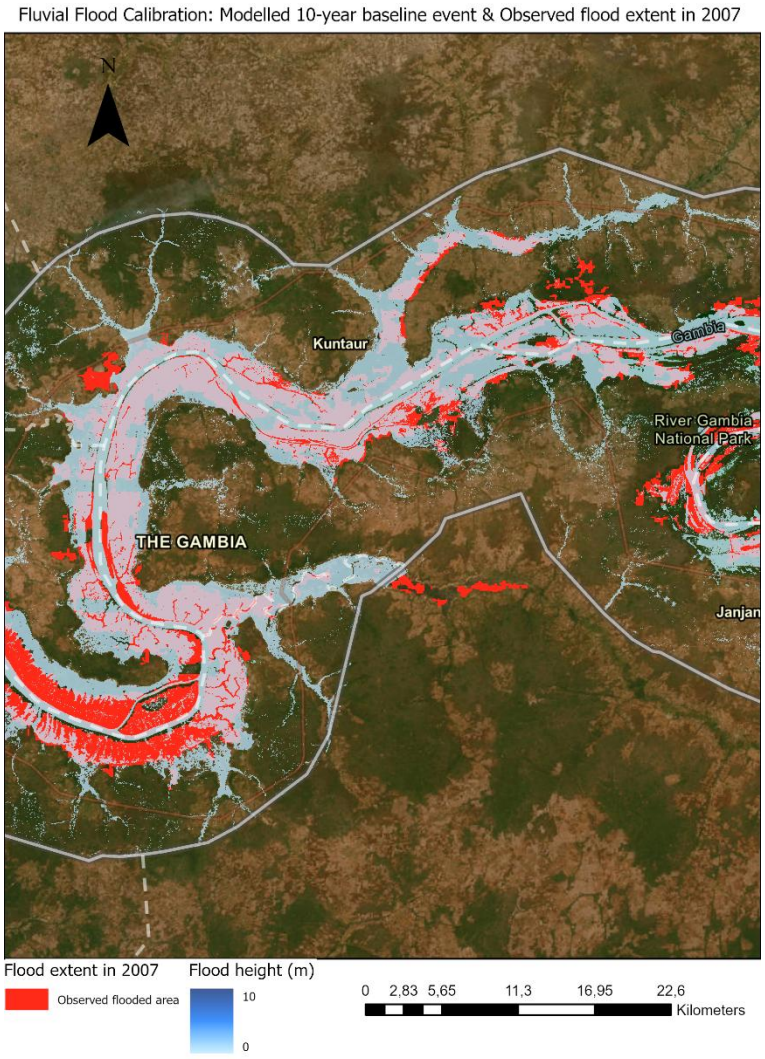

Figure 5-10: Calibration flood simulation results with satellite-based observations (Source: UNOSAT).

[42] https://reliefweb.int/map/gambia/flood-water-identification-central-gambia-18-sep-2007

In conclusion, given the limited availability of ground-truth data, the level of alignment achieved speaks to the robustness of the approach and the general reliability of the datasets used.

Nonetheless, several limitations of the satellite-based map affect the precision of the calibration. In particular, the imagery may not accurately capture rapid-onset flooding in urban areas, since the timing of the satellite fly-over often does not coincide with the peak flood event. Additionally, the resolution and quality of the satellite data can be insufficient to resolve finer-scale inundation pathways or small, localized flash flood events. These constraints highlight the challenges of relying on remote sensing in data-scarce environments.

Nevertheless, considering these factors, the overall calibration still provides a valuable validation of the modelling process.

6. CONCLUSIONS

This flood hazard assessment for The Gambia reveals significant current hazard from multiple flood types, with projections generally indicating intensification of the flood events under future climate scenarios. The analysis demonstrates distinct spatial patterns in flood intensities across the country, with different regions showing varying susceptibility to coastal, pluvial, and fluvial flooding. These patterns have important implications for infrastructure planning and adaptation strategies.

The assessment indicates that climate change will substantially influence flooding patterns across The Gambia, with both SSP2-4.5 and SSP5-8.5 scenarios projecting increased flood hazards by 2050. However, the nature and severity of these changes vary significantly by region and flood type, necessitating locally tailored adaptation approaches.

6.1 Coastal flooding

The coastal flood assessment reveals particular hazard in the Greater Banjul Area and the Gambia River estuarine area. Some key findings include:

- Current coastal floods are concentrated in low-lying areas around Banjul, with significant inundation during extreme water level events.
- Mangrove areas west of Banjul show high inundation levels, underlining their crucial role and potential in flood attenuation.
- Sea level rise will amplify coastal flood risks, with projected increases in flood depths under the SSP5-8.5 climate scenario of 0.25 meters by 2050 and 0.42m by 2070.
- The combination of sea level rise and storm surge creates compound effects that will increasingly challenge coastal infrastructure.
- Banjul and Brikama regions show the highest projected increases in flood depths for extreme events between the current and 2050 time horizons.

These findings suggest an urgent need for coastal adaptation strategies, particularly for critical infrastructure in the Greater Banjul Area.

6.2 Pluvial flooding

The analysis of rainfall-driven flooding reveals widespread pluvial flood hazard across The Gambia, with distinct spatial patterns:

- Eastern regions, particularly Basse, show the highest susceptibility to pluvial flooding and the largest projected increases in flood depth under future climate scenarios.
- Urban areas demonstrate particular vulnerability to local flash flooding, with Kanifing showing significant localized impacts around Kotu Stream.
- Short-duration, high-intensity rainfall events are projected to increase in frequency and severity under future climate scenarios, leading to increased flooding.
- The east-west gradient in increased flood exposure suggests the need for regionally differentiated adaptation strategies.

These patterns highlight the importance of improving urban drainage systems and localized flood management strategies.

6.3 Fluvial flooding

The assessment of riverine flooding reveals complex interactions between river dynamics and flood exposure:

- The Gambia River and its tributaries have extensive flood plains, particularly in middle river regions (Mansa Konko, Kuntaur, and Janjanbureh) which also show the most significant fluvial flood hazard.
- Under future climate scenarios, the effect of increased sea levels is transmitted up the Gambia River as far as the tidal effect, resulting in increased flooding in the lower river regions under these scenarios.

- Up to 2050, the 7-day precipitation change ratio for future climate scenarios is positive, reflecting increased long-duration rainfall; however after 2050 it then reflects a pronounced decline in total cumulative rainfall under the high-emission scenario SSP5-8.5. This shift points to a strong decrease in long-duration extreme precipitation, and thus in the magnitude of fluvial floods between 2050 and 2070.
- The spatial pattern of fluvial flood hazard contrasts with pluvial hazard patterns requiring integrated flood management.

The validation against 2007 flood events demonstrates the model's capability to capture major flood patterns with sufficient accuracy for the purposes of this assessment.

6.4 Limitations

The flood hazard assessment contains several important limitations that should be considered when interpreting and applying its results, as follows:

6.4.1 Data Limitations

Limited availability of high-resolution elevation data affects model accuracy, particularly in urban areas and flood plains with high canopy cover where small-scale topographic features significantly influence flood patterns. The scarcity of historical flood records and discharge measurements restricted model validation capabilities, though the 2007 flood event provided some verification opportunities. Future climate projects, especially for extreme events, carry inherent uncertainties despite the use of state-of-the-art modelling techniques. Lack of ground-truth data also constrain the ability to comprehensively verify model performance across all simulations.

6.4.2 Methodological Constraints

The assessment necessarily simplified several complex processes. Urban drainage systems were not represented due to limited infrastructure data and the time necessary to incorporate such into a model. Compound flooding effects, where multiple flood types occur simultaneously, may be underestimated despite considering basic interactions between coastal, pluvial, and fluvial flooding. The models' temporal and spatial resolution limits their ability to fully capture rapid-onset urban flooding and small-scale topographic features that influence local flood patterns. Furthermore, the model is currently limited to providing only one discharge boundary condition. This limits the analysis of large river systems with extensive tributaries.

6.4.3 Additional Considerations

Future land-use changes were not incorporated into the models.

The coastal flood modelling excluded wave effects.

Existing and planned flood protection infrastructure were not represented in the model.

The model does not take aquifer recharge and a decrease in soil permeability after drought events into account.

While these limitations are significant, they do not invalidate the assessment's findings but rather provide context for their interpretation. The results offer a robust foundation for flood risk management while highlighting areas where future research and more detailed modelling could enhance understanding of flood hazard in The Gambia.

ANNEX 1. LIST OF FLOOD HAZARD MAPS

Below a list of the flood hazard maps produced is provided.

For each flood type there are 42 files available as .tif format.

Flood Type	Climate Scenario	Time Horizon	Return Period
Fluvial	Historical	2025	2
Fluvial	Historical	2025	5
Fluvial	Historical	2025	10
Fluvial	Historical	2025	20
Fluvial	Historical	2025	50
Fluvial	Historical	2025	100
Fluvial	SSP245	2030	2
Fluvial	SSP245	2030	5
Fluvial	SSP245	2030	10
Fluvial	SSP245	2030	20
Fluvial	SSP245	2030	50
Fluvial	SSP245	2030	100
Fluvial	SSP245	2050	2
Fluvial	SSP245	2050	5
Fluvial	SSP245	2050	10
Fluvial	SSP245	2050	20
Fluvial	SSP245	2050	50
Fluvial	SSP245	2050	100
Fluvial	SSP245	2070	2
Fluvial	SSP245	2070	5
Fluvial	SSP245	2070	10
Fluvial	SSP245	2070	20
Fluvial	SSP245	2070	50
Fluvial	SSP245	2070	100
Fluvial	SSP585	2030	2
Fluvial	SSP585	2030	5
Fluvial	SSP585	2030	10
Fluvial	SSP585	2030	20
Fluvial	SSP585	2030	50
Fluvial	SSP585	2030	100
Fluvial	SSP585	2050	2
Fluvial	SSP585	2050	5
Fluvial	SSP585	2050	10
Fluvial	SSP585	2050	20
Fluvial	SSP585	2050	50
Fluvial	SSP585	2050	100
Fluvial	SSP585	2070	2
Fluvial	SSP585	2070	5
Fluvial	SSP585	2070	10
Fluvial	SSP585	2070	20

Fluvial	SSP585	2070	50
Fluvial	SSP585	2070	100
Pluvial	Historical	2025	2
Pluvial	Historical	2025	5
Pluvial	Historical	2025	10
Pluvial	Historical	2025	20
Pluvial	Historical	2025	50
Pluvial	Historical	2025	100
Pluvial	SSP245	2030	2
Pluvial	SSP245	2030	5
Pluvial	SSP245	2030	10
Pluvial	SSP245	2030	20
Pluvial	SSP245	2030	50
Pluvial	SSP245	2030	100
Pluvial	SSP245	2050	2
Pluvial	SSP245	2050	5
Pluvial	SSP245	2050	10
Pluvial	SSP245	2050	20
Pluvial	SSP245	2050	50
Pluvial	SSP245	2050	100
Pluvial	SSP245	2070	2
Pluvial	SSP245	2070	5
Pluvial	SSP245	2070	10
Pluvial	SSP245	2070	20
Pluvial	SSP245	2070	50
Pluvial	SSP245	2070	100
Pluvial	SSP585	2030	2
Pluvial	SSP585	2030	5
Pluvial	SSP585	2030	10
Pluvial	SSP585	2030	20
Pluvial	SSP585	2030	50
Pluvial	SSP585	2030	100
Pluvial	SSP585	2050	2
Pluvial	SSP585	2050	5
Pluvial	SSP585	2050	10
Pluvial	SSP585	2050	20
Pluvial	SSP585	2050	50
Pluvial	SSP585	2050	100
Pluvial	SSP585	2070	2
Pluvial	SSP585	2070	5
Pluvial	SSP585	2070	10
Pluvial	SSP585	2070	20
Pluvial	SSP585	2070	50
Pluvial	SSP585	2070	100
Coastal	Historical	2025	2

Coastal	Historical	2025	5
Coastal	Historical	2025	10
Coastal	Historical	2025	20
Coastal	Historical	2025	50
Coastal	Historical	2025	100
Coastal	SSP245	2030	2
Coastal	SSP245	2030	5
Coastal	SSP245	2030	10
Coastal	SSP245	2030	20
Coastal	SSP245	2030	50
Coastal	SSP245	2030	100
Coastal	SSP245	2050	2
Coastal	SSP245	2050	5
Coastal	SSP245	2050	10
Coastal	SSP245	2050	20
Coastal	SSP245	2050	50
Coastal	SSP245	2050	100
Coastal	SSP245	2070	2
Coastal	SSP245	2070	5
Coastal	SSP245	2070	10
Coastal	SSP245	2070	20
Coastal	SSP245	2070	50
Coastal	SSP245	2070	100
Coastal	SSP585	2030	2
Coastal	SSP585	2030	5
Coastal	SSP585	2030	10
Coastal	SSP585	2030	20
Coastal	SSP585	2030	50
Coastal	SSP585	2030	100
Coastal	SSP585	2050	2
Coastal	SSP585	2050	5
Coastal	SSP585	2050	10
Coastal	SSP585	2050	20
Coastal	SSP585	2050	50
Coastal	SSP585	2050	100
Coastal	SSP585	2070	2
Coastal	SSP585	2070	5
Coastal	SSP585	2070	10
Coastal	SSP585	2070	20
Coastal	SSP585	2070	50
Coastal	SSP585	2070	100

GLOBAL
CENTER ON
ADAPTATION

ANTOINE PLATEKADE 1006
3072 ME ROTTERDAM
THE NETHERLANDS
+31(0)88-088-6800
WWW.GCA.ORG